ELUCIDATION OF MOLECULAR EVENTS UNDERLYING

HYPOXIA INDUCED DYSFUNCTIONS IN 3T3-L1 ADIPOCYTES

AND POSSIBLE AMELIORATION WITH BILOBALIDE AND CURCUMIN

Thesis submitted to
Cochin University of Science and Technology
in partial fulfilment of the requirements for the degree of

Doctor of Philosophy
in
Biotechnology
under the Faculty of Science

By

PRIYANKA. A
(Reg. No. 3870)

Under the supervision of
Dr. K. G. RAGHU

Agroprocessing and Natural Products Division
Council of Scientific and Industrial Research–National Institute for
Interdisciplinary Science and Technology (CSIR-NIIST)
Thiruvananthapuram – 695 019, Kerala, India.

JUNE 2015

COUNCIL OF SCIENTIFIC & INDUSTRIAL RESEARCH
NATIONAL INSTITUTE FOR INTERDISCIPLINARY SCIENCE & TECHNOLOGY
GOVERNMENT OF INDIA
Thiruvananthapuram-695 019, Kerala, India

Telephone: 91-471-2515486
Fax: 91-471-2491712

Dr. K. G. Raghu
Principal Scientist
Agroprocessing and Natural Products Division

CERTIFICATE

This is to certify that the work embodied in the thesis entitled "**ELUCIDATION OF MOLECULAR EVENTS UNDERLYING HYPOXIA INDUCED DYSFUNCTIONS IN 3T3-L1 ADIPOCYTES AND POSSIBLE AMELIORATION WITH BILOBALIDE AND CURCUMIN**" has been carried out by **Ms. Priyanka. A**, under my supervision and guidance at Agroprocessing and Natural Products Division of Council of Scientific and Industrial Research-National Institute for Interdisciplinary Science and Technology (CSIR-NIIST), Thiruvananthapuram in partial fulfilment of the requirements for the award of degree of Doctor of Philosophy in Biotechnology under Faculty of Science, Cochin University of Science and Technology, Kochi, Kerala, India and the same has not been submitted elsewhere for any other degree. All the relevant corrections, modifications and recommendations suggested by the audience and the doctoral committee members during the pre-synopsis seminar of **Ms. Priyanka. A** has been incorporated in the thesis.

K. G. Raghu
(Thesis Supervisor)

Thiruvananthapuram,
June, 2015.

e-mail: raghukgopal2009@gmail.com; raghukgopal@rediffmail.com

i

DECLARATION

I hereby declare that thesis entitled *"**ELUCIDATION OF MOLECULAR EVENTS UNDERLYING HYPOXIA INDUCED DYSFUNCTIONS IN 3T3-L1 ADIPOCYTES AND POSSIBLE AMELIORATION WITH BILOBALIDE AND CURCUMIN***"* embodies the results of investigations carried out by me at Agroprocessing and Natural Products Division of Council of Scientific and Industrial Research - National Institute for Interdisciplinary Science and Technology (CSIR-NIIST), Thiruvananthapuram as a full time research scholar under the supervision of Dr. K. G. Raghu and the same has not been submitted elsewhere for any other degree. In keeping with the general practice of reporting scientific observations, due acknowledgement has been made wherever the work described is based on the findings of other investigators.

Priyanka. A

Thiruvananthapuram,
June 2015.

ii

DEDICATED TO MY BELOVED

PARENTS, HUSBAND, & SON…

ACKNOWLEDGEMENT

Priyanka. A

CONTENTS

CHAPTER 2: HYPOXIA INDUCED OXIDATIVE STRESS AND ENDOPLASMIC RETICULUM STRESS IN 3T3-L1 ADIPOCYTES AND POSSIBLE PROTECTION WITH BILOBALIDE AND CURCUMIN

CHAPTER 3: EFFECT OF HYPOXIA ON MITOCHONDRIAL FUNCTIONS IN 3T3-L1 ADIPOCYTES AND POSSIBLE AMELIORATION WITH BILOBALIDE AND CURCUMIN

CHAPTER 4: HYPOXIA INDUCED INFLAMMATION AND INSULIN RESISTANCE IN 3T3-L1 ADIPOCYTES AND POSSIBLE ATTENUATION WITH BILOBALIDE AND CURCUMIN

LIST OF TABLES

LIST OF FIGURES

LIST OF **ABBREVIATIONS**

2-NBDG : 2-(N-(7-Nitrobenz-2-oxa-1,3-diazol-4-yl)Amino)-2-Deoxyglucose

ABTS : 2, 2'-azino-bis(3-ethylbenzothiazoline-6-sulphonic acid)

ANGPTL4 : Angiopoietin-like 4

ARE : Antioxidant response element

ATCC : American Type Culture Collection

ATF-6 : Activating transcription factor 6

ATH : Adipose tissue hypoxia

ATP : Adenosine triphosphate

BCA : Bicinchoninic acid

BiP : Binding immunoglobulin protein

BMI : Body mass index

CAT : Catalase

CHOP : CCAAT-enhancer-binding protein homologous protein

CRP : C-reactive protein

DAB : 3, 3'-diaminobenzidine

DALY : The disability-adjusted life year

DCPIP : Dichlorophenolindophenol

DMEM : Dulbecco's modified eagle medium

Drp 1 : Dynamin related protein 1

DTT : Dithiothreitol

EDTA : Ethylene diamine tetraacetic acid

eIF2α : Eukaryotic Initiation Factor 2 alpha

ELISA : Enzyme-linked immunosorbent assay

ETC	: Electron transport chain
FBS	: Foetal bovine serum
FFA	: Free fatty acid
FIS 1	: Fission protein 1
GLUT-1	: Glucose transporter 1
GPx	: Glutathione peroxidase
GR	: Glutathione reductase
GRP78	: Glucose-regulated protein 78
GSH	: Glutathione
HEPES	: 4-(2-Hydroxyethyl)-1-piperazine ethane sulfonic acid
HIF-1α	: Hypoxia inducible factor 1 alpha
HO-1	: Heme oxygenase 1
IFN-γ	: Interferon gamma
IL-1β	: Interleukin 1beta
IL-6	: Interleukin 6
IRE-1α	: Inositol-requiring enzyme 1alpha
IRS-1	: Insulin receptor substrate 1
JNK	: c-Jun N-terminal kinase
Keap1	: Kelch-like erythroid cell-derived protein 1
MCP-1	: Monocyte chemotactic protein 1
MFN-1	: Mitofusin-1
MMP2	: Matrix metalloproteinase 9
mPTP	: Mitochondrial permeability transition pore
mtDNA	: Mitochondrial DNA

MTT	: 3-(4, 5-dimethylthiazol- 2-yl)-2,5-diphenyl tetrazolium bromide
NBT	: Nitro blue tetrazolium
NCA	: N acetylcysteine
NEFAs	: Non esterified fatty acids
NF-κB	: Nuclear factor kappa-light-chain-enhancer of activated B
NRF-1	: Nuclear respiratory factor 1
Nrf-2	: Nuclear factor erythroid 2-related factor 2
OPA1	: Optic atrophy 1
OXPHOS	: Oxidative phosphorylation
PBS	: Phosphate buffered saline
PDI	: Protein disulfide isomerase
PDK-1	: Pyruvate dehydrogenase kinase
PERK	: Protein kinase RNA-like endoplasmic reticulum kinase
PHD	: Prolyl hydroxylase domain
PMS	: Phenazine methosulfate
PO_2	: Oxygen partial pressure
PPAR	: Peroxisome prolifarator activated receptor
PVDF	: Polyvinylidene difluoride
qRT PCR	: quantitative real time polymerase chain reaction
RIPA buffer	: Radioimmunoprecipitation buffer
ROS	: Reactive oxygen species
SCAT	: Subcutaneous adipose tissue
SDS	: Sodium dodecyl sulphate
SOD	: Superoxide dismutase

T2DM	: Type 2 diabetes mellitus
TAGs	: Triacylglycerol
TBST	: Tris buffered saline-tween 20
TCA	: Tricarboxylic acid
Tfam	: Transcription factor A, mitochondrial
TLR4	: Toll-like receptor 4
TMB	: 3,3', 5,5'-Tetramethylbenzidine
TNF-α	: Tumor necrosis factor alpha
UCP1	: Uncoupling protein 1
UPR	: Unfolded protein response
VAT	: Visceral adipose tissue
VEGF	: Vascular endothelial growth factor
WAT	: White adipose tissue
WHO	: World Health Organization
XBP1	: X-box binding protein 1
$\Delta\psi m$	: Mitochondrial membrane potential

SYNOPSIS

Obesity and related complications have increased substantially over the past few decades. It is a prominent risk factor for insulin resistance, hypertension, type 2 diabetes and cancer. Obesity is characterised by excessive expansion of adipocyte size and adipose tissue mass. This enlargement of adipocyte size (140-180 μm) exceeds the normal oxygen diffusion distance (100 μm) and compromises the effective oxygen supply, which lead to local hypoxia. The response to low O_2 levels is accomplished through the activation of specific transcription factor, hypoxia inducible factor 1 (HIF-1). The HIF-1α subunit of this heterodimeric transcription factor is considered as the molecular oxygen sensor. When cellular O_2 levels are sufficient, this protein is continuously synthesized but is immediately targeted for proteasome degradation. The low O_2 level induces stabilization, nuclear translocation, and activation of this transcription factor. HIF-1α expression is directly linked to adiposity and is decreased following weight loss. So the hypoxia-signaling pathway is expected to provide a new target for the treatment of obesity-associated complications. Inhibition or downregulation of the HIF-1 pathway could be an effective target for the treatment of obesity related hypoxia.

In this study, we evaluated the effect of hypoxia on functions of 3T3-L1 adipocytes emphasising on oxidative stress, endoplasmic reticulum (ER) stress, mitochondrial dysfunctions, inflammation, and insulin resistance. We also evaluated the protective role of two phytochemicals, bilobalide and curcumin, on hypoxia induced alterations. Hypoxia was induced in differentiated 3T3-L1 adipocytes on 9th day by incubating in hypoxic chamber at an atmosphere of 1% O_2, 94% N_2, 5% CO_2, and at $37^{o}C$ for 24 hrs. The control cells were incubated in an atmosphere of 21% O_2 and 5% CO_2 at $37^{o}C$. The cells were treated with different concentrations of bilobalide (10 μM, 20 μM & 50 μM) and curcumin (5 μM, 10 μM & 20 μM) during hypoxic period (24hrs). Acriflavine (5 μM) is used as positive control which is an HIF-1α inhibitor.

The thesis is divided into 5 chapters including summary and conclusion. A general introduction dealing with obesity and its prevalence, obesity related metabolic complications, importance of adipose tissue in obesity, adipose tissue hypoxia, the effect of hypoxia on key functions of adipocytes, and the role of natural products in obesity related

complications, a brief note on the pharmacological properties of bilobalide and curcumin etc., along with aims and objectives of the study have been described in chapter 1.

The chapter 2 highlights how hypoxia affects the physiological functions of 3T3-L1 adipocytes, emphasizing on HIF-1α expression, lactate release, oxidative stress and ER stress and possible protection with bilobalide and curcumin. The results revealed that hypoxia significantly altered all the vital parameters of adipocyte biology. There was a significant increase in HIF-1α expression, lactate release, ROS production, lipid and protein oxidation, in hypoxia treated groups compared with normoxic group. In addition, a reduction in antioxidant enzymes status was observed in hypoxic group. The expression of Nrf2/HO-1 and ER stress markers (GRP78, ERO1-Lα, PDI, PERK, IRE-1α, ATF-6 & CHOP) were significantly upregulated in hypoxic groups compared to normoxia. Bilobalide and curcumin attenuated the expression of HIF-1α, the hypoxic marker and protected 3T3-L1 adipocytes from hypoxia induced oxidative stress and ER stress.

Chapter 3 depicts hypoxia induced mitochondrial dysfunctions in 3T3-L1 adipocytes and its protection by bilobalide and curcumin. Various parameters relevant to mitochondrial functions like superoxide production, aconitase activity, transmembrane potential, integrity of mitochondrial permeability transition pore, oxygen consumption rate and ATP content, proteins involved in oxidative phosphorylation, expression of genes involved in mitochondrial biogenesis and proteins involved in mitochondrial structural dynamics were analysed in all the normoxic and hypoxic groups. Hypoxia impaired all the vital parameters relevant to mitochondrial functions in differentiated 3T3-L1 cells. Bilobalide and curcumin protected 3T3-L1 adipocytes from adverse effects of hypoxia by enhancing mitochondrial biogenesis, mitochondrial functional performances and by controlling mitochondrial dynamics via downregulating HIF-1α expression.

Chapter 4 explains the crosstalk between hypoxia induced inflammation, and insulin resistance and, also secretion of proangiogenic factors in 3T3-L1 adipocytes and possible reversal with bilobalide and curcumin. Hypoxia significantly increased the release of TNF-α, IL-6, IL-10, MCP-1 and IFN-γ, leptin, and resistin, the adipokines that induce inflammation and insulin resistance in adipocytes. But the secretion of adiponectin, a beneficial antidiabetic adipokine was significantly reduced in hypoxia treated adipocytes. Hypoxia also showed an increased mRNA expression of TLR4, the receptors of free fatty acids. Enhanced TLR4 activation in combination with increased glycerol release activated

inflammatory pathways, NF-κB and JNK signaling in hypoxic groups. Activation of NF-κB and JNK signaling pathways by hypoxia and subsequent higher expression of cytokines impair insulin signaling cascade by mediating serine phosphorylation of IRS-1 and by downregulating the expression of IRS-2. However, we observed an increased basal glucose uptake in hypoxia, in response to increased GLUT1 expression. But there were no significant changes in expression of GLUT4 after 24hrs of hypoxia. Bilobalide and curcumin ameliorated hypoxia-induced inflammation in 3T3-L1 adipocytes and improved insulin signaling. Hypoxia also increased the release proangiogenic factors (MMP-2, MMP-9, VEGF, angiopoietin like protein 4) in 3T3-L1 adipocytes. Bilobalide and curcumin significantly reduced the expression of proangiogenic factors via reducing hypoxia and inflammation.

Chapter 5 describes the overall summary and conclusion of the study. Based on these results we presume that HIF-1α represent a viable therapeutic target for the treatment of obesity related hypoxia.

CHAPTER 1

INTRODUCTION

1.1 Obesity

1.1.1 Obesity as a global epidemic

There has been an exponential rise in the prevalence of overweight and obesity in recent years, which has reached epidemic proportions. In fact, the worldwide prevalence of obesity has almost doubled in the last 20 years and it is currently the fifth leading risk for global death (WHO, 2015). Obesity is an independent risk factor for a number of chronic diseases including hypertension, cardiovascular disease, and diabetes (Poirier and Eckel, 2002; Ye, 2013). Obesity also increases the risk of developing certain cancers such as breast and colon cancer, in addition to respiratory disorders such as sleep apnea (Pischon et al., 2008; Vgontzas et al., 1994). Economic growth, modernization, urbanization and globalization of food markets are the main contributors to the obesity epidemic. Therefore, the development of effective anti-obesity therapies represents a high priority area for the research-based pharmaceutical industry.

Most countries show progressive increases in the prevalence of overweight and obesity, including the USA, Europe, the Middle East and Asia. Obesity is less common in sub-Saharan Africa (except for South Africa) and is increasingly prevalent among urban populations in India and China (Williams and Fruhbeck, 2009). Worldwide, at least 3.4 million people die each year as a result of being obese, and an estimated 3.8% of global DALYs are caused by obesity. However, the phenomenon is not only restricted to industrialized societies, this increase is often faster in developing countries than in the developed world. A few developed countries such as the United Kingdom and Germany experienced a drop in the prevalence rate of obesity in the past decade, but the prevalence of obesity continues to rise in many other parts of the world, especially in the Asia Pacific region (Chan and Woo, 2010). More than 50% of obese individuals in the world live in ten countries (listed in order of number of obese individuals): USA, China, India, Russia, Brazil, Mexico, Egypt, Germany, Pakistan, and Indonesia. The USA accounted for 13% of obese people worldwide in 2013, with China and India jointly accounting for 15% (Ng et al., 2014). Childhood obesity prevalence also remains very high in developed countries. It is reported that about 10% of school children aged between 5 to 17 years around the globe

are overweight out of which 70% grow up to become obese adults. Obesity adversely affects both physical and psychological health of the child (Li et al., 2004; Siddiqui and Bose, 2012).

1.1.2 Definition for overweight and obesity

Overweight and obesity are defined as abnormal or excessive fat accumulation that may impair health. Body mass index (BMI) is a simple index of weight-for-height that is commonly used to classify overweight and obesity in adults. It is defined as a person's weight in kilograms divided by the square of his height in meters.

$$BMI = (Weight\ in\ kg)/(height\ in\ m)^2$$

The WHO definition is:

- a BMI greater than or equal to 25 is overweight
- a BMI greater than or equal to 30 is obesity.

BMI provides the most useful population-level measure of overweight and obesity as it is the same for both sexes and for all ages of adults. The BMI classes are detailed in Table 1.1.

Table 1.1 Classification of overweight and obesity in adults according to BMI

Classification BMI	kg/m^2	Risk of co-morbidities
Underweight	<18.5	Low
Normal range	18.5 – 24.9	Average
Overweight	25 -29.9	Increased
Obese class I	30 -34.9	Moderate
Obese class II	35 -39.9	Severe
Obese class III	≥ 40	Very severe

WHO, 2015.

1.1.3 Possible causes of the obesity epidemic

Obesity results from the failure of the homeostatic mechanisms that normally regulate energy intake and expenditure. The etiology of obesity is multifactorial. It involves complex interactions among the genetic background, hormones and different social and environmental factors, such as sedentary lifestyle and unhealthy dietary habit (Chan and Woo, 2010; Table 1.3).

Table 1.2 Causes of obesity

'Common', 'idiopathic' or 'lifestyle-related'
  ➢ Genetic susceptibility (polygenic)
  ➢ Obesogenic environment
    (overconsumption of energy and/or decreased
    expenditure)
	>95% of cases

Secondary causes
  ➢ Drugs
    (e.g. corticosteroids, antipsychotics, antiepileptics)
  ➢ Endocrine disorders
    (e.g. Cushing syndrome, hypothalamic damage)
  ➢ Specific genetic syndromes
    (e.g. Prader-Willi syndrome)
  ➢ Mutations affecting energy control mechanisms
    (e.g. leptin mutations)
	<5% of cases

Williams and Frühbeck, 2009.

1.1.4 Metabolic complications of obesity

Obesity is associated with a large number of diseases and metabolic abnormalities, many of which have high risk of morbidity and mortality (Fig. 1.1). This include hypertension, type 2 diabetes mellitus, dyslipidemia, gall bladder disease, osteoarthritis, coronary heart disease, stroke, obstructive sleep apnea, other respiratory problems and various malignancies (Pi-Sunyer, 2002).
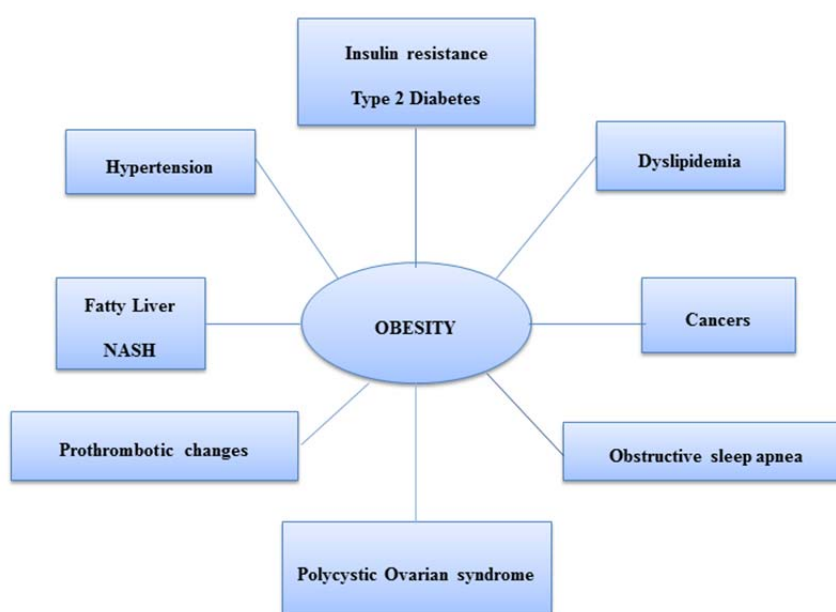
Fig. 1.1 Metabolic syndrome and some other disorders associated with obesity

1.2 Importance of adipose tissue in obesity

The classical perception of adipose tissue as a lipid storage depot has now been replaced by the notion that adipose tissue is an active endocrine organ playing a central role in lipid and glucose metabolism and produces a large number of hormones and cytokines. White adipose tissue (WAT) has now moved centre stage in energy balance and obesity research.

Adipose tissue comprises a variety of cell types, including endothelial cells, blood cells, fibroblasts, pericytes, preadipocytes, macrophages, and other immune cells. However, the predominant cells present in adipose tissue are mature adipocytes (Géloën et al., 1989). The adipocytes are broadly classified into three main types: white, brown, or beige (brite). The important function of white adipocytes is to store energy in the form of triglyceride, provide a long-term fuel reserve for the animal. The brown adipocytes dissipate energy in a heat-producing process called thermogenesis and practically absent in adult humans, but are found in foetuses and new-born infants (Fonseca-Alaniz et al., 2007). It generates heat via the mitochondrial uncoupling protein UCP1 (Stephens, 2012). Beige cells resemble white fat cells in having extremely low basal expression of UCP1, but, like classical brown fat, they respond to cyclic AMP stimulation with high UCP1 expression and respiration rates (Wu et al., 2012; Stephens, 2012).

There are differences between adipose tissue, subcutaneous adipose tissue (SCAT) present in subcutaneous areas and visceral adipose tissue (VAT) present in the abdominal cavity. VAT adipocytes are more metabolically active, more sensitive to lipolysis and more insulin-resistant than SCAT adipocytes. VAT has a greater capacity to generate free fatty acids and to uptake glucose than SCAT and is more sensitive to adrenergic stimulation, while SCAT is more avid in absorption of circulating free fatty acids and triglycerides. VAT carries a greater prediction of mortality than SCAT (Ibrahim, 2010).

1.2.1 Physiological role of white adipocytes

The primary functions of WAT are to insulate and cushion the body and store excess energy. In the adipocytes, energy is stored in the form of triacylglycerols (TAGs), composed of three fatty acids esterified to one molecule of glycerol. After an overnight fast or during prolonged exercise, when the body needs energy, TAGs can be hydrolysed into

non-esterified fatty acids (NEFAs) and released into the circulation. In the blood, NEFAs are bound to albumin and transported to target tissues, including skeletal muscle and liver, where they are used as energy substrates (Rosen and Spiegelman, 2006).

The discovery of leptin production in 1994 by adipocytes marked the first indication that adipose tissue also functions as an endocrine organ. Further studies revealed that adipocytes secrete a large number of cytokines known as adipokines. These adipokines can act on the adipose tissue itself in an auto- and/or paracrine fashion or be released into the circulation to regulate other organ's metabolism (Guilherme et al., 2008). These adipokines are involved in glucose metabolism (e.g. adiponectin, resistin), lipid metabolism (e.g. cholesteryl ester transfer protein), inflammation (e.g. TNF-α, IL-6, IL-10), feeding behaviour (leptin) and so on (Fig. 1.2).
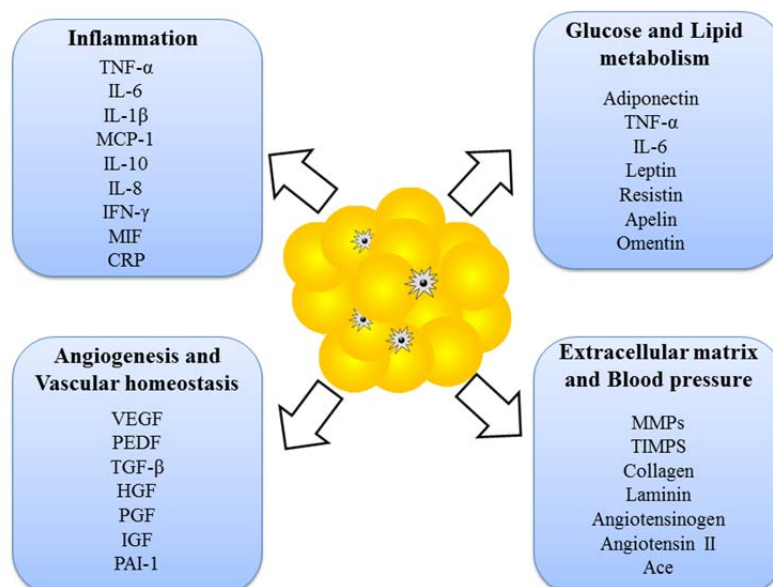
Fig. 1.2 Overview of adipokines released by adipose tissue and their role in adipocyte biology

1.3 Adipose tissue hypoxia (ATH)

Obesity is characterised by excessive enlargement of adipose tissue to store energy in the form of triglyceride. Hyperplasia (cell number increase) and hypertrophy (cell size increase) are two possible growth mechanisms of adipose tissue (Jo et al., 2009). This enlargement of adipocyte size (140-180 µM) exceeds the normal oxygen diffusion distance (100 µm) and compromises the effective oxygen supply which leads to localized hypoxia (Trayhurn and Wood, 2004). The role of hypoxia in chronic

inflammation in adipose tissue was first proposed in a review article in 2004 (Trayhurn and Wood, 2004). The adipose tissue hypoxia is known in genetic and diet induced obese mice as well as in obese individuals (Ye et al., 2007; Hosogai et al., 2007). *In vitro* studies also demonstrate the role of hypoxia in adipocyte dysfunctions such as inflammation, insulin resistance, cytokine secretion, and so forth (Wang et al., 2007).

Table.1.3 Oxygen level in WAT and other tissues

Tissue	PO_2, mmHg
Inspired air (at sea level)	160
Alveolar blood from lungs	104
General tissue oxygenation	40-50
Brain	4-8
Retina	2-25
Tumours	1-10
White adipose tissue, lean mice	47.9
White adipose tissue, obese mice	15.2
White adipose tissue, humans (I)	lean 55.4/obese 44.7
White adipose tissue, humans (II)	lean 46.8/obese 67.4

Trayhurn, 2013.

Adipocytes have only a limited capacity for hypertrophy; one reason for this is considered the diffusion limit of oxygen, which is at most 100 μm. This limits adequate oxygen supply in adipocytes, resulting in decreased oxygen tension. A PO_2 of 48 mmHg was recorded in the white fat of lean mice, a level that is similar to the general level of tissue oxygenation (Table 1.3). But, for obese mice, the PO_2 was three fold lower at 15.2 mmHg (Ye, 2009). Cell culture and other *in vitro* studies on the molecular and cellular responses of adipocytes to hypoxia have usually employed either 1% or 2% O_2, with 1% being the most widely used O_2 concentration, 1% O_2 is equivalent to a PO_2 7.6 mmHg, which is close to the level observed in WAT of very obese mice (ob/ob) (Trayhurn, 2013). The reference point almost always employed is the 21% O_2.

1.3.1 Possible causes of adipose tissue hypoxia

Ye (2009), proposes the reasons for adipose tissue hypoxia in obesity. One possibility may be related to the reduction in adipose tissue blood flow that is seen in both obese humans and animals. Reductions in capillary density may also contribute to adipose tissue hypoxia. Another possible cause of adipose tissue hypoxia may be the increase in adipocyte size that is seen with obesity. The diffusion distance of oxygen is 100-120 μm at most. In the obese state, adipocyte size increases up to 140-180 μm. Therefore, this increased size may block diffusion with oxygen not being able to reach the cells outside the 120 μm range, causing hypoxia.

1.3.2 Demonstration of hypoxia in adipose tissue in obesity

The adipose tissue hypoxia in obese groups can be confirmed by different methods. The first is the direct measurement of the interstitial partial pressure of oxygen via the insertion of an optical oxygen probe. The second approach involves detection via a chemical hypoxic probe, pimonidazole hydrochloride, which reacts with proteins in a low-oxygen environment leading to the generation of new protein adducts. The probe can then be stained for and measured via western blot or enzyme-linked immunosorbent assay (ELISA). In the third technique, a group of widely accepted hypoxia-responsive genes are used as markers of hypoxia. These genes include hypoxia inducible factor-1α (HIF-1α), vascular endothelial growth factor (VEGF), glucose transporter 1 (GLUT1), heme oxygenase 1 (HO-1), and pyruvate dehydrogenase kinase-1 (PDK1). Of these, HIF-1α is the transcription factor that controls the expression of the other four genes in response to hypoxia. The fourth technique is a lactate assay in the adipose tissue, with lactate being used as an indirect indicator of hypoxia (Ye, 2009).

1.3.3 Hypoxia signaling pathway

The transcription factor, HIF-1 is a key regulator that facilitates adaptation and survival of cells and organism from normoxia (21% O_2) to hypoxia (1% O_2) (Wang et al., 1995). The HIF-1 transcription factor was first identified based on its ability to activate the erythropoetin gene in response to hypoxia (Semenza et al., 1991; Wang and Semenza, 1993). HIF-1 is considered as a master signal mediator of hypoxia. It consists of an oxygen sensitive α subunit (HIF1-α) and a constitutively expressed β subunit (ARNT or HIF-1β). HIF-1 function is primarily regulated by HIF-1α protein stability. Under normoxic

conditions, oxygen can mediate the hydroxylation at proline residues of HIF-1α in a Fe2+ and α-ketoglutarate-dependent manner by a family of prolyl hydroxylases (PHDs). Following hydroxylation, HIF-1α is ubiquitinated by the E3 ubiquitin ligase, von Hippel-Lindau tumour suppressor (VHL), and degraded via the proteasome pathway. Under hypoxia, PHDs are inactive due to lack of substrate, and HIF-1α is no longer subjected to hydroxylation and degradation, and can then bind to HIF-1β, and activate transcription of HIF target genes (Fig. 1.3) (Brahimi-Horn et al., 2005). HIF target genes like Glut 1, Hemox, PDK1, NF-κB and VEGF, facilitate cell survival in a low-oxygen environment, by promoting glycolytic metabolism, angiogenesis, or maintenance of redox status (Ye, 2009). But its expression in adipose tissue may also be involved in some of the inflammatory and metabolic complications seen in the obese state (Trayhurn and Wood, 2004; Trayhurn et al., 2008a, b; Wang et al., 2007). HIF-1α expression is directly linked to adiposity and is decreased following weight loss. Therefore inhibition or downregulation of the HIF-1 pathway could be an effective target for the treatment of obesity related hypoxia.
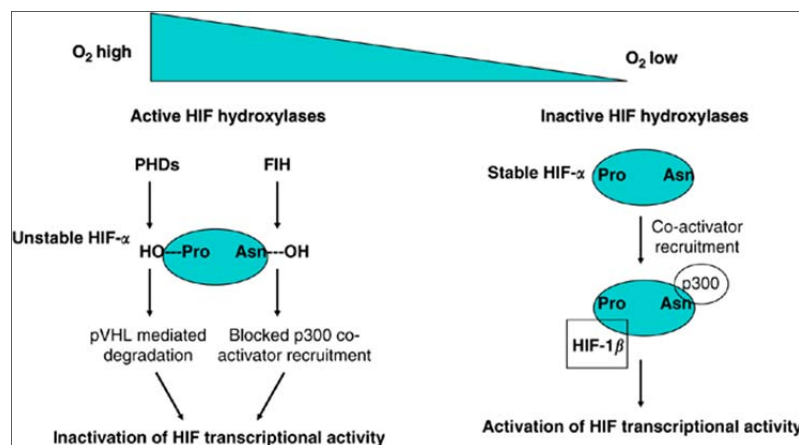
Fig. 1.3 Diagrammatic view of the molecular signaling response to hypoxia through the hypoxia-inducible factor (HIF) system: In the presence of oxygen, PHDs bind to HIF-1α and catalyse the Fe (II)-dependent hydroxylation of specific proline residues. Once hydroxylated, HIF-1α binds rapidly to the VHL tumour-suppressor protein (an E3 Ligase), which results in its polyubiquitylation and proteasome-mediated degradation. An extra oxygen-dependent hydroxylation event takes place at asparagine residue, mediated by FIH and this modification prevents the association between HIF-1α and p300/CBP. In the presence of low oxygen, HIF-1α is stabilized and can translocate to the nucleus. HIF-1α dimerizes with HIF-1β and associates with co-activator proteins p300/CBP to transactivate target genes containing hypoxia responsive elements (Trayhurn et al., 2008b).

1.4 Effects of hypoxia on key functions of white adipocytes

Hypoxia has pervasive effects on the function of adipocytes and appears to be a key factor in adipose tissue dysfunctions in obesity (Fig. 1.4). It is considered as an important cause for the inflammatory response in adipose tissue in the obese state. Other factors which induce inflammation include ER stress, free fatty acid and oxidative stress, all of these can be initiated by hypoxia (Trayhurn et al., 2008a). Adipose tissue hypoxia also impairs mitochondrial function and insulin signaling in adipocytes (Zhang et al., 2010; Jang et al., 2013; Halberg et al., 2009).
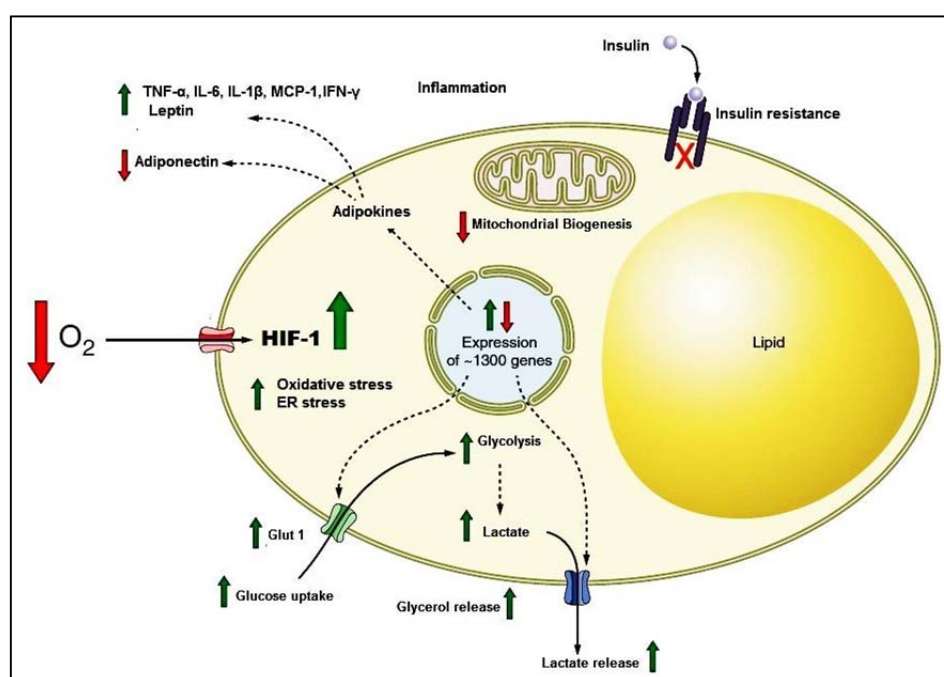
Fig. 1.4 Schematic representation of the effect of hypoxia on key functions of adipocytes: The effect of hypoxia on oxidative stress, ER stress, mitochondrial functions, adipokines release, glucose uptake, and insulin signaling is shown (Trayhurn, 2013).

1.4.1 Adipose tissue hypoxia and oxidative stress

Reactive oxygen species (ROS) are byproduct of the normal metabolism of oxygen and have important roles in cell signaling and homeostasis. An imbalance between ROS production and the cellular antioxidant defence system leads to oxidative stress (D Marchi et al., 2013). It has been reported that obesity may induce systemic oxidative stress. Biomarkers of oxidative damage are higher in individuals with obesity and correlate directly with BMI and the percentage of body fat (Pihl et al., 2006). Adipose tissue hypoxia in obesity is one of the reasons for oxidative stress. Reactive oxygen species

(ROS) are derived from many sources including mitochondria, xanthine oxidase, uncoupled nitric oxide synthases and NADPH oxidase (Mueller et al., 2005). In hypoxia, mitochondria act as major source of ROS production. Under hypoxic conditions, mitochondria participate in a ROS burst generated at complex III of the electron transport chain (Liu et al., 2002). Mitochondria function as O_2 sensors and signal hypoxia by releasing ROS to the cytosol. The resulting oxidant signal then mediates an inhibition of PHDs, leading to HIF1-α stabilization (Guzy et al., 2015).

Biomarkers of oxidative stress are defined as molecules that are modified by interactions with ROS and enzymes of the antioxidant system that change in response to increased redox stress. DNA, proteins, lipids including phospholipids and carbohydrates can be modified by excessive ROS *in vivo.* Of these modifications, some are known to have direct effects on function of the molecule (e.g. inhibit enzyme function), but others merely reflect the degree of oxidative stress in the local environment. Lipid peroxidation, oxidative protein modifications, and oxidized low-density lipoprotein and oxidized phospholipids are major biological markers of oxidative stress (Ho et al., 2013).

The activity of antioxidant enzymes like superoxide dismutase (SOD), catalase (CAT) and glutathione peroxidase (GPx) represent endogenous antioxidant system of the cells. Of these, SOD decomposes superoxide radicals and produce H_2O_2. H_2O_2 is subsequently removed to water by CAT in the peroxisomes, or by GPx oxidizing GSH in the cytosol (Hermes-Lima and Zenteno-Savín, 2002). The activities of these enzymes are inversely associated with oxidative stress.

ROS levels also influence the expression of key genes involved in regulating cellular and systemic oxidative stress. A prime example is Nuclear factor (erythroid-derived 2)-like 2 (Nrf-2), a transcription factor that is upregulated in response to oxidative stress and drives the increased expression of numerous cellular antioxidant enzymes. Heme oxygenase-1 (HO-1) is another example of stress-inducible protein. HO-1 gene expression is mainly regulated by the Nrf2-antioxidant response element (ARE) pathway, and induction of this enzyme protects cells against oxidative stress-induced cell death and tissue injury (Singh et al., 2010).

1.4.1.1 The kelch-like ECH-associated protein 1 (Keap1)/Nrf2 pathway

The Nrf2 is a prime transcriptional activator that plays a central role in inducible expression of many cytoprotective genes in response to oxidative and electrophilic stresses. Target genes of Nrf2 are involved in the glutathione synthesis, elimination of reactive oxygen species (ROS), xenobiotic metabolism and drug transport (Kobayashi et al., 2004; Kobayashi and Yamamoto, 2005). Keap1 is essential for the regulation of activity of Nrf2. Under normal conditions, Nrf2 is constantly degraded via the ubiquitin–proteasome pathway in a Keap1-dependent manner (Itoh et al., 1997; Motohashi and Yamamoto, 2004). In the presence of electrophiles or ROS, Nrf2 degradation ceases, stabilized Nrf2 accumulates in nuclei, heterodimerizes with small Maf proteins and activates target genes for cytoprotection through antioxidant response element (ARE) ∕ electrophile response element (Fig. 1.5; Itoh et al., 2004).
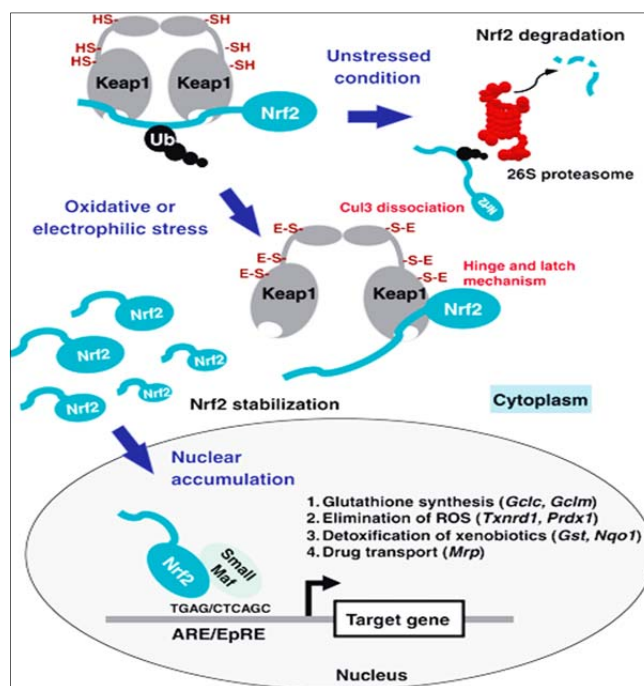
Fig. 1.5 Nrf2-antioxidant response element signaling pathway: Under unstressed conditions, Nrf2 is constantly degraded via the ubiquitin–proteasome pathway in a Keap1-dependent manner. When oxidative or electrophilic stress inactivates Keap1, Nrf2 is stabilized and de novo synthesized Nrf2 translocates into nuclei. Nrf2 heterodimerizes with small Maf proteins and activates target genes for cytoprotection through antioxidant ∕ electrophile response element (ARE∕ EpRE) (Taguchi et al., 2011).

Therefore, understanding the mechanism that regulates ROS formation is important to protect adipocytes from hypoxic injury. Hypoxia induces ROS production in

almost all cell types. Previous studies revealed that hypoxia significantly increased oxidative stress in adipocytes and treatment with antioxidants N-acetyl cysteine (NCA) and CAT significantly abolished hypoxia induced ROS production (Regazzetti et al., 2009).

1.4.2 Adipose tissue hypoxia and endoplasmic reticulum stress

The endoplasmic reticulum (ER) is a central organelle of each eukaryotic cell where, protein folding and secretion, calcium homeostasis and lipid biosynthesis take place (Gething and Sambrook, 1992). It is also a site for posttranslational modifications (glycation, disulphide formations etc) of newly synthesised proteins. It is the organelle in which proteins are folded into their proper conformation and in which multi subunit proteins are assembled (Kaufman, 1999). The lumen of the ER contains molecular chaperones and folding enzymes including glucose regulated protein 78/ immunoglobulin heavy chain binding protein (Grp78/BiP), Grp94, protein disulfide isomerase (PDI), calnexin, and calreticulin. Only properly folded proteins are exported to the Golgi organelle, while incompletely folded proteins are retained in the ER to complete the folding process or are delivered to the cytosol to undergo endoplasmic reticulum–associated degradation. Under normal physiologic conditions, there is equilibrium between ER protein load and folding capacity. Perturbations in ER homeostasis is due to increased protein synthesis, accumulation of misfolded proteins, or alterations in the calcium or redox balance of the ER lead to a condition called ER stress (Ron and Walter, 2007).

To cope with this stress, cells have developed a protective mechanism called the unfolded protein response (UPR) or ER stress response (Fig 1.6). The initial objective of this response includes the attenuation of protein translation to lessen the protein processing load in the ER. There is also an upregulation of genes involved in ER protein folding including chaperones such as BiP/GRP78, enzymes mediating folding such as protein disulfide isomerase, ER structural components, and components of the ER-associated degradation pathway (ERAD) (Oslowski and Urano, 2011).

The ER stress response is initiated when the capacity of ER-resident chaperone proteins is exceeded by the load of misfolded proteins. BiP/GRP78, a transmembrane protein that spans the ER lumen, associates with the UPR sensors PKR-like ER kinase (PERK), inositol-requiring enzyme 1 (IRE1), and activating transcription factor 6 (ATF6) and represses their activity. The accumulation of misfolded proteins results in the

saturation of ER chaperones, including BiP/GRP78. The sequestering of BiP by misfolded proteins results in the loss of BiP-mediated repression of the UPR sensors resulting in their activation. Prolonged ER stress typically results in cell death by apoptosis (Lin et al., 2008).

1.4.2.1 GRP78/BiP

Molecular chaperones and among them Grp78/BiP plays an important role in the protein folding process. Grp78/BiP participates in the translocation of nascent polypeptide chains into the ER and also recognizes unfolded or misfolded proteins in the lumen of the ER. As an ER-resident protein Grp78/BiP contains a typical signal sequence at the NH2-terminus (to guide it into the ER) and a KDEL sequence at the C-terminus (to hold it in the ER). The ADP-bound form of Grp78/BiP has high affinity for other proteins while exchange of ADP for ATP releases the substrates and allows for further folding. Grp78/BiP cycles between monomeric and oligomeric states. Oligomeric Grp78/BiP forms a storage pool. Only monomeric Grp78/BiP associates with unfolded proteins. Accumulation of unfolded proteins in the ER lumen increases the monomeric Grp78/BiP pool (Gething, 1999).

1.4.2.2 Unfolded protein response

Three major transducers of the UPR have been identified: PERK, IRE1 and ATF-6. These factors transmit signals from the ER to the cytoplasm or nucleus, and activate three pathways: i) suppression of protein translation to avoid the generation of more unfolded proteins; ii) induction of genes encoding ER molecular chaperones to facilitate protein folding; and iii) activation of ER-associated degradation (ERAD) to reduce unfolded protein accumulation in the ER. If these strategies fail, the cells are unable to maintain ER homeostasis and undergo apoptosis (Kawasaki et al., 2012).

The first response to ER stress is attenuation of transient global translation. This is mediated by the PERK signaling pathway. PERK binds to the chaperone protein Grp78 under normal conditions. As unfolded proteins accumulate during ER stress, Grp78 dissociates, allowing PERK to autophosphorylate and dimerize. Once activated, it phosphorylates α-subunit of eukaryotic translational initiating factor 2 (eIF-2α), resulting in translational attenuation. Phosphorylated eIF-2α preferentially enhances translation of ATF4 transcription factor that induces expression of UPR target genes (Shi et al., 1998).

Activation of IRE1 by ER stress is typical of receptor kinase proteins, which homodimerize and transphosphorylate. Activation of IRE1 by dimerization and phosphorylation causes IRE1-mediated splicing of XBP1 mRNA. Translation of spliced XBP1 mRNA produces a transcription factor that upregulates UPR target genes (Calfon et al., 2002).

ATF6 activation involves an unusual mechanism called regulated intramembrane proteolysis. The protein translocates from the ER to the Golgi where it is proteolytically processed. In Golgi, the full length 90-kDa ATF6 is proteolytically processed to release a 50-kDa transcription factor that translocates to the nucleus and activates UPR target genes. Some target genes of the UPR pathway include genes encoding ER-resident chaperones and genes involved in ER stress induced apoptosis (Lai et al., 2007).
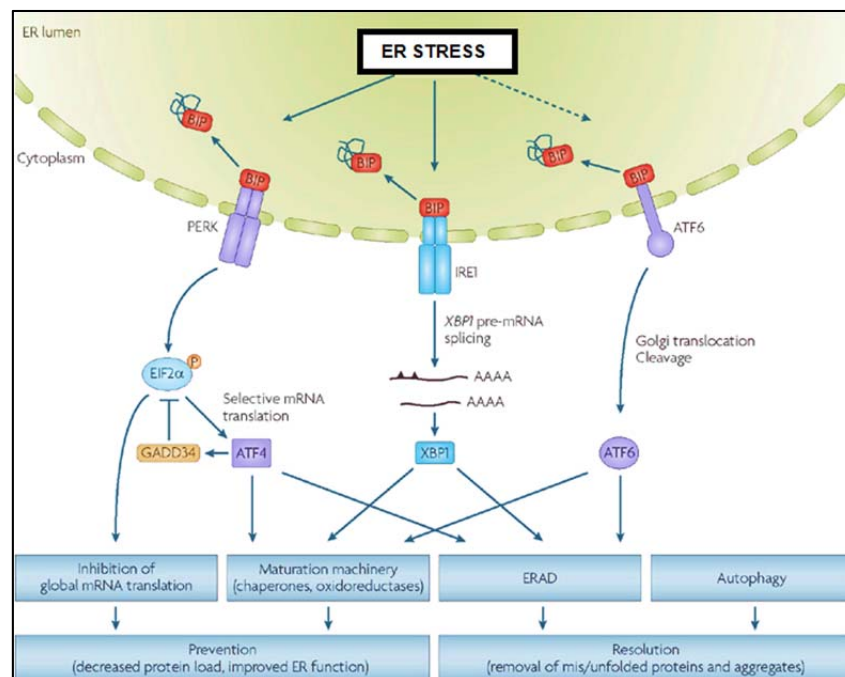
Fig. 1.6 ER stress pathway: Protein misfolding in the ER induces the UPR. There are 3 signaling arms of the UPR that are activated upon increased protein misfolding: activation of (1) IRE1 leads to spliced (s) (XBP-1) and (2) ATF6 which leads to transcriptional up-regulation of chaperone proteins. The third arm involves PERK, which oversees the attenuation of nascent protein translation via phosphorylation of eukaryotic initiation factor 2 alpha (eIF2α) (Wouters and Koritzinsky, 2008).

CHOP is the first identified protein that mediates ER stress-induced apoptosis. All three UPR signaling pathways are involved in inducing CHOP transcription, although the PERK pathway is essential. CHOP is also known as growth-arrest and DNA-damage-

inducible gene 153 (GADD153). It is induced by ER stress more than growth arrest or DNA damage. During prolonged ER stress, CHOP is one of the most highly upregulated genes, which downregulates the expression of the anti-apoptotic protein Bcl-2 and induces GADD34 and ERO1 and promote ER stress induced apoptosis (Wang et al., 1996).

Accumulating evidence suggests prolonged ER stress in the development and progression of many diseases, including neurodegeneration, atherosclerosis, type 2 diabetes, liver disease, and cancer. Recent study reported the up-regulation of ER stress markers such as BiP, phosphorylated PERK, and phosphorylated eIF2α in adipose tissue and the liver of ob/ob mice (Ozcan et al., 2004). However, the triggers that induce ER stress in obesity remained unclear. ER stress in obesity is thought to be induced by an augmented demand for protein synthesis under nutrient excess. Obesity related hypoxia is known to induce ER stress (Hosogai et al., 2007). So the better understandings of the molecular mechanism of ER stress response during obesity related hypoxia provide a potential strategy to treat obesity related complications.

1.4.3 Adipose tissue hypoxia and mitochondrial dysfunctions

Mitochondria play a central role in cellular bioenergetics. In mitochondria, the energy supplied by nutrients is converted to adenosine triphosphate (ATP) via tricarboxylic acid (TCA) cycle and oxidative phosphorylation (OXPHOS) process of the respiratory chain. In addition to supplying cellular energy, mitochondria are involved in several cellular stresses and human diseases (Lane, 2006). Mitochondria have an important role in the pathophysiology of obesity. The mitochondria of obese individuals are different from those of lean individuals. Alterations in mitochondrial morphology, impaired mitochondrial bioenergetics, increased mitochondrial lipid peroxides, decreased ATP content, and other mitochondrial dysfunctions increase the risks of developing metabolic complications associated with obesity (Grattagliano et al., 2012). Obesity is also accompanied by a decrease in the expression of adipose mitochondrial genes in ob/ob mice and impaired adipose mitochondria in db/db mice (Rong et al., 2007).

Mitochondria play a key role in oxygen homeostasis in adipocytes. HIF-1α is a major mediator of the hypoxia signal involved in mitochondrial dysfunction. It has been demonstrated that HIF-1α functions as a negative regulator of mitochondrial biogenesis and oxygen utilization. Therefore in adipose tissue hypoxia, mitochondria act as O_2

sensors, convey signals to HIF-1 directly or indirectly, which in turn triggers a cascade of events involving stabilization of HIF-1α, ER stress, inflammation and insulin resistance (Ali et al., 2012).

Mitochondria are considered as the main source of reactive oxygen species (ROS). Previous studies report increased ROS production in adipose tissue of obese mice, accompanied by augmented expression of NADPH oxidase and decreased expression of antioxidant enzymes (Furukawa et al., 2004). Hypoxia in obese adipose tissue is considered as a mediator of mitochondrial ROS production. Under normal oxygen tensions, cells catabolise glucose to pyruvate via glycolytic enzymes. Pyruvate is then taken up by the mitochondria for further catabolism through the TCA or Krebs cycle, which transfers electrons to the respiratory chain. Electron transport through this chain results in ATP production and terminates in the donation of electrons to oxygen. But in low oxygen tension, there is a paucity of oxygen as final electron acceptor; hypoxic cells are then forced to undergo anaerobic glycolysis. Hypoxic activation of HIF-1 promotes ATP production through increased anaerobic glycolysis. Increased ATP production, however, may not be sufficient for hypoxic adaptation, since hypoxia paradoxically causes oxidative stress from uncontrolled mitochondrial generation of reactive oxygen species (ROS). Under hypoxic conditions, perturbation in electron transport is associated with leakage of electrons from the respiratory chain, resulting in increased superoxide production that could be toxic to cells (Kim et al., 2006).

Increased ROS production adversely affects mitochondrial membrane potential ($\Delta\psi$m) and ATP synthesis. $\Delta\psi$m is an important parameter of mitochondrial function and has been used as an indicator of cell health. The $\Delta\psi$m is the electrochemical gradient built across the inner membrane by the respiratory chain complexes, constitutes a distinguishing feature of mitochondria. In normal physiological cell functioning, maintenance of $\Delta\psi$m, is essential for ATP synthesis. $\Delta\psi$m, is highly negative, approximately -180 mV, due to the chemiosmotic gradient of protons across the inner mitochondrial membrane. This energy is used to synthesise ATP by the respiratory chain. $\Delta\psi$m also provides the driving force for Ca^{2+} uptake into mitochondria by the Ca^{2+} uniporter, and it is now generally accepted that it is this Ca^{2+} signal in the mitochondria which stimulates ATP production in response to increased demand of energy by the cell (Andrew et al., 2004). Many studies support the dissipation of $\Delta\psi$m in obese subjects. Mitochondria isolated from the liver of high-fat fed

rats exhibit impaired mitochondrial membrane potential, oxygen consumption and cellular ATP levels (Teodoro et al., 2013).

The mitochondrial permeability transition pore (mPTP) is a Ca^{2+} dependent, non-selective pore located on the inner mitochondrial membrane. It facilitates the exchange of molecules between the mitochondrial matrix and cytoplasm, and opening of the mPTP occurs in response to physiological stressors. It opens in response to elevated matrix Ca^{2+} concentrations, increasing the permeability of the mitochondrial membrane to molecules less than 1500 Da in weight, and resulting in cell death (Zoratti and Szabo, 1995). Under normal physiological conditions, mPTP is closed; if matrix $[Ca^{2+}]$ increases, the pore opens, causing a mitochondrial permeability transition (mPTP) and resulting in mitochondrial swelling. Conditions associated with obesity such as oxidative stress, mitochondrial membrane potential dissipation and depletion of adenine nucleotides also influence mPTP opening. Recent study reports opening of the mitochondrial permeability transition pore links mitochondrial dysfunction to insulin resistance in skeletal muscle of HFD mice (Taddeo et al., 2014).

Mitochondrial biogenesis can be defined as growth and division of pre-existing mitochondria. Mitochondrial biogenesis involves the coordinated action of both nuclear and mitochondrial encoded genomes. PGC-1α is a central regulator of mitochondrial biogenesis. PGC-1α acts as co-transcriptional regulation factor that induces mitochondrial biogenesis by activating different transcription factors, including NRF-1 and NRF-2, which promote the expression of Tfam. NRF-1 and NRF-2 are important contributors to the sequence of events leading to the increase in transcription of key mitochondrial enzymes, and they have been shown to interact with Tfam, which drives transcription and replication of mtDNA (Virbasius and Scarpulla, 1994). Decreased expression of markers of mitochondrial biogenesis and metabolism were found in overweight and obese insulin-resistant subjects (Heilbronn et al., 2007). Studies also reported that transgenic as well as high fat diet obese mice had less mitochondrial density compared to lean control (Zhang et al., 2010).
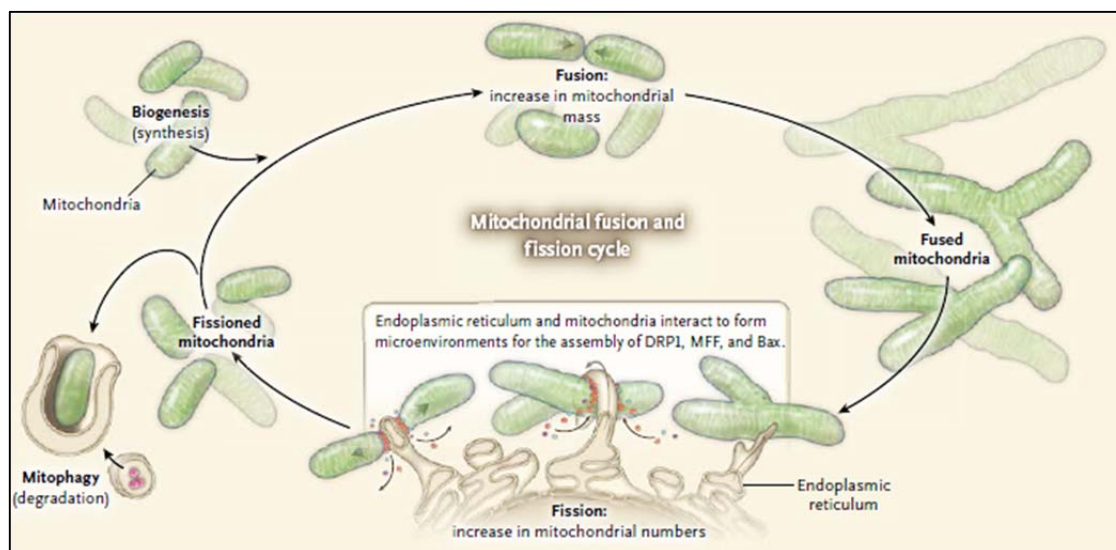
Fig. 1.7 Mitochondrial fusion and fission cycle: Mitochondrial biogenesis increases mitochondrial numbers and replaces damaged mitochondria. Fusion dilutes damage that accumulates in the mitochondria, including mitochondrial DNA mutations and oxidized proteins. When mitochondrial damage exceeds a critical level, fission supports mitochondrial quality control by dividing a mitochondrion into a larger, polarized healthy portion (which can reintegrate with the network) and a smaller depolarized, abnormal portion. The small depolarised abnormal portion packaged into autophagic vacuoles that are transported to lysosomes for elimination by mitophagy (Archer, 2013).

Mitochondria are dynamic organelles that continually undergo fusion and fission (Fig. 1.7). These opposing processes work in concert to maintain the shape, size, and number of mitochondria, and their physiological function. Dysregulation of mitochondrial dynamics alters mitochondrial morphology, metabolism, and intracellular signaling, and it has been implicated in various human diseases, including T2DM and obesity (Chan, 2012; Bach et al., 2005). In mammals, three large GTPases are essential for mitochondrial fusion. The mitofusins Mfn1 and Mfn2 are transmembrane GTPases embedded in the mitochondrial outer membrane. OPA1 is a dynamin related GTPase associated with the mitochondrial inner membrane or intermembrane space. Mitochondrial fusion is a multistep process. Outer membrane fusion depends on the mitofusins Mfn1 and Mfn2. Inner membrane fusion depends on the OPA1. Depletion of any of these three GTPases results in severely reduced levels of mitochondrial fusion. Studies have identified two classes of molecules that are necessary for the fission of mitochondria. The central player appears to be Drp1, a dynamin-related protein. Drp1 assembles on mitochondrial tubules and is thought to mediate constriction and scission. Much of Drp1 resides in the cytosol, and therefore a second class of proteins on the mitochondrial surface is necessary to

efficiently recruit Drp1 for fission. This second class potentially includes Fis1, Mff, MiD49, and MiD51 (Archer, 2013; Lee et al., 2004). Mitochondrial fusion and fission result in content exchange between mitochondria. These exchange events keep the mitochondrial population homogeneous and functional. Mitochondrial dynamics is involved in multiple mitochondrial functions, including mtDNA stability, respiratory function, apoptosis, response to cellular stress, and mitochondrial degradation (Chan, 2012).

1.4.4 Adipose tissue hypoxia and inflammation
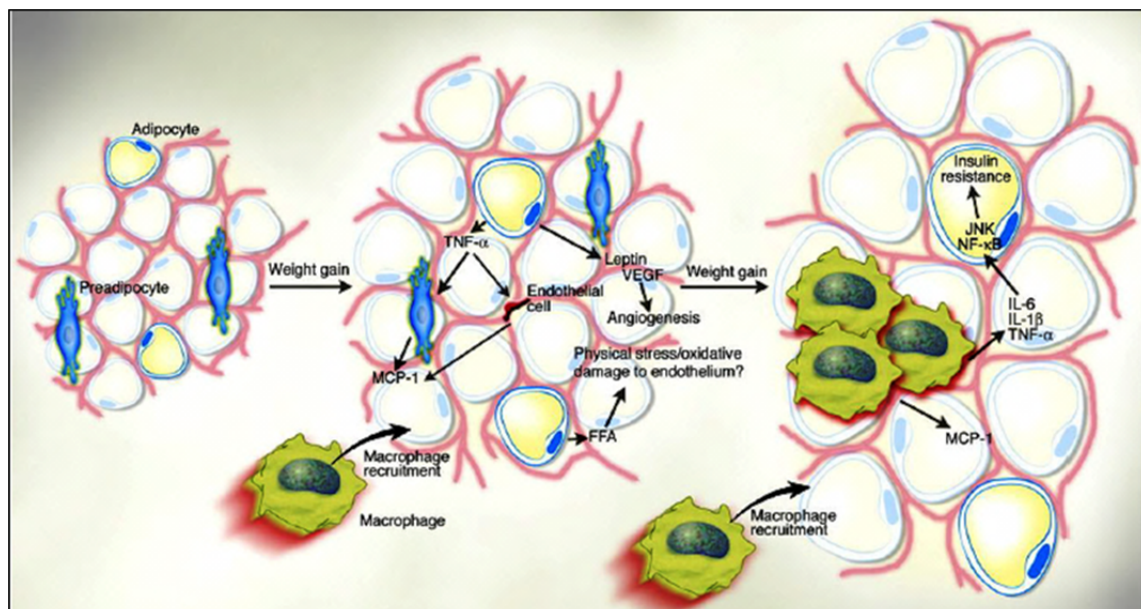
Fig. 1.8 Obesity-induced inflammatory changes in adipose tissue: Obese adipose tissue is characterized by inflammation and progressive infiltration by macrophages as obesity develops (Wellen and Hotamisligil, 2003).

In obesity research, the link between chronic inflammation and fat accumulation is well established (Fig. 1.8). The initial observation of TNF-α elevation in adipose tissue of obese mice provides the first evidence for the chronic inflammation (Hotamisligil et al., 1993). Thereafter, the concept of obesity induced inflammation was confirmed by abundant literature identifying increases in many other inflammatory cytokines, such as plasma C-reactive protein (CRP), interleukin 6 (IL-6), plasminogen activator inhibitor-1 (PAI-1), in models of obesity. Activation of inflammatory kinases such as NF-κB and JNK

provides additional evidence for activation of intracellular inflammatory pathways in obesity (Yuan et al., 2001; Hirosumi et al., 2002).

Adipose tissue is a major source of chronic inflammation in obesity. In adipose tissue, adipocytes and adipose tissue macrophages are the major cell types responsible for the production of inflammatory cytokines. Macrophages and adipocytes are activated during the process of adipose tissue expansion. Recent studies suggest that the adipose tissue expansion induces a local hypoxia. The hypoxia response serves as a common root for all of the stress responses in adipose tissue including inflammatory stress (Ye, 2009; Hosogai et al., 2007). Hypoxia directly promotes the chronic inflammation through activation of transcription factors (NF-κB and HIF-1) in adipocytes and macrophages (Ye et al., 2007). The representative adipokines include TNF-α, IL-6, MCP-1, IL-1β, leptin, adiponectin and resistin.

TNF-α: It is a pro-inflammatory cytokine secreted predominantly by monocytes macrophage, and adipocytes. It has wide ranging biological effects on lipid metabolism, coagulation and endothelial function. In humans, TNF-α level are higher in plasma and adipose tissue of subjects with obesity, and circulating levels reduce with weight loss (Kern et al., 1995; Ziccardi et al., 2002). Previous study reports the interplay between obesity, inflammation and insulin resistance and showed that TNF-α expression was elevated in adipose tissue isolated from different obese rodent models. Hotamisligil et al., also showed that immuno-neutralization of TNF-α in obese rat ameliorated insulin resistance (Hotamisligil et al., 1993). Corresponding *in vitro* experiments demonstrated that by activating IKKβ, TNF-α stimulation leads to serine phosphorylation of IRS-1 which attenuates its ability to transduce insulin mediated cellular events (Hotamisligil et al., 1996). Mice genetically deficient in TNF-α or the TNF-α receptor 1 gene (Tnfr1) do not develop insulin resistance caused by high fat feeding or obesity (Uysal et al., 1997). TNF-α treatment of cultured 3T3-L1 adipocytes leads to reduced expression of the insulin receptor, IRS-1 and Glut4 genes, as well as a decrease in insulin stimulated glucose uptake (de Luca and Olefsky, 2008).

IL-6: IL-6 is an inflammatory cytokine produced and secreted from WAT and act as pathogenic mediator of insulin resistance. IL-6 levels are positively correlated with body mass and plasma free fatty acid concentrations. It has been demonstrated that IL-6 inhibits

the insulin signaling pathway by upregulating SOCS3 expression, which in turn impair insulin-induced insulin receptor and IRS-1 phosphorylation in adipocytes (Senn et al., 2002; Senn et al., 2003). IL-6 can promote fatty acid oxidation and glucose uptake in skeletal muscle. IL-6 also modulates insulin resistance through several distinct mechanisms, including c-Jun N-terminal kinase 1 (JNK1) mediated serine phosphorylation of IRS-1, and IκB kinase mediated NF-κB activation (Kelly et al., 2004).

MCP-1: MCP-1 (also called CCL2) is a chemoattractive protein that recruits immune cells to sites of inflammation. The adipose tissue expression of MCP-1 increases in proportion to adiposity and decreases following treatment with TZDs and following bariatric surgery. MCP-1 gene expression in adipose tissue is increased in diet-induced insulin resistance and in ob/ob and db/db mice. Two independent studies convincingly showed that the adipocyte-specific overexpression of MCP-1 in mice was sufficient to increase macrophage recruitment to adipose tissue and cause systemic insulin resistance (Kamei et al., 2006; Kanda et al., 2006) notably, MCP-1 expression in adipocytes resulted in hepatic steatosis and insulin resistance in liver and muscle as well as in fat cells. Concordantly, mice deficient in CCR2, a major cell surface receptor for MCP-1, have fewer monocytes recruited to fat cells and are protected against the development of obesity-induced insulin resistance (Weisberg et al., 2006).

IL-1: IL-1α and IL-1β are proinflammatory cytokines that binds to IL-1 receptors and shows similar functions. Il1α−/− mice have lower fasting glucose and insulin levels and improved insulin sensitivity as compared with wild type controls (Matsuki et al., 2003). mRNA expression of IL-lβ was increased in the epididymal fat pads of insulin resistant HFD-fed mice and ob/ob mice compared with low-fat-fed mice and wild type mice, respectively (Lagathu et al., 2006). IL-1β together with IL-6 concentrations predicts risk for T2D in humans better than either cytokine alone (Shoelson et al., 2007).

Resistin: Resistin is an inflammatory cytokine produced in adipocytes and immune cells whose expression is suppressed by TZDs and up-regulated by proinflammatory cytokines. In rodents, circulating levels of resistin were increased in obesity (Rajala et al., 2004), and both gain and loss of function studies (Satoh et al., 2003; Kim et al., 2004) demonstrated a role for resistin in mediating hepatic or skeletal muscle insulin resistance. Like many other

proinflammatory cytokines, resistin stimulates intracellular signaling through NF-κB activation, which in turn promotes the synthesis of other proinflammatory cytokines, including TNF-α, IL-6, MCP-1, etc. Consistent with the feed forward, "positive feedback loop" nature of NF-κB-mediated inflammatory signaling, various proinflammatory stimuli also induce the expression of resistin. In addition to its potential roles in insulin resistance, resistin may play a role in the inflammation associated with the pathogenesis of CVD (Jamaluddin et al., 2012).

Adiponectin: Adiponectin is a 30-kDa secretory hormone produced predominantly by adipocytes, expression, and secretions are elevated during adipocyte differentiation (Carbone et al., 2012). There are three major isoforms of adiponectin; low molecular weight (LMW), formed from three adiponectin monomers, middle-molecular weight (MMW) which is an octomer, and high- molecular weight (HMW) consisting of 12 or more monomers (Magkos and Sidossis, 2007). HMW adiponectin is the most biologically active form and best reflective of the reduction in total adiponectin levels associated with obesity (Almeda-Valdes et al., 2010). Adiponectin can enhance FA oxidation and improve insulin sensitivity (Carbone et al., 2012); suppressing gluconeogenesis in the liver thus reducing circulating glucose levels, also increasing glucose uptake in the muscle by enhanced GLUT4 expression. In the liver, adiponectin stimulates glucose and FA oxidation through activation of the AMPK pathway and reduces lipogenesis by minimizing SREBP-1c expression (Utzschneider and Kahn, 2006).

Leptin: Leptin is the product of the ob gene. It is involved in the regulation of energy homeostasis and is almost exclusively expressed and produced by WAT and more particularly by differentiated mature adipocytes (Ahima and Flier, 2008). Circulating levels and adipose tissue mRNA expression of leptin are strongly associated with BMI and fat mass in obesity (Varela and Horvatha, 2012). Thus, leptin appears as a real marker of adipose tissue mass in lean humans where the subcutaneous fraction represents about 80 % of total fat. In animal models, expression of leptin is increased in conditions that are associated with release of pro-inflammatory cytokines such as TNF-α and IL-6 in monocytes and macrophages. Vice versa, TNF-α and IL-6 are capable of stimulating adipocyte leptin production. Leptin has also been reported to improve insulin sensitivity through activation of AMP-activated protein kinase (AMPK) (Minokoshi et al., 2012).

Moreover, the leptin-signaling pathway, activate suppressor of cytokine signaling (SOCS)-3, which inturn inhibit insulin signaling (Howard and Flier, 2006). Taken together, it is suggested that leptin has proinflammatory effects and is involved in the pathogenesis of insulin resistance. However, the underlying mechanism of leptin in the etiology of obesity-associated adipose tissue inflammation and insulin resistance needs to be further elucidated.

1.4.4.1 Role of free fatty acid stimulation of toll-like receptor 4 in inflammation

TLR4 belongs to the family of toll-like receptors that function as pattern recognition receptors that guard against microbial infections as part of the innate immune system. TLR4, in particular, is stimulated by lipopolysaccharide (LPS), an endotoxin released by gram-negative bacteria. TLR4 stimulation results in the activation of both Ikkβ/NF-κB and JNK/AP-1 signaling, culminating in the expression and secretion of pro-inflammatory cytokines/chemokines (Iwasaki and Medzhitov, 2004).

The role of TLR4 as a key component in fatty acid-induced inflammation was first identified in studies examining the ability of dietary fatty acids to activate the inflammatory response via TLR4 signaling in cultured macrophages. The link between TLR4 and fatty acid and obesity-induced insulin resistance was further assessed by Shi et al, (2006). This study found that FFA activate the NF-κB signaling pathway in primary macrophages from wild type mice but not in macrophages derived from TLR4 deficient (Tlr4−/−) mice. In addition, they demonstrated that saturated fatty acids are the most potent inducers of this inflammatory response. In *in vivo* studies, they found that obese mice have increased TLR4 expression in adipose tissue compared to lean controls. Previous studies also showed the role of TLR4 in the development of lipid and obesity-induced insulin resistance and suggest that TLR4 can act as a potential sensor of elevated tissue and/or serum FFA concentrations that are commonly associated with obesity (Shi et al., 2006; Zhu et al., 2010).

1.4.4.2 NF-κB and JNK pathway

The IKKβ/NF-κB pathway is a dominant inflammation signaling pathway. The pathway has been under active investigation in the obesity field after IKKβ was found to induce insulin resistance in obese mice (Yuan et al., 2001; Arkan et al., 2005). The serine kinase IKK has three major isoforms including IKKα (IKK1), IKKβ (IKK2) and IKKγ, in

which IKKβ is required for NF-kB activation. In obesity, IKKβ is activated by several intracellular signals, such as ROS, ER stress, DAG, and Ceramide. IKKβ is also activated by the extracellular stimuli including TNF-α, IL-1, fatty acids, and hypoxia (Ye and Keller, 2010). IKKβ induces NF-κB activation by phosphorylation of the Inhibitor Kappa B alpha (IkBα). In the classical pathway, NF-κB activation is mediated by IKKβ-induced phosphorylation, proteasome-mediated degradation of IkBα (Karin and Ben-Neriah, 2010). It induces transcription of inflammatory cytokines (TNF-α, IL-1β, IL-6, MCP-1, etc). In the alternative pathway, NF-κB is activated by hypoxia in the absence of IkBα degradation (Ye, 2009). This type of NF-κB activation in adipocytes and macrophages contributes to chronic inflammation in the adipose tissue of obese individuals.

The c-Jun NH$_2$-terminal kinase (JNK) belongs to a family of mitogen-activated kinases (MAPKs), together with extracellular regulated kinases (ERKs) and p38. The JNK subgroup of MAPKs is encoded by three loci; Jnk1 and Jnk2 are ubiquitously expressed, and Jnk3 is expressed primarily in heart, testis, and brain (Maeda, 2010). Stimuli that have been shown to activate JNK pathways during metabolic dysregulation include TNF-α, IL-1, TLR, or free fatty acids, intracellular stresses including ROS and ER stress, ceramides, and various PKC isoforms. Obesity-induced JNK activation promotes the phosphorylation of IRS-1 at serine sites that negatively regulate normal signaling through the insulin receptor/IRS-1 axis. By contrast, evidence has not been reported for obesity-induced effects on transcription factors such as AP-1 that are regulated by JNK (Ye and Keller, 2010).

1.4.4.3 Molecular pathways that link inflammation and insulin resistance

The NF-κB and JNK-MAPK pathways link obesity, inflammation, and insulin resistance. The NF-κB pathway is activated by inhibitor of NF-κB (IκB) kinase β (IKKβ), and the c-Jun NH2-terminal kinase (JNK) pathway. These pathways are activated by many of the same proinflammatory stimuli including cytokines such as TNF-α and IL-6 which in addition to being activators of NF-κB are also NF-κB-regulated products. Both pathways are also activated by pattern recognition receptors, such as the receptor for advanced glycation end products and the toll-like receptors, which are gatekeepers of the innate immune system. In addition to being activated by bacterial, viral, and fungal products, toll-like receptors can be activated by free fatty acids. Reactive oxygen species, endoplasmic

reticulum stress, hypoxia and ceramides are increased by adiposity, and all have also been shown to activate both JNK and NF-κB (Mc Ardle et al., 2013).

JNK1 and NF-κB contribute to insulin resistance and type 2 diabetes through multiple mechanisms. Serine/threonine phosphorylation of insulin receptor substrates 1 and 2 (IRS1&2) is believed to be an important mediator of insulin resistance because it results in uncoupling of insulin receptor activation from downstream signaling (Tanti et al., 1994). This hypothesis is supported by a study showing that mice expressing an IRS-1 variant in which the serine phosphorylation sites Ser-302, Ser-307, and Ser-612 were replaced by alanines (IRS-1 Ser3Ala), are protected from high-fat diet-induced insulin resistance (Morino et al., 2008). By contrast, mice expressing an IRS-1 variant with only Ser-307 mutated to alanine are more susceptible to developing insulin resistance when fed a high-fat diet (Copps et al., 2010). Therefore, the inhibitory action of IRS-1 serine/threonine phosphorylation on insulin signaling could be independent from Ser-307 phosphorylation. Another mechanism by which JNK1 and NF-κB promote insulin resistance is by induction of proinflammatory cytokines. Interestingly, NF-κB induced insulin resistance is nearly fully reversed with neutralizing antibodies against IL-6 (Cai et al., 2005). Jnk1$^{-/-}$ mice show decreased expression of proinflammatory cytokines in models of diet-induced insulin resistance (Tuncman et al., 2006), and a conditional deletion of Jnk1 in adipocytes decreases IL-6 serum levels and improves hepatic insulin sensitivity (Sabio et al., 2008).

1.5 Inflammation and angiogenesis

Angiogenesis corresponds to the formation of new vessels from the pre-existing vascular network. This phenomenon has critical role in physiological and pathophysiological remodelling processes (Carmeliet and Jain, 2000). Inflammation and hypoxia, the main angiogenesis regulators described in non-neoplasic tissues, may represent two possible candidates for angiogenesis regulation in growing adipose tissue. VEGF, leptin and MMP-2 and -9 are factors involved in the process of angiogenesis, it is suggested that hypoxic adipocytes may increase their secretion of angiogenic factors to stimulate the formation of new blood vessels. Hypoxia, in adipocytes, stimulates the HIF-1α pathway and enhances the expression of proangiogenic factors such as leptin, VEGF, MMP-2, and MMP-9. Lolmède et al. (2003) demonstrated rapid accumulation of HIF-1α protein and up regulation of the expression of leptin, VEGF, and MMP-2 and MMP-9 in

3T3-F442A adipocytes, exposed $CoCl_2$, the hypoxia-mimetic agents. Emerging evidence shows that modulators of angiogenesis affect the expansion and metabolism of fat mass by regulating the growth and remodelling of the adipose tissue vasculature. Pharmacological manipulation of adipose tissue neovascularization by angiogenic stimulators and inhibitors might therefore offer a novel therapeutic option for the treatment of obesity and related metabolic disorders (Cao, 2010).

1.6 Natural products and HIF-1α

Preventing and treating obesity have become a major public health priority. Even after several decades of intensive research activity, progress has been very limited. Reversing hypoxia, or attenuating the O_2-signaling pathways, through the HIFs or other regulatory factors, presents novel opportunities and targets providing adiposity is not itself enhanced. Natural compounds seem to be an alternative in an attempt to identify new inhibitors of the HIF-1 signaling pathway. During the past few years many studies tried to identify natural compounds able to interfere with or inhibit the HIF-1 activity. It is reported that dietary quinones, semiquinones, phenolics, vitamins, amino acids, isoprenoids, and vasoactive compounds can down-regulate the HIF-1 pathways. Unfortunately, many of these identified compounds are very toxic and cannot be used in human therapy (Manolescu et al., 2009). In present study we analysed the protective roles of two phytochemicals, bilobalide and curcumin against hypoxia induced dysfunctions.

1.6.1 Bilobalide

Bilobalide is a naturally occurring sesquiterpene trilactone from *Gingko biloba* (Fig. 1.9), the best known example of a living fossil (Singh et al., 2008). *Gingko biloba* extract (EGb 761) is a popular and standardised natural extract used worldwide for the treatment of numerous ailments. Bilobalide is one of the predominant components of this extract constituent that accounts for 2.9% of the standardized *Ginkgo biloba* extract EGb 761 (Yoshitake et al., 2010). As a single chemical entity, bilobalide possesses several pharmacological activities, including preventing ischemia-induced edema formation, cerebral ischemia and neurodegenerative diseases (Van Beek and Montoro, 2009).

Ginkgo biloba L. could be one of natural product candidates for treating metabolic syndromes. In traditional Chinese medicine, fruits and seeds of *Ginkgo biloba* L. have been used for the treatment of asthma, cough and enuresis (Smith and Luo, 2004). EGb761, a

standardized extract of *Ginkgo biloba* leaves, is the more widely used version of the herbal medicine in the USA and Europe, largely because of its better quality control, safety, and tolerability, as compared to other types of *Ginkgo biloba* preparations. As a dietary supplement, EGb761 exerts multiple therapeutic effects on several diseases; these effects included improvements in peripheral blood circulation, increases in cerebral blood perfusion, and prevention of neurodegenerative disorders, such as Alzheimer's disease (Man et al., 2008; DeFeudis and Drieu, 2000). Like *Ginkgo biloba* leaves, EGb761 is also an effective free radical scavenger. Its flavonoid fraction exhibits antioxidant and free radical-scavenging actions (Eckert et al., 2003). Recently, it was reported that EGb761 can protect pancreatic beta cells against HFD-induced apoptosis in rats (Choi et al., 2007). In addition, it has been observed that EGb761 could increase insulin secretion from INS-1 cells and also reduce insulin resistance in a high-fat-fed mouse model (Choi et al., 2007; Cong et al., 2011).
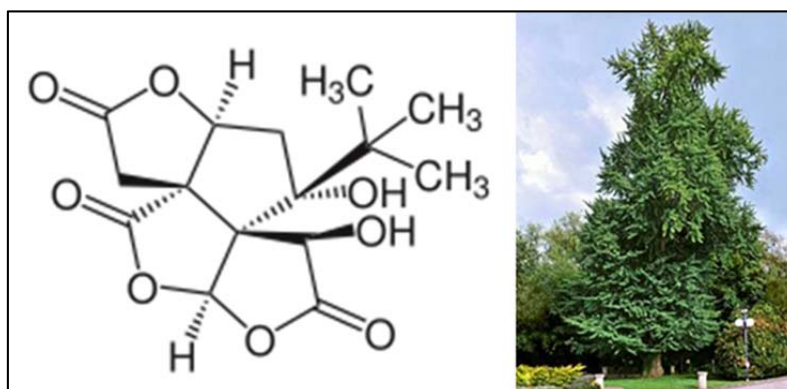
Fig. 1.9 The compound selected for the study: **Structure of bilobalide, and figure of *Ginkgo biloba* L plant**

EGb 761 upregulates the expression of antioxidant enzymes such as mitochondrial SOD, GPx, and HO-1 (Li et al., 2005; Saleem et al., 2008; Shah et al., 2011). Additionally, EGb 761 increases mRNA and protein levels of GST-P1 and NQO1 *in vitro* through the Nrf2-Keap1-ARE signaling pathway (Liu et al., 2007). Liu et al., suggest that EGb 761 may have dual effects on Keap1; first, EGb 761 interacts with keap1 (or Nrf2) to dissociate the Nrf2-Keap1 complex, facilitating the release and nuclear translocation of Nrf2; second, EGb 761 reduced expression or enhanced degradation of Keap1 enables Nrf2 nuclear translocation.

Both EGb 761 and bilobalide protects mitochondria from ischemia induced alterations (Janssens et al., 1995; Janssens et al., 1999). Bilobalide allows mitochondria to maintain their respiratory activity under ischemic conditions by protecting complex I and III activities as long as some oxygen is present, thus delaying the onset of ischemia-induced damage (Janssens et al., 2000). The nonflavone fraction is responsible for the antihypoxic activity of EGb 761. Zhu et al., 2007, reported that ginkgolides, the main constituent of the nonflavone fraction of EGb 761, have a significant protective role against chemical and physical hypoxia-induced injury in neurons and PC12 cells.

1.6.2 Curcumin

Curcumin is the major active component of turmeric, a yellow compound originally isolated from the plant *Curcuma longa* (Fig. 1.10). It is a member of the curcuminoid family and has been used for centuries in traditional medicines. As a spice, it provides curry with its distinctive colour and flavour. Furthermore, traditional Indian medicine has considered curcumin as a drug effective for various respiratory conditions (asthma, bronchial hyperactivity, and allergy) as well as for other disorders including anorexia, cough, hepatic diseases, and sinusitis (Goel et al., 2008).
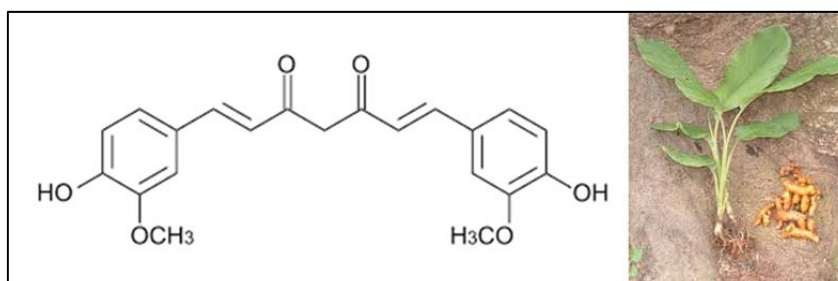
Fig. 1.10 The compound selected for the study: Structure of curcumin, and figure of *Curcuma longa* plant

Curcumin, a dietary polyphenol has been shown to possess antioxidant, anti-inflammatory, anticancer, anti-angiogenesis, chemopreventive and chemotherapeutic properties (Shao et al., 2012). The first report referring to curcumin's effect on disease in humans was published in The Lancet by Oppenheimer on 1937 (Oppenheimer, 1937). Studies have shown that curcumin inhibits a number of signaling pathways and molecular targets involved in inflammation and obesity-related metabolic diseases. Curcumin can inhibit the IKK signaling complex that is responsible for the phosphorylation of IκB,

thereby blocking improper activation of NF-κB induced by various inflammatory agents (Singh and Aggarwal, 1995). Anti-obesity effects of curcumin are also linked with the inhibition of inflammatory and angiogenic biomarkers such as COX-2 and vascular endothelial growth factor (VEGF) (Aggarwal et al., 2006). Curcumin has known to downregulate the expression of various NF-κB-regulated proinflammatory adipocytokines, chemokines (such as MCP-1, MCP-4, and eotaxin) and interleukins (IL-1 IL-6, IL-8 etc) (Woo et al., 2007; Wang et al., 2009) in obese subjects. Several studies have shown that curcumin blocks the leptin signaling by reducing the phosphorylation levels of the leptin receptor (Ob-R) and increases the induction of adiponectin, which improves obesity-associated inflammation (Shao et al., 2012). These finding support the existence of direct and indirect molecular mechanisms by which curcumin inhibits several inflammatory pathways that are responsible for obesity and obesity-related metabolic diseases.

Moreover, curcumin has been identified as a potent inducer of HO-1, a redox-sensitive inducible protein via regulation of Nrf2 and the antioxidant-responsive element (ARE), which provides protection against various forms of stress. Curcumin stimulates HO-1 gene activity through inactivation of the Nrf2–Keap1 complex, leading to increased Nrf2 binding to the resident HO-1 and AREs (Yang et al., 2009)

There are reports on inhibitory effect of curcumin on HIF-1 activation by degrading aryl hydrocarbon receptor nuclear translocator in cancer studies (Choi et al., 2006). The antiangiogenic activity of curcumin in HepG2 hepatocellular carcinoma cells was hypothesized to be mediated by the inhibition of HIF-1 and down-regulation of VEGF (Yoysungnoen et al., 2008). These findings suggest that curcumin may play pivotal role in inhibition of HIF-1α mediated hypoxia response. The major disadvantage of curcumin is its poor absorption and bioavailability.

1.7 Scope of present study and objectives

Obesity research has become a priority in current healthcare research due to its increased social and economic consequences. Therefore, studies focusing on understanding the underlying mechanisms that link obesity and metabolic dysfunction may provide new pharmaceutical targets and innovative therapies for the prevention and treatment of metabolic diseases. Recent studies have shown the emerging role of ATH in obesity. This links obesity with other metabolic syndromes. Hypoxia is mainly responsible for

inflammation, insulin resistance and all other obesity related complications in obese individuals and that leads to metabolic syndromes. So there is a high demand for anti-obese phytoceuticals to control and manage the complications resulting from adipose tissue hypoxia. Reversing hypoxia, or attenuating the O_2-signaling pathways, through the HIFs or other regulatory factors, presents novel opportunities and targets. In present study we evaluated the effect of hypoxia on key functions of adipocyte biology using the cell line '3T3-L1 adipocytes' and possible attenuation with phytochemicals curcumin and bilobalide.

The main aims and objectives of the present study are

1. To investigate how hypoxia affects the physiological functions of 3T3-L1 adipocytes, emphasizing on HIF-1α expression, lactate release, oxidative stress and ER stress and also evaluate the protective role of curcumin and bilobalide on hypoxia induced alterations in adipocytes.

2. To evaluate the effect of hypoxia on adipocyte mitochondria emphasising on intracellular reactive oxygen species (ROS) levels, mitochondrial superoxide production, aconitase activity, mitochondrial membrane potential (Δψ) and mitochondrial transition pore opening (mPTP opening), ATP production and oxygen consumption, proteins involved in oxidative phosphorylation, mitochondrial mass and mitochondrial DNA (mtDNA) copy number, expression of genes and proteins involved in mitochondrial biogenesis and proteins involved in mitochondrial structural dynamics and possible protection with bilobalide and curcumin.

3. To study the crosstalk between hypoxia induced inflammation and insulin resistance, and, also the secretion of proangiogenic factors in 3T3-L1 adipocytes and possible reversal with phytochemicals bilobalide and curcumin.

1.8 Societal impact of present study

Obesity and overweight have significant implications for health, social care and the economy. Being obese or overweight increases the risk of developing a range of serious diseases, including heart disease and cancers. The impact of obesity on the health of adults has long been established. In addition, rising levels of childhood obesity has

consequences for the physical and mental health of children and young people in both the short and the longer term. The ideal anti-obesity drug would produce sustained weight loss with minimal side effects. However, most of the anti-obesity drugs that were approved and marketed have now been withdrawn due to serious adverse effects. Natural products may be an excellent alternative strategy for developing future effective, safe anti-obesity drugs. A variety of natural products, including crude extracts and isolated pure natural compounds can induce body weight reduction and prevent obesity related complications. Understanding the underlying mechanisms that link obesity and metabolic dysfunction may provide new pharmaceutical targets. Recent studies have shown the emerging role of ATH in obesity mediated metabolic complications. Reversing hypoxia through the HIFs or other regulatory factors, presents a novel therapeutic target for obesity treatment. The present study suggested natural compounds as an alternative attempt to identify new inhibitors of the HIF-1, for treating obesity related complications.

References

Aggarwal BB, Shishodia S, Sandur SK, Pandey MK, Sethi G. (2006). Inflammation and cancer: how hot is the link? *Biochem Pharmacol*, 72: 1605-1612.

Ahima RS, Flier JS. (2000). Leptin. *Annu Rev Physiol,* 62: 413.

Ali SS, Hsiao M, Zhao HW, Dugan LL, Haddad GG, Zhou D. (2012). Hypoxia-Adaptation Involves Mitochondrial Metabolic Depression and Decreased ROS Leakage. *PLoS ONE,* 7: e36801. doi:10.1371/journal.pone.0036801.

Almeda-Valdes P, Cuevas-Ramos D, Mehta R, Gomez-Perez FJ, Cruz-Bautista I, Arellano-Campos O, Navarrete-Lopez M, Aguilar-Salinas CA. (2010). Total and high molecular weight adiponectin have similar utility for the identification of insulin resistance. *Cardiovasc Diabetol*, 23: 9-26.

Andrew P, Halestrap AH, Clarke SJ, Javadov SA. (2004). Mitochondrial permeability transition pore opening during myocardial reperfusion-a target for cardioprotection. *Cardiovasc Res*, 61: 372-385.

Archer SL. (2013). Mitochondrial dynamics—mitochondrial fission and fusion in human diseases. *J Med*, 369: 2236-2251.

Arkan MC, Hevener AL, Greten FR, Maeda S, Li ZW, Long JM, Wynshaw-Boris A, Poli G, Olefsky J, Karin M. (2005). IKK-beta links inflammation to obesity-induced insulin resistance. *Nat Med*, 11: 191-198.

Bach D, Naon D, Pich S, Soriano FX, Vega N, Rieusset J, Laville M, Guillet C, Boirie Y, Wallberg-Henriksson H, Manco M, Calvani M, Castagneto M, Palacín M, Mingrone G, Zierath JR, Vidal H, Zorzano A. (2005). Expression of Mfn2, the Charcot-Marie-Tooth neuropathy type 2A gene, in human skeletal muscle: effects of type 2 diabetes, obesity, weight loss, and the regulatory role of tumor necrosis factor alpha and interleukin-6. *Diabetes*, 54: 2685-2693.

Brahimi-Horn C, Mazure N, Pouyssegur J. (2005). Signalling via the hypoxia-inducible factor-1alpha requires multiple posttranslational modifications. *Cell Signal*, 17: 1-9.

Cai D, Yuan M, Frantz DF, Melendez PA, Hansen L, Lee J, Shoelson SE. (2005). Local and systemic insulin resistance resulting from hepatic activation of IKK-beta and NF-kappaB. *Nat Med*, 11: 183-190.

Calfon M, Zeng H, Urano F, Till JH, Hubbard SR, Harding HP, Clark SG, Ron D. (2002). IRE1 couples endoplasmic reticulum load to secretory capacity by processing the XBP-1 mRNA. *Nature*, 415: 92-96.

Cao Y. (2010). Adipose tissue angiogenesis as a therapeutic target for obesity and metabolic diseases. *Nat Rev Drug Discov*, 9: 107-115.

Carbone F, La Rocca C, Matarese G. (2012). Immunological functions of leptin and adiponectin. *Biochimie*. 94: 2082-2088.

Carmeliet P, Jain RK. (2000). Angiogenesis in cancer and other diseases. *Nature*, 407: 249-257.

Chan DC. (2012). Fusion and Fission: Interlinked Processes Critical for Mitochondrial Health. *Annu Rev Genet*, 46: 265-287.

Chan R, Woo J. (2010). Prevention of Overweight and Obesity: How Effective is the Current Public Health Approach. *Int J Environ Res Public Health*, 7: 765-783.

Choi H, Chun YS, Kim SW, Kim MS, Park JW. (2006). Curcumin inhibits hypoxia-inducible factor-1 by degrading aryl hydrocarbon receptor nuclear translocator: a mechanism of tumor growth inhibition. *Mol Pharmacol*, 70: 1664-1671.

Choi SE, Shin HC, Kim HE, Lee SJ, Jang HJ, Lee KW, Kang Y. (2007). Involvement of Ca2+, CaMK II and PKA in EGb 761-induced insulin secretion in INS-1 cells. *J Ethnopharmacol,* 110: 49-55.

Cong W, Tao R, Tian J, Zhao J, Liu Q, Ye F. (2011). EGb761, an extract of Ginkgo biloba leaves, reduces insulin resistance in a high-fat-fed mouse model. *Acta Pharmaceutica Sinica B*, 1: 24-20.

Copps KD, Hancer NJ, Opare-Ado L, Qiu W, Walsh C, White MF. (2010). IRS-1 serine 307 promotes insulin sensitivity in mice. *Cell Metab*, 11: 84-92.

de Luca C, Olefsky JM. (2000). Inflammation and insulin resistance. *FEBS Lett*, 582: 97-105.

De Marchi E, Baldassari F, Bononi A, Wieckowski MR, Pinton P. (2013). Oxidative Stress in Cardiovascular Diseases and Obesity: Role of p66Shc and Protein Kinase C. Oxidative Medicine and Cellular Longevity. *Oxid Med Cell Longev*, 2013: 564961. doi: 10.1155/2013/564961.

DeFeudis FV, Drieu K. (2000). Ginkgo biloba extract (EGb 761) and CNS functions: basic studies and clinical applications. *Curr Drug Targets*, 1: 25-58.

Eckert A, Keil U, Kressmann S, Schindowski K, Leutner S, Leutz S, Müller WE. (2003). Effects of EGb 761 Ginkgo biloba extract on mitochondrial function and oxidative stress. *Pharmacopsychiatry*, 36: S15-S23.

Fonseca-Alaniz MH, Takada J, Alonso-Vale MIC, Lima FB. (2007). Adipose tissue as an endocrine organ: from theory to practice. *J Pediatr*, 83: S192-S203.

Furukawa S, Fujita T, Shimabukuro M, Iwaki M, Yamada Y, Nakajima Y, Nakayama O, Makishima M, Matsuda M, Shimomura I. (2004). Increased oxidative stress in obesity and its impact on metabolic syndrome. *J Clin Invest*, 114: 1752-1761.

Géloën A, Collet AJ, Guay G, Bukowiecki LJ. (1989). Insulin stimulates *in vivo* cell proliferation in white adipose tissue. *Am J Physiol*, 256: C190-C196.

Gething MJ, Sambrook J (1992). Protein folding in the cell. *Nature*, 355: 33-45.

Gething MJ. (1999). Role and regulation of the ER chaperone BiP. *Semin Cell Dev Biol*, 10: 465-472.

Goel A, Kunnumakkara AB, Aggarwal BB. (2008). Curcumin as ''Curecumin'': From kitchen to clinic. *Biochem Pharmacol*, 75: 787-809.

Grattagliano I, de Bari O, Bernardo TC, Oliveira PJ, Wang DQ, Portincasa P. (2012). Role of mitochondria in nonalcoholic fatty liver disease-from origin to propagation. *Clin Biochem,* 45: 610-618.

Guilherme A, Virbasius JV, Puri V, Czech MP. (2008). Adipocyte dysfunctions linking obesity to insulin resistance and type 2 diabetes. *Nat Rev Mol Cell Biol*, 9: 367-377.

Guzy RD, Hoyos B, Robin E, Chen H, Liu L, Mansfield KD, Simon MC, Hammerling U, Schumacker PT. (2005). Mitochondrial complex III is required for hypoxia-induced ROS production and cellular oxygen sensing. *Cell Metab*, 1: 401-408.

Halberg N, Khan T, Trujillo ME, Wernstedt-Asterholm I, Attie AD, Sherwani S, Wang ZV, Landskroner-Eiger S, Dineen S, Magalang UJ, Brekken RA, Scherer PE. (2009). Hypoxia-inducible factor 1a induces fibrosis and insulin resistance in white adipose tissue. *Mol Cell Biol*, 29: 4467-4483.

Heilbronn LK, Gan SK, Turner N, Campbell LV, Chisholm DJ. (2007). Markers of mitochondrial biogenesis and metabolism are lower in overweight and obese insulin-resistant subjects. *J Clin Endocrinol Metab*, 92: 1467-1473.

Hermes-Lima M, Zenteno-Savín T. (2002). Animal response to drastic changes in oxygen availability and physiological oxidative stress. *Comp Biochem Physiol C Toxicol Pharmaco*l, 133: 537-556.

Hirosumi J, Tuncman G, Chang L, Gorgun C, Uysal K, Maeda K, Karin M, Hotamisligil GS. (2002*).* A central role for JNK in obesity and insulin resistance. *Nature*, 420: 333-336.

Ho E, Karimi Galougahi K, Liu C-C, Bhindi R, Figtree GA. (2013). Biological markers of oxidative stress: applications to cardiovascular research and practice. *Redox Biol*, 1: 483-491.

Hosogai N, Fukuhara A, Oshima K, Miyata Y, Tanaka S, Segawa K, Furukawa S, Tochino Y, Komuro R, Matsuda M, Shimomura I. (2007). Adipose tissue hypoxia in obesity and its impact on adipocytokine dysregulation. *Diabetes*, 56: 901-911.

Hotamisligil GS, Peraldi P, Budavari A, Ellis R, White MF, Spiegelman BM. (1996). IRS-1-mediated inhibition of insulin receptor tyrosine kinase activity in TNF-alpha- and obesity-induced insulin resistance. *Science*, 271: 665-668

Hotamisligil GS, Shargill NS, Spiegelman BM. (1993). Adipose expression of tumor necrosis factor-alpha: direct role in obesity-linked insulin resistance. *Science*, 259: 87-91.

Howard JK, Flier JS. (2006). Attenuation of leptin and insulin signaling by SOCS proteins. *Trends Endocrinol Metab*, 17: 365-371.

Ibrahim MM. (2010). Subcutaneous and visceral adipose tissue: structural and functional differences. *Obes Rev*, 11: 11-18.

Itoh K, Chiba T, Takahashi S, Ishii T, Igarashi K, Katoh Y, Oyake T, Hayashi N, Satoh K, Hatayama I, Yamamoto M, Nabeshima Y. (1997). An Nrf2/small Maf heterodimer mediates the induction of phase II detoxifying enzyme genes through antioxidant response elements. *Biochem Biophys Res Commun*, 236: 313-322.

Itoh K, Tong KI, Yamamoto M. (2004). Molecular mechanism activating Nrf2-Keap1 pathway in regulation of adaptive response to electrophiles. *Free Radic Biol Med*, 36:1208-1213

Iwasaki A, Medzhitov R. (2004). Toll-like receptor control of the adaptive immune responses. *Nat Immunol*, 5: 987-995.

Jamaluddin MS, Weakley SM, Yao Q, Chen C. (2012). Resistin: functional roles and therapeutic considerations for cardiovascular disease. *Br J Pharmacol*, 165: 622-632.

Jang MK, Son Y, Jung MH. (2013). ATF3 plays a role in adipocyte hypoxia-mediated mitochondrial dysfunction in obesity. *Biochem Biophys Res Commun*, 431: 421-427.

Janssens D, Delaive E, Remacle J, Michiels C. (2000). Protection by bilobalide of the ischaemia-induced alterations of the mitochondrial respiratory activity. *Fundam Clin Pharmacol*, 14: 193-201.

Janssens D, Michiels C, Delaive E, Eliaers F, Drieu K, Remacle J. (1995). Protection of hypoxia-induced ATP decrease in endothelial cells by ginkgo biloba extract and bilobalide. *Biochem Pharmacol*, 50: 991-999.

Janssens D, Remacle J, Drieu K, Michiels C. (1999). Protection of mitochondrial respiration activity by bilobalide. *Biochem Pharmacol*, 58: 109-119.

Jo J, Gavrilova O, Pack S, Jou W, Mullen S, Sumner AE, Cushman SW, Periwal V. (2009). Hypertrophy and/or Hyperplasia: Dynamics of Adipose Tissue Growth. *PLoS Comput Biol*, 5: e1000324. doi:10.1371/journal.pcbi.1000324.

Kamei N, Tobe K, Suzuki R, Ohsugi M, Watanabe T, Kubota N, Ohtsuka-Kowatari N, Kumagai K, Sakamoto K, Kobayashi M, Yamauchi T, Ueki K, Oishi Y, Nishimura S, Manabe I, Hashimoto H, Ohnishi Y, Ogata H, Tokuyama K, Tsunoda M, Ide T, Murakami K, Nagai R, Kadowaki T. (2006). Overexpression of monocyte chemoattractant protein-1 in adipose tissues causes macrophage recruitment and insulin resistance. *J Biol Chem*, 281: 26602-26614.

Kanda H, Tateya S, Tamori Y, Kotani K, Hiasa K, Kitazawa R, Kitazawa S, Miyachi H, Maeda S, Egashira K, Kasuga M. (2006). MCP-1 contributes to macrophage infiltration into adipose tissue, insulin resistance, and hepatic steatosis in obesity. *J Clin Invest*, 116: 1494-1505.

Karin M, Ben-Neriah Y. (2000). Phosphorylation meets ubiquitination: the control of NF-[kappa]B activity. *Annu Rev Immunol*, 18: 621-663.

Kaufman RJ. (1999). Stress signaling from the lumen of the endoplasmic reticulum: coordination of gene transcriptional and translational controls. *Genes Dev*, 13: 1211-1233.

Kawasaki N, Asada R, Saito A, Kanemoto S, Imaizumi K. (2012). Obesity-induced endoplasmic reticulum stress causes chronic inflammation in adipose tissue. *Sci Rep*, 2: 799. doi: 10.1038/srep00799.

Kelly M, Keller C, Avilucea PR, Keller P, Luo Z, Xiang X, Giralt M, Hidalgo J, Saha AK, Pedersen BK, Ruderman NB. (2004). AMPK activity is diminished in tissues of IL-6 knockout mice: the effect of exercise. *Biochem Biophys Res Commun,* 320: 449-454.

Kern PA, Saghizadeh M, Ong JM, Bosch RJ, Deem R, Simsolo RB. (1995). The expression of tumor necrosis factor in human adipose tissue. Regulation by obesity, weight loss, and relationship to lipoprotein lipase. *J Clin Invest*, 95: 2111-2119.

Kim JW, Tchernyshyov I, Semenza GL, Dang CV. (2006). HIF-1-mediated expression of pyruvate dehydrogenase kinase: a metabolic switch required for cellular adaptation to hypoxia. *Cell Metab,* 3: 177-185.

Kim KH, Zhao L, Moon Y, Kang C, Sul HS. (2004). Dominant inhibitory adipocyte-specific secretory factor (ADSF)/resistin enhances adipogenesis and improves insulin sensitivity. *Proc Natl Acad Sci* U S A, 101: 6780-6785.

Kobayashi A, Ohta T, Yamamoto M. (2004). Unique function of the Nrf2–Keap1 pathway in the inducible expression of antioxidant and detoxifying enzymes. *Methods Enzymol*, 378: 273-286.

Kobayashi M, Yamamoto M. (2005). Molecular mechanisms activating the Nrf2-Keap1 pathway of antioxidant gene regulation. *Antioxid Redox Signal*, 7: 385-394.

Lagathu C, Yvan-Charvet L, Bastard JP, Maachi M, QuignardBoulange A, Capeau J, Caron M. (2006). Long-term treatment with interleukin-1 induces insulin resistance in murine and human adipocytes. *Diabetologia*, 49: 2162-2173.

Lai E, Teodoro T and Volchuk A. (2007). Endoplasmic reticulum stress: signaling the unfolded protein response. *Physiology*, 22: 193-201.

Lane N. (2006). Mitochondrial disease: powerhouse of disease. *Nature*, 440: 600-602.

Lee YJ, Jeong SY, Karbowski M, Smith CL, Youle RJ. (2004). Roles of the mammalian mitochondrial fission and fusion mediators Fis1, Drp1, and Opa1 in apoptosis. *Mol Biol Cell*, 15: 5001-5011.

Li K, Yao P, Zhou SL, Song FF. (2005). Protective effects of extract of Ginkgo biloba against ethanol-induced oxidative injury in rat testes. *J Hygiene Res*, 34: 559-562.

Li X, Li S, Ulusoy E, Chen W, Srinivasan SR, Berenson GS. (2004). Childhood adiposity as a predictor of cardiac mass in adulthood: The Bogalusa Heart Study. *Circulation*, 110: 3488-3492.

Lin JH, Walter P, Yen TSB. (2008). Endoplasmic Reticulum Stress in Disease Pathogenesis. *Annu Rev Pathol Mech Dis*, 3: 399-425.

Liu XP, Goldring CE, Copple IM, Wang HY, Wei W, Kitteringham NR, Park BK. (2007). Extract of Ginkgo biloba induces phase 2 genes through Keap1-Nrf2-ARE signaling pathway. *Life Sci*, 80: 1586-1591.

Liu Y, Fiskum G, Schubert D. (2002). Generation of reactive oxygen species by the mitochondrial electron transport chain. *J Neurochem*, 80: 780-787.

Lolmède K, Durand de Saint Front V, Galitzky J, Lafontan M, Bouloumié A. (2003). Effects of hypoxia on the expression of proangiogenic factors in differentiated 3T3F442A adipocytes. *Int J Obes Relat Metab Disord*, 27: 1187-1195.

Maeda S. (2010). NF-κB, JNK, and TLR signaling pathways in Hepatocarcinogenesis. *Gastroenterol Res Pract*, 2010: 367694. doi: 10.1155/2010/367694

Magkos F, Sidossis LS (2007). Recent advances in the measurement of adiponectin isoform distribution. *Curr Opin Clin Nutr Metab Care*, 10: 571-575.

Man SC, Durairajan SS, Kum WF, Lu JH, Huang JD, Cheng CF, Chung V, Xu M, Li M. (2008). Systematic review on the efficacy and safety of herbal medicines for Alzheimer's disease. *J Alzheimers Dis*, 14: 209-223.

Manolescu B, Oprea E, Busu C, Cercasov C. (2009). Natural compounds and the hypoxia-inducible factor (HIF) signalling pathway. *Biochimie*, 91: 1347-1358.

Matsuki T, Horai R, Sudo K, Iwakura Y. (2003). IL-1 plays an important role in lipid metabolism by regulating insulin levels under physiological conditions. *J Exp Med*, 198: 877-888.

Mc Ardle MA, Finucane OM, Connaughton RM, McMorrow AM, Roche HM. (2013). Mechanisms of obesity-induced inflammation and insulin resistance: insights into the emerging role of nutritional strategies. *Front Endocrinol*, 4: 52. doi:10.3389/fendo.2013.00052.

Minokoshi Y, Toda C, Okamoto S. (2012). Regulatory role of leptin in glucose and lipid metabolism in skeletal muscle. *Indian J Endocrinol Metab*, 16: S562-S568.

Morino K, Neschen S, Bilz S, Sono S, Tsirigotis D, Reznick RM, Moore I, Nagai Y, Samuel V, Sebastian D, White M, Philbrick W, Shulman GI. (2008). Muscle specific IRS-1 Ser-Ala transgenic mice are protected from fat-induced insulin resistance in skeletal muscle. *Diabetes*, 57: 2644-2651.

Motohashi H, Yamamoto M. (2004). Nrf2-Keap1 defines a physiologically important stress response mechanism. *Trends Mol Med*, 10: 549-557.

Mueller CF, Laude K, McNally JS, Harrison DG. (2005). ATVB in focus: redox mechanisms in blood vessels. *Arterioscler Thromb Vasc Biol*, 25: 274-278

Ng M, Fleming T, Robinson M, Thomson B, Graetz N, Margono C, Mullany EC, Biryukov S, Abbafati C, Abera SF, Abraham JP, Abu-Rmeileh NM, Achoki T, AlBuhairan FS, Alemu ZA, Alfonso R, Ali MK, Ali R, Guzman NA, Ammar W, Anwari P, Banerjee A, Barquera S, Basu S, Bennett DA, Bhutta Z, Blore J, Cabral N, Nonato IC, Chang JC, Chowdhury R, Courville KJ, Criqui MH, Cundiff DK, Dabhadkar KC, Dandona L, Davis A, Dayama A, Dharmaratne SD, Ding EL, Durrani AM, Esteghamati A, Farzadfar F, Fay DF, Feigin VL, Flaxman A, Forouzanfar MH, Goto A, Green MA, Gupta R, Hafezi-Nejad N, Hankey GJ, Harewood HC, Havmoeller R, Hay S, Hernandez L, Husseini A, Idrisov BT, Ikeda N, Islami F, Jahangir E, Jassal SK, Jee SH, Jeffreys M, Jonas JB, Kabagambe EK, Khalifa SE, Kengne AP, Khader YS, Khang YH, Kim D, Kimokoti RW, Kinge JM, Kokubo Y, Kosen S, Kwan G, Lai T, Leinsalu M, Li Y, Liang X, Liu S, Logroscino G, Lotufo PA, Lu Y, Ma J, Mainoo NK, Mensah GA, Merriman TR, Mokdad AH, Moschandreas J, Naghavi M, Naheed A, Nand D, Narayan KM, Nelson EL, Neuhouser ML, Nisar MI, Ohkubo T, Oti SO, Pedroza A, Prabhakaran D, Roy N, Sampson U, Seo H, Sepanlou SG, Shibuya K, Shiri R, Shiue I, Singh GM, Singh JA, Skirbekk V, Stapelberg NJ, Sturua L, Sykes BL, Tobias M, Tran BX, Trasande L, Toyoshima H, van de Vijver S, Vasankari TJ, Veerman JL, Velasquez-Melendez G, Vlassov VV, Vollset SE, Vos T, Wang C, Wang X, Weiderpass E, Werdecker A, Wright JL, Yang YC, Yatsuya H, Yoon J, Yoon SJ, Zhao Y, Zhou M, Zhu S, Lopez AD, Murray CJ, Gakidou E. (2014). Global, regional, and national prevalence of overweight and obesity in children and adults during 1980–2013: a systematic analysis for the Global Burden of Disease Study 2013. *Lancet*, 384: 766-781.

Oppenheimer A. (1937). Turmeric (curcumin) in biliary diseases. *Lancet*, 229: 619-621.

Oslowski CM, Urano F. (2011). Measuring ER stress and the unfolded protein response using mammalian tissue culture system. *Methods Enzymol*, 490: 71-92.

Ozcan U, Cao Q, Yilmaz E, Lee AH, Iwakoshi NN, Ozdelen E, Tuncman G, Görgün C, Glimcher LH, Hotamisligil GS. (2004). Endoplasmic reticulum stress links obesity, insulin action, and type 2 diabetes. *Science*, 306: 457-461.

Pihl E, Zilmer K, Kullisaar T, Kairane C, Mägi A, Zilmer M. (2006). Atherogenic inflammatory and oxidative stress markers in relation to overweight values in male former athletes. *Int J Obes*, 30: 141-146.

Pischon T, Nöthlings U, Boeing H. (2008). Obesity and cancer. *Proc Nutr Soc*, 67: 128-145.

Pi-Sunyer FX. (2002). The obesity epidemic: pathophysiology and consequences of obesity. *Obes Res*, 2: 97S-104S.

Poirier P, Eckel RH. (2002). Obesity and cardiovascular disease. *Curr Atheroscler Rep*, 4: 448-453.

Rajala MW, Qi Y, Patel HR, Takahashi N, Banerjee R, Pajvani UB, Sinha MK, Gingerich RL, Scherer PE, Ahima RS. (2004). Regulation of resistin expression and circulating levels in obesity, diabetes, and fasting. *Diabetes*, 53:1671-1679.

Regazzetti C, Peraldi P, Grémeaux T, Najem-Lendom R, Ben-Sahra I, Cormont M, Giorgetti-Peraldi S. (2009). Hypoxia decreases insulin signaling pathways in adipocytes. *Diabetes*, 58: 95-103.

Ron D, Walter P. (2007). Signal integration in the endoplasmic reticulum unfolded protein response. *Nat Rev Mol Cell Biol*, 8: 519-529.

Rong JX, Qiu Y, Hansen MK, Zhu L, Zhang V, Xie M, Okamoto Y, Mattie MD, Higashiyama H, Asano S, Strum JC, Ryan TE. (2007). Adipose mitochondrial biogenesis is suppressed in db/db and high-fat diet-fed mice and improved by rosiglitazone. *Diabetes*, 56: 1751-1760.

Rosen ED, Spiegelman BM. (2006). Adipocytes as regulators of energy balance and glucose homeostasis. *Nature*, 444: 847-853.

Sabio G, Das M, Mora A, Zhang Z, Jun JY, Ko HJ, Barrett T, Kim JK, Davis RJ. (2008). A stress signaling pathway in adipose tissue regulates hepatic insulin resistance. *Science*, 322: 1539-1543.

Saleem S, Zhuang H, Biswal S, Christen Y, Doré S. (2008). Ginkgo biloba extract neuroprotective action is dependent on heme oxygenase 1 in ischemic reperfusion brain injury. *Stroke*, 39: 3389-3396.

Satoh H, Nguyen MT, Miles PD, Imamura T, Usui I, Olefsky JM. (2004). Adenovirus-mediated chronic "hyper-resistinemia" leads to *in-vivo* insulin resistance in normal rats. *J Clin Invest*, 114: 224-231.

Semenza GL, Nejfelt MK, Chi SM, and Antonarakis SE. (1991). Hypoxia-inducible nuclear factors bind to an enhancer element located 3′ to the human erythropoietin gene. *Proc Natl Acad Sci USA*, 88: 5680-5684.

Senn JJ, Klover PJ, Nowak IA, Mooney RA. (2002). Interleukin-6 induces cellular insulin resistance in hepatocytes. *Diabetes*, 51: 3391-3399.

Senn JJ, Klover PJ, Nowak IA, Zimmers TA, Koniaris LG, Furlanetto RW Mooney RA. (2003). Suppressor of cytokine signaling-3 (SOCS-3), a potential mediator of interleukin-6-dependent insulin resistance in hepatocytes. *J Biol Chem*, 278: 13740-13746.

Shah ZA, Nada SE, Doré S. (2011). Heme oxygenase 1, beneficial role in permanent ischemic stroke and in Gingko biloba (EGb 761) neuroprotection. *Neuroscience*, 18: 248-255.

Shao W, Yu Z, Chiang Y, Yang Y, Chai T, Foltz W, Lu H, Fantus IG, Jin T (2012) Curcumin prevents high fat diet induced insulin resistance and obesity via attenuating lipogenesis in liver and inflammatory pathway in adipocytes. *PLoS ONE*, 7: e28784. doi:10.1371/journal.pone.0028784.

Shi H, Kokoeva MV, Inouye K, Tzameli I, Yin H, Flier JS. (2006). TLR4 links innate immunity and fatty acid-induced insulin resistance. *J Clin Invest*, 116: 3015-3025.

Shi Y, Vattem KM, Sood R, An J, Liang J, Stramm L, Wek RC. (1998). Identification and characterization of pancreatic eukaryotic initiation factor 2 alpha-subunit kinase, PEK, involved in translational control. *Mol Cell Biol*, 18: 7499-7509.

Shoelson SE, Herrero L, Naaz A. (2007). Obesity, inflammation, and insulin resistance. *Gastroenterology*, 132: 2169-2180.

Siddiqui NI, Bose S. (2012). Prevalence and trends of obesity in Indian school children of different socioeconomic class. *Ind J Basic Appl Med Res*, 5: 393-398.

Singh B, Kaur P, Gopichand, Singh RD, Ahuja PS. (2008). Biology and chemistry of *Ginkgo biloba*. *Fitoterapia*, 79: 401-418.

Singh S, Aggarwal BB. (1995). Activation of transcription factor NF-κB is suppressed by curcumin (diferuloylmethane). *J Biol Chem*, 270: 4995-5000.

Singh S, Vrishni S, Singh BK, Rahman I, Kakkar P. (2010). Nrf2-ARE stress response mechanism: a control point in oxidative stress-mediated dysfunctions and chronic inflammatory diseases. *Free Rad Res*, 44: 1267-1288.

Smith JV, Luo Y. (2004). Studies on molecular mechanisms of Ginkgo biloba extract. *Appl Microbiol Biotechnol*, 64: 465-472.

Stephens JM. (2012). The Fat Controller: Adipocyte Development. *PLoS Biol*, 10: e1001436. doi:10.1371/journal.pbio.1001436.

Taddeo EP, Laker RC, Breen DS, Akhtar YN, Kenwood BM, Liao JA, Zhang M, Fazakerley DJ, Tomsig JL, Harris TE, Keller SR, Chow JD, Lynch KR, Chokki M, Molkentin JD, Turner N, James DE, Yan Z, Hoehn KL. (2013). Opening of the mitochondrial permeability transition pore links mitochondrial dysfunction to insulin resistance in skeletal muscle. *Mol Metab*, 3: 124-134.

Taguchi K, Motohashi H, Yamamoto M. (2011). Molecular mechanisms of the Keap1–Nrf2 pathway in stress response and cancer evolution. Genes Cells. 16: 123-140.

Tanti JF, Grémeaux T, van Obberghen E, Le Marchand-Brustel Y. (1994). Serine/threonine phosphorylation of insulin receptor substrate 1 modulates insulin receptor signaling. *J Biol Chem*, 269: 6051-6057.

Teodoro JS, Duarte FV, Gomes AP, Varela AT, Peixoto FM, Rolo AP, Palmeira CM. (2013). Berberine reverts hepatic mitochondrial dysfunction in high-fat fed rats: a possible role for SirT3 activation. *Mitochondrion*, 13: 637-646.

Trayhurn P, Wang B, Wood IS. (2008a). Hypoxia and the endocrine and signalling role of white adipose tissue. *Arch Physiol Biochem*, 114: 267-276.

Trayhurn P, Wang B, Wood IS. (2008b). Hypoxia in adipose tissue: a basis for the Dysregulation of tissue function in obesity? *Br J Nutr*, 100: 227-235.

Trayhurn P, Wood IS. (2004). Adipokines: inflammation and the pleiotropic role of white adipose tissue. *Br J Nutr*, 92: 347-355.

Trayhurn P. (2013). Hypoxia and Adipose tissue function and Dysfunction in obesity. *Physiol Rev*, 93: 1-21.

Tuncman G, Hirosumi J, Solinas G, Chang L, Karin M, Hotamisligil GS. (2006). Functional in vivo interactions between JNK1 and JNK2 isoforms in obesity and insulin resistance. *Proc Natl Acad Sci USA*, 103: 10741-10746.

Utzschneider KM, Kahn SE. (2006). The role of insulin resistance in non-alcoholic fatty liver disease. *J Clin Endocrinol Metab*, 91: 4753-4761.

Uysal KT, Wiesbrock SM, Marino MW, Hotamisligil GS. (1997). Protection from obesity-induced insulin resistance in mice lacking TNF-alpha function. *Nature*, 389: 610-614.

Van Beek TA, Montoro P. (2009). Chemical analysis and quality control of Ginkgo biloba leaves, extracts, and phytopharmaceuticals. *J Chromatogr A*, 1216: 2002-2032.

Varela L, Horvatha TL. (2012). Leptin and insulin pathways in POMC and AgRP neurons that modulate energy balance and glucose homeostasis. *EMBO Rep*, 13: 1079-1086.

Vgontzas AN, Tan TL, Bixler EO, Martin LF, Shubert D, Kales A. (1994). Sleep apnea and sleep disruption in obese patients. *Arch Intern Med*, 154: 1705-1711.

Virbasius JV, Scarpulla RC. (1994). Activation of the human mitochondrial transcription factor A gene by nuclear respiratory factors: a potential regulatory link between nuclear and mitochondrial gene expression in organelle biogenesis. *Proc Natl Acad Sci USA*, 91: 1309-1313.

Wang B, Wood IS, Trayhurn P. (2007). Dysregulation of the expression and secretion of inflammation-related adipokines by hypoxia in human adipocytes. *Pfl€ugers Archiv. Eur J Physiol*, 455: 479-492.

Wang GL, Jiang BH, Rue EA, Semenza GL. (1995). Hypoxia-inducible factor 1 is a basic-helix-loop-helix-PAS heterodimer regulated by cellular O_2 tension. *Proc Natl Acad Sci USA*, 92: 5510-5514.

Wang GL, Semenza GL. (1993). Desferrioxamine induces erythropoietin gene expression and hypoxia-inducible factor 1 DNA-binding activity: implications for models of hypoxia signal transduction. *Blood*, 82: 3610-3615.

Wang SL, Li Y, Wen Y, Chen YF, Na LX, Li ST, Sun CH. (2009). Curcumin, a potential inhibitor of up-regulation of TNF-alpha and IL-6 induced by palmitate in 3T3-L1 adipocytes through NF-kappaB and JNK pathway. *Biomed Environ Sci*, 22: 32-39.

Wang XZ, Lawson B, Brewer JW, Zinszner H, Sanjay A, Mi LJ, Boorstein R, Kreibich G, Hendershot LM, Ron D. (1996). Signals from the stressed endoplasmic reticulum

induce C/EBP-homologous protein (CHOP/GADD153). *Mol Cell Biol,* 16: 4273-4280.

Weisberg SP, Hunter D, Huber R, Lemieux J, Slaymaker S, Vaddi K, Charo I, Leibel RL, Ferrante AW Jr. (2006). CCR2 modulates inflammatory and metabolic effects of high-fat feeding. *J Clin Invest,* 116: 115-124.

Wellen KE, Hotamisligil GS. (2003). Obesity-induced inflammatory changes in adipose tissue. *J Clin Invest*, 112: 1785-1788.

Williams G, Frühbeck G. (2009). Obesity: Science to Practice. John Wiley & Sons, Ltd, Chichester, UK. doi: 10.1002/9780470712221.ch23.

Woo HM, Kang JH, Kawada T, Yoo H, Sung MK, Yu R. (2007). Active spice-derived components can inhibit inflammatory responses of adipose tissue in obesity by suppressing inflammatory actions of macrophages and release of monocyte chemoattractant protein-1 from adipocytes. *Life Sci,* 80: 926-931.

World Health Organization (2015). Fact sheet: obesity and overweight. Available online: http://www.who.int/mediacentre/factsheets/fs311/en/.

Wouters BG, Koritzinsky M. (2008). Hypoxia signalling through mTOR and the unfolded protein response in cancer. *Nat Rev Cancer*, 8: 851-864.

Wu J, Boström P, Sparks LM, Ye L, Choi JH, Giang AH, Khandekar M, Virtanen KA, Nuutila P, Schaart G, Huang K, Tu H, van Marken Lichtenbelt WD, Hoeks J, Enerbäck S, Schrauwen P, Spiegelman BM. (2012). Beige adipocytes are a distinct type of thermogenic fat cell in mouse and human. *Cell*, 150: 366-376.

Yang C, Zhang X, Fan H, Liu Y. (2009). Curcumin upregulates transcription factor Nrf2, HO-1 expression and protects rat brains against focal ischemia. *Brain Res*, 1282: 133-141.

Ye J, Gao Z, Yin J, He H. (2007). Hypoxia is a potential risk factor for chronic inflammation and adiponectin reduction in adipose tissue of ob/ob and dietary obese mice. *Am J Physiol Endocrinol Metab*, 293: E1118-E1128.

Ye J, Keller JN. (2010). Regulation of energy metabolism by inflammation: A feedback response in obesity and calorie restriction. *Aging*, 2: 361-368.

Ye J. (2009). Emerging role of adipose tissue hypoxia in obesity and insulin resistance. *Int J Obes (Lond)*, 33: 54-66.

Ye J. (2013). Mechanisms of insulin resistance in obesity. *Front Med*, 7: 14-24.

Yoshitake T, Yoshitake S, Kehr J. (2010). The Ginkgo biloba extract EGb 761® and its main constituent flavonoids and ginkgolides increase extracellular dopamine levels in the rat prefrontal cortex. *Br J Pharmacol*, 159: 659-668.

Yoysungnoen P, Wirachwong P, Changtam C, Suksamrarn A, Patumraj S. (2008). Anti-cancer and anti-angiogenic effects of curcumin and tetrahydrocurcumin on implanted hepatocellular carcinoma in nude mice. *World J Gastroenterol*, 14: 2003-2009.

Yuan M, Konstantopoulos N, Lee J, Hansen L, Li ZW, Karin M, Shoelson SE. (2001). Reversal of obesity and diet-induced insulin resistance with salicylates or targeted disruption of ikkbeta. *Science*, 293: 1673-1677.

Zhang X, Lam KS, Ye H, Chung SK, Zhou M, Wang Y, Xu A. (2010) Adipose tissue-specific inhibition of hypoxia-inducible factor 1 induces obesity and glucose intolerance by impeding energy expenditure in mice. *J Biol Chem*, 22: 32869-32877.

Zhu L, Wu XM, Yang L, Du F, Qian ZM. (2007). Up-regulation of HIF-1α expression induced by ginkgolides in hypoxic neurons. *Brain Res*, 1166: 1-8.

Zhu MJ, Du M, Nathanielsz PW, Ford SP. (2010). Maternal obesity up-regulates inflammatory signaling pathways and enhances cytokine expression in the mid-gestation sheep placenta. *Placenta*, 31: 387-391.

Ziccardi P, Nappo F, Giugliano G, Esposito K, Marfella R, Cioffi M, D'Andrea F, Molinari AM, Giugliano D. (2002). Reduction of inflammatory cytokine concentrations and improvement of endothelial functions in obese women after weight loss over one year. *Circulation*, 105: 804-809.

Zoratti M, Szabo I. (1995). The mitochondrial permeability transition. *Biochim Biophys Acta*, 1241: 139-176.

CHAPTER 2

HYPOXIA INDUCED OXIDATIVE STRESS AND ENDOPLASMIC RETICULUM STRESS IN 3T3-L1 ADIPOCYTES AND POSSIBLE PROTECTION WITH BILOBALIDE AND CURCUMIN

2.1 Introduction

Obesity is a major public health concern because of its strong predispositions to certain diseases, such as type 2 diabetes, cardiovascular diseases and numerous cancers (Bergman et al., 2001; Bianchini et al., 2002). Obesity is characterised by excessive expansion of adipocyte size and adipose tissue mass (Weisberg et al., 2003). This enlargement of adipocyte size (140-180 μm) exceeds the normal oxygen diffusion distance (100 μm) and compromises the effective oxygen supply. This leads to local hypoxia which is considered as a possible contributor to obesity-related metabolic complications (Trayhurn and Wood, 2004).

The response to low O_2 levels is accomplished through the activation of hypoxia inducible factor-1 (HIF-1). HIF-1 is a heterodimeric transcription factor, consisting of α and β subunits, which directs a broad range of responses in hypoxic cells (Maxwell et al., 1997). The HIF-1α subunit is considered as the molecular oxygen sensor (Semenza, 2004). When cellular O_2 levels are sufficient, this protein is continuously synthesized but is immediately targeted for proteasome degradation. The low O_2 level induces stabilization, nuclear translocation, and activation of this transcription factor (Rocha, 2007). HIF-1α expression is directly linked to adiposity and is decreased following weight loss (Jiang et al., 2011).

An important metabolic change in hypoxia is the shift from aerobic to anaerobic glycolysis. The anaerobic glycolysis is maintained by conversion of pyruvate to lactate, a reaction catalysed by lactate dehydrogenase A (Koukourakis et al., 2005). This is also an adaptation to low O_2 tension. This increased release of lactate, is maintained by pyruvate dehydrogenase kinase-1 (PDK1), by inhibiting the conversion of pyruvate to acetyl CoA. PDK1 is up-regulated in hypoxia and is under the control of the HIF-1 (Kim et al., 2006).

The growing body of evidence suggests oxidative stress, associated with increased formation of reactive oxygen species (ROS), also contributes1 to the pathophysiology of hypoxic injury (Millar et al., 2007; Guzy et al., 2005; Zhang et al., 2013). Overproduction

of ROS has been shown to be accompanied with a decline in endogenous antioxidant defense system. Increased ROS accumulation also leads to proteins, nucleic acids and intracellular membranes modifications, subsequently impairing cellular functions (Prabhakar et al., 2007).

HO-1 is a stress-associated protein induced by hypoxia and its expression is regulated by HIF-1 (Lee et al., 1997). In addition to hypoxia, HO-1 is dramatically induced by a variety of other stresses. At the transcriptional level, HO-1 gene expression is mainly regulated by the Nrf2/ARE pathway, and induction of this enzyme protects cells against oxidative stress-induced cell death and tissue injury (He et al., 2014). Under normal physiological conditions, Nrf2 is sequestered in the cytosol by Keap1 and is targeted for proteasomal degradation. In the presence ROS, Nrf2 is released from Keap1 and then translocate into the nucleus, activating the transcription of target antioxidant genes, including HO-1 (Jeong et al., 2006; Cheng et al., 2011). Therefore, activation of Nrf2 is critical for cellular rescue pathways against oxidative stress.

Endoplasmic reticulum (ER) stress is known to be initiated by hypoxia and oxidative stress. In oxidative stress, ROS oxidizes nascent proteins and increases misfolded and unfolded proteins in the ER. ROS also acts on calcium channels in the ER membrane, followed by stimulation of calcium release from the ER. Decreased concentration of the total calcium in the ER lumen ultimately impairs protein folding of nascent proteins (Malhotra and Kaufman, 2007). Protein folding in the ER requires disulfide bond formation catalysed sequentially by ERO 1 and protein disulfide isomerase (PDI). The final electron acceptor downstream of ERO 1 is molecular oxygen. Although ERO 1 is transcriptionally induced by HIF during hypoxia, in the absence of oxygen, it cannot fold proteins containing disulfide bonds (Gess et al., 2003). These findings underscore the critical role of molecular oxygen in sustaining ER folding and strongly suggest that the accumulation of misfolded proteins in the ER is a natural consequence of hypoxia.

Hence UPR pathway links with other stress signals induced by hypoxia (HIF pathway) and oxidative stress (Nrf2 pathway), and contributes to the progression of various diseases (Chiang and Inagi, 2010; Inagi et al., 2013). So understanding the relationship between hypoxia, oxidative stress and unfolded protein response is essential to develop new therapeutic targets against adipose tissue hypoxia related complications in obesity.

In this chapter, we reported how hypoxia affects the physiological functions of 3T3-L1 adipocytes, emphasizing on HIF-1α expression, lactate release, oxidative stress and ER stress. We also evaluated the protective role of bilobalide and curcumin on hypoxia induced alterations in 3T3-L1 adipocytes.

2.2 Materials and Methods

2.2.1 Chemicals and cell culture reagents

Curcumin, bilobalide, acriflavine, 3-isobutyl-1-methylxanthine (IBMX), dexamethasone, insulin, 3-(4,5-dimethylthiazol-2-yl)-2,5-diphenyl tetrazolium bromide (MTT), dimethyl sulfoxide (DMSO), 2′,7′dichlorodihydrofluorescein diacetate (DCFH-DA), bovine serum albumin, trizma, phenazine methosulphate (PMS), nitroblue tetrazolium (NBT), nicotinamide adenine dinucleotide (NADH) and Dulbecco's Modified Eagle's Medium (DMEM) were purchased from Sigma Aldrich (St. Louis, MO, USA). Foetal calf serum (FCS) was from Gibco (Langley, OK, USA) and foetal bovine serum (FBS) and supplements were from Hi-media Pvt Ltd (Mumbai, India). All other chemicals used were of analytical grade.

2.2.2 Cell culture

3T3-L1 preadipocytes (ATCC) were maintained in DMEM (4.5 g/L; high glucose) supplemented with 10% FBS, antibiotic (100 U penicillin/mL and 100 μg streptomycin/mL) and incubated at 5% CO_2 and 37°C. To induce differentiation, 2-days post confluent 3T3-L1 preadipocytes were stimulated for 48 hours (hrs) with 0.5 mM isobutyl methyl xanthine, 0.25 mM dexamethasone, and 1 μg/ml insulin in DMEM. Then differentiated adipocytes were maintained in and refed every 2 days with DMEM containing 1 μg/ml insulin.

2.2.3 Hypoxia induction and treatment

In order to induce hypoxia, differentiated 3T3-L1 adipocytes at 9th day were incubated in a hypoxic chamber (Galaxy 48R, New Brunswick, Eppendorf, Germany) at an atmosphere of 1% O_2, 94% N_2, 5% CO_2, and at 37°C for 24 hrs. The control cells were incubated in an atmosphere of 21% O_2 and 5% CO_2 at 37°C. The cells were treated with different concentrations (10, 20, & 50 μM) of bilobalide, (5, 10, & 20 μM) of curcumin or

acriflavine (5 µM; positive control) during hypoxic period (24 hrs). For mRNA expression and protein expression studies, only higher doses of test materials were used. Acriflavine was used as positive control, which is an HIF-1α inhibitor and prevent transcriptional activities of HIF-1 (Jiang et al., 2013; Lee et al., 2009).

2.2.4 Cell viability by MTT assay

The cytotoxicity of bilobalide (10, 20, & 50 µM), curcumin (5, 10, & 20 µM) and acriflavine (5 µM) were assessed in differentiated 3T3 L1 cells after 24 hrs of treatment by MTT assay. The protective property of bilobalide, curcumin, and acriflavine against hypoxia induced cell death was also checked. In brief, MTT solution (5 mg/mL) was added to each well and incubated for 4 hrs at 37°C. The blue-coloured tetrazolium crystals resulting from mitochondrial enzymatic activity on the MTT substrate were dissolved in DMSO. Then the plates were read at 570 nm after 45 minutes (mins) on multimode reader (Biotek Synergy 4, USA).

2.2.5 Molecular docking study

Docking experiments of bilobalide, curcumin and acriflavine into the HIF-1α was performed using Autodock 4.2 and iGEMDOCK v2.1 software with default docking parameters. These docking softwares were used to determine the appropriate binding and conformations of the ligand to the receptor. The 3D model of HIF-1α (PDB id:4AJY) was retrieved from the Brookhaven Protein Data Bank (PDB) (http:// www.rcsb.org/pdb/), acriflavine (CAS No: 8063-24-9.mol), bilobalide (ChemSpider ID: 66258.mol) and curcumin (ChemSpider ID:839564.mol) structures were downloaded from Chemical Book (http://www.chemicalbook.com/) and Chemspider (http://www.chemspider.com/) and converted to PDB file using Chem3D Pro 10. The docking fitness of the ligand molecules to HIF-1α and the amino acids of the receptor (HIF-1α) involved in interactions were predicted using iGEMDOCK. The interaction table and the binding energy of HIF-1α were analysed using iGEMDOCK.

2.2.6 HIF-1α transcription factor Assay

After normoxic and hypoxic treatments, nuclear extracts of the cells were isolated using Cayman's nuclear extraction assay kit (Cayman chemical company, MI, USA). The HIF-1α was then estimated in nuclear extract using HIF-1α transcription factor assay kit

(Cayman chemical company, MI, USA). Cayman's HIF-1α transcription factor assay is a non-radioactive, sensitive method for detecting specific transcription factor DNA binding activity in nuclear extracts and whole cell lysate. A specific double stranded DNA (dsDNA) consensus sequence containing the HIF-1α response element was immobilized to the wells of a 96-well plate. HIF-1α contained in a nuclear extract bound specifically to the HIF-1α response element. The HIF transcription factor complex was then detected by addition of a specific primary antibody directed against HIF-1α. A secondary antibody conjugated to HRP was added to provide a sensitive colorimetric readout at 450 nm.

2.2.7 Detection of lactate release

The concentration of lactate was determined in conditioned medium with lactate assay kit (Cayman chemical company, MI, USA). Lactate assay provides a fluorescence-based method for detecting lactate in biological samples. In this assay, lactate dehydrogenase catalyzes the oxidation of lactate to pyruvate, along with the concomitant reduction of NAD+ to NADH. NADH reacts with the fluorescent substrate to yield a highly fluorescent product. The fluorescent product were then analysed with an excitation wavelength of 530-540 nm and an emission wavelength of 585-595 nm.

2.2.8 Detection of intracellular reactive oxygen species (ROS)

Intracellular ROS content was determined by oxidative conversion of cell-permeable DCFH-DA to fluorescent 2',7' dichlorofluorescein (DCF) (Wang and Joseph, 1999). In brief DCFH-DA stain in serum-free medium was added in the cell and incubated at $37^{o}C$ for 20 mins. After three washes, images of the cells were collected using spinning disk microscope (BD Pathway 855; BD Biosciences, USA) using AttoVision 1.5.3 software.

2.2.9 Estimation of lipid peroxidation and protein carbonyl content

The levels of lipid peroxidation in cell lysates were estimated according to the method of Niehius and Samuelsson, 1968. In brief, cells after treatment, were washed twice in cold PBS, scraped off the dishes, and then suspended in 12 ml of PBS supplemented with 150 μM butylated hydroxytoluene (BHT). After centrifugation at 2,000 g for 5 mins, the supernatant was discarded, and the cells were resuspended in 150 μl of PBS with BHT. The cell suspension (100 μl) was combined with freshly made 50 μl 30%

trichloroacetic acid, 0.75% thiobarbituric acid, and 0.5 N HCl, and incubated for 15 mins at 100°C. The reaction mixture was then centrifuged for 8 mins at 13,500 g. The absorbance of the supernatant was measured at 532 nm.

The protein carbonyl content in cell lysate was estimated using protein carbonyl assay kit (Cayman Chemical Company, USA) as per the manufacturer's instructions.This assay utilizes the DNPH reaction to measure the protein carbonyl content in the sample. The amount of protein-hydrozone produced was quantified spectrophotometrically at an absorbance between 360-385 nm.

2.2.10 Estimation of superoxide dismutase (SOD) and catalase (CAT) activity :

Superoxide dismutase (SOD) activity was estimated by method of Kakkar et al., 1984. The assay of SOD is based on the inhibition of the formation of NADH-PMS-NBT formazan. In brief, the assay mixture contained 1.2 ml of sodium pyrophosphate buffer, 0.1 ml of PMS, 0.3 ml of NBT, 0.2 ml of the cell extract and water in a total volume of 2.8 ml. The reaction was initiated by the addition of 0.2 ml of NADH. The mixture was incubated at 30°C for 90s and arrested by the addition of 1.0 ml of glacial acetic acid. The reaction mixture was then shaken with 4.0 ml of n-butanol, allowed to stand for 10 mins and centrifuged. The intensity of the chromogen in the butanol layer was measured at 560 nm in a multimode reader.

CAT activity was determined by the method of Cohen et al., 1970, where decomposed hydrogen peroxide is measured by reacting it with excess of $KMnO_4$ and residual $KMnO_4$ is measured spectrophotometrically at 480 nm.

2.2.11 Estimation of glutathione peroxidase (GPx) activity

GPx activity was quantified according to the method of Gunzler et al., 1974. In brief, to 0.2 ml of the Tris buffer (0.4 M), 0.2 ml of EDTA (0.4 mM), 0.1 ml of sodium azide (10 mM), and 0.5 ml of cell lysate were added and mixed; to this, 0.2 ml of GSH was added, followed by H_2O_2. The reaction was stopped after 10 mins by adding 0.5 ml of 10% trichloroacetic acid (TCA). After centrifugation, the supernatant was read at 412 nm.

2.2.12 Estimation of glutathione reductase (GR) activity

The GR activity was done according to the procedure of David and Richard, 1983. In brief, the assay system contained 0.1 M phosphate buffer, 15 mM ethylene diamine

tetraacetic acid (EDTA), 65.3 mM oxidized glutathione, and 0.1 ml of sample, and the volume was made up to 2 ml using distilled water. The tubes were incubated for 3 mins and 0.1 ml of 9.6 mM nicotinamide adenine dinucleotide phosphate (NADPH) was added. The absorbance was read at 340 nm in Tecan multiplate reader (Tecan Infinite 200 PRO, Tecan, Austria). Controls were set up that contained water instead of oxidized glutathione.

2.2.13 Estimation of reduced glutathione (GSH) activity

GSH content in the cell lysate was measured following the method described by Moran et al., 1979. GSH is measured by its reaction with DTNB (Ellman's reaction) to give a compound that absorbs at 420 nm.

2.2.14 Estimation of total antioxidant activity

Total antioxidant activity was determined in cell lysate using total antioxidant assay kit (Cayman chemical company, MI, USA) as per the manufacturer's instructions. This assay was based on the ability of antioxidants in the sample to inhibit the oxidation of ABTS* (2, 2'- Azino-di-[3-ethylbenzthiazoline sulphonate]) to reduced ABTS**+ by metmyoglobin. The amount of ABTS**+ produced was monitored by measuring the absorbance at 405 nm. In brief, after respective treatment the cells were collected by centrifugation (2000×g) for 10 mins at 4 °C. The pellets were sonicated and centrifuged at 10,000×g for 15 mins at 4 °C. For assay, 10 μl of the sample (supernatant) and 10 μl standards was added in two different wells. 10 μl metmyoglobin and 150 μl of chromogen were added to both wells. The reaction was initiated by adding H_2O_2. The wells were incubated for 5 mins at room temperature and then absorbance was read at 405 nm.

2.2.15 Nrf2 translocation assay

Nrf2 transcription factor was determined in cytosolic and nuclear extract using Nrf2 transcription factor assay kit (Cayman chemical company, MI, USA). In brief, after hypoxic and normoxic treatments, cytosolic and nuclear extracts of the cells were isolated using Cayman's nuclear extraction assay kit (Cayman chemical company, MI, USA). The Nrf2 containing cytosolic and nuclear extracts were then added to the well coated with specific double stranded DNA (dsDNA) sequence containing the Nrf2 response element. Nrf2 contained in the extracts, bound specifically to the Nrf2 response element. Nrf2 was detected by addition of a specific primary antibody directed against Nrf2. A secondary

antibody conjugated to HRP was added to provide a sensitive colorimetric readout at 450 nm.

2.2.16 Determination of heme oxygenase-1 (HO-1) activity

HO-1 activity assay was determined according to the method reported by Foresti, 1994. The amount of extracted bilirubin was calculated using the difference in absorption between 464 and 530 nm using an extinction coefficient of 40 mM^{-1} cm^{-1} for bilirubin.

2.2.17 Determination of expression of p-eIF-1α by indirect ELISA

Indirect ELISA was carried out using specific primary antibody (1:500 dilutions) and HRP-conjugated secondary antibody (1:1000 dilutions) by the method of Engvall and Perlman, 1971, with slight modification. The amounts of phosphorylated eIF-2α expressed in the cells were quantitated by Indirect ELISA. Cell lysate precoated to ELISA plates (96 well, NUNC) served as antigen. After blocking (5% non-fat dry milk) and washing (50 mM Tris, pH 7.5, 150 mM NaCl, 0.01% Tween-20), the plates were incubated with specific primary antibody against p-eIF-2α for 2 hrs at room temperature. The plates were washed and then treated with HRP-conjugated secondary antibody. The colour developed using 3, 3' 5 5'- tetramethylbenzidine (TMB) substrate solution (BD bioscience) was measured spectrophotometrically at 450 nm in a plate reader (Biotek, USA).

2.2.18 Quantitative real-time PCR

Total RNA from 3T3-L1 adipocytes was extracted using Trizol reagent (Invitrogen, Carlsbad, CA). 2 μg of total RNA was reverse transcribed using Super Script III reverse transcriptase and random hexamers (Life technologies, Invitrogen, USA). The gene expression levels were analysed by quantitative real-time RT-PCR, conducted using the CFX96 Real Time PCR system (Bio-rad, USA) using the following conditions: an initial denaturation for 10 min at 95ºC, followed by 39 cycles of 15 s denaturation at 95ºC, 30 s annealing at the optimal primer temperature and 10 s extension at 72ºC. Each sample was assayed in triplicate in a 20 μL reaction volume containing 1 μL cDNA, 10 μL SYBR Green master mix (Power SYBR® Green PCR Master Mix, life technologies, Invitrogen, USA), 5.81 μL DEPC water and 1.6 μL of each primer. Negative controls (no template) were run as well to ensure the absence of contamination. Analysis was performed according to the ΔΔCt method using β-actin as the housekeeping gene. Specific primers for

each gene were designed to amplify a single product, as confirmed by dissociation curve analysis after the real-time PCR run.

$$\text{Fold change} = 2^{-\Delta(\Delta CT)}$$

where ΔCT = CT, target - CT, β-actin and $\Delta\Delta CT = \Delta CT$, stimulated- ΔCT, control, CT (threshold cycle) is the intersection between an amplification curve and a threshold line.

Table. 2.1 Nucleotide sequence of qRT-PCR primers

mRNA		Primer sequence
Hif-1a	Forward	5'-TCAAGTCAGCAACGTGGAAG-3'
	Reverse	5'-TATCGAGGCTGTGTCGACTG-3'
Pdk-1	Forward	5'-AGCAGGTAATGACACCTGGG-3'
	Reverse	5'-CCTCTAGGCAAGTGGCAAAG-3'
Grp78	Forward	5'-CCACTTCATCTTACCATTTA-3'
	Reverse	5'-ATCTGCATCTGAGTTTAATC-3'
Chop	Forward	5'-GTCCAGCTGGGAGCTGGAAG-3'
	Reverse	3'-GTCCAGCTGGGAGCTGGAAG-3'
β-Actin	Forward	5'-AGTACCCCATTGAACGC-3'
	Reverse	5'-TGTCAGCAATGCCTGGGTAC-3'

2.2.19 Western blot analysis

Fully differentiated 3T3-L1 cells after respective treatments were lysed in RIPA buffer containing protease inhibitor cocktail (Sigma Aldrich, St Louis, MO, USA). After incubation, the cell suspensions were centrifuged at 12000 rpm for 15 min at 4°C, and the supernatants were collected. Proteins content in the supernatants were quantified using the bicinchoninic acid protein (BCA) assay kit (Pierce, Rockford, IL, USA) in accordance with the manufacturer's instructions. Equal amount of proteins (50 μg) were separated by 10% sodium dodecyl sulfate-polyacrylamide electrophoresis (SDS-PAGE) and transferred to Polyvinylidene difluoride (PVDF) membranes using turbo transblot apparatus (BD Bioscience). The membranes were blocked with 5% BSA in TBST for 1 hrs at room temperature. The membrane was washed 3 times with TBST for 10 mins each. The membrane was incubated at 4ºC overnight in 5% BSA in TBST containing primary antibodies to one of the following: HIF-1α 1:200, PDK1 1:500, HO1 1:500, GRP78 1:500, ERO1-Lα 1:500, PDI 1:500, IRE-1α 1:500, PERK 1:500, ATF6 1:500, CHOP 1:500 or β-ACTIN 1:1000. After washing with TBST, the membrane was incubated with peroxidase-conjugated corresponding secondary antibodies for 1 hr at room temperature. After

washing, membranes were developed using 3, 3'-diaminobenzidine tablets (DAB) (Sigma Aldrich, St Louis, MO, USA) and H_2O_2. The immunoblot results were analysed in quantity one software using Gel doc (BD Bioscience).

2.2.20 Statistical analysis

Results were expressed as mean ± standard deviation of the control and treated cells. Data were subjected to one-way ANOVA and the significance of differences between means were calculated by Duncan' s multiple range test using SPSS for Windows, standard version 7.5.1 (SPSS, Inc.), and significance was accepted at P≤0.05.

2.3 Results

2.3.1 Cell viability in normoxic and hypoxic adipocytes

Cell viability was assessed in normoxic group, hypoxic group, bilobalide and curcumin treated hypoxic groups by MTT assay. The different doses of bilobalide (10, 20 and 50 µM), curcumin (5, 10, and 20 µM) and acriflavine (5 µM) did not cause any significant toxicity after 24 hrs of treatment (data not given).
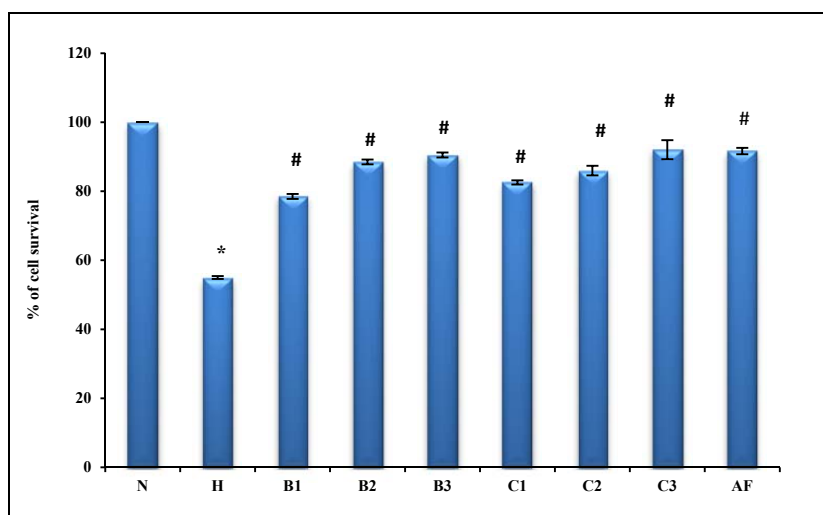
Fig. 2.1 Cell viability evaluated by MTT assay: The bar diagram represent % of viability of 3T3-L1 cells under hypoxia and treated with different concentrations of bilobalide (B1-10 µM, B2-20 µM, B3-50 µM) and curcumin (C1-5 µM, C2-10 µM, C3-20 µM) and acriflavine (AF-5 µM). The cell viability of normoxia is adjusted to 100%.Values are means, with standard deviations represented by vertical bars (n=6).* Mean value are significantly different from the control cells (P≤0.05). # Mean values are significantly different from hypoxia treated cells (P≤0.05).

Cells exposed to 24 hrs of hypoxia exhibited a significant decrease in cell viability (45%; Fig. 2.1; P≤0.05. The treatment with 10, 20, 50 µM bilobalide and 5, 10, and 20 µM curcumin reduced cell injury significantly (21.5%, 11.5% and 9.5% & 17.4%, 14% and 7.9%; Fig. 2.1; P≤0.05) in a dose dependent manner. Acriflavine treatment also showed protection against hypoxia induced cell injury (8.3%; Fig.2.1; P≤0.05) compared to hypoxic cells.

2.3.2 HIF-1α expression in normoxic and hypoxic adipocytes
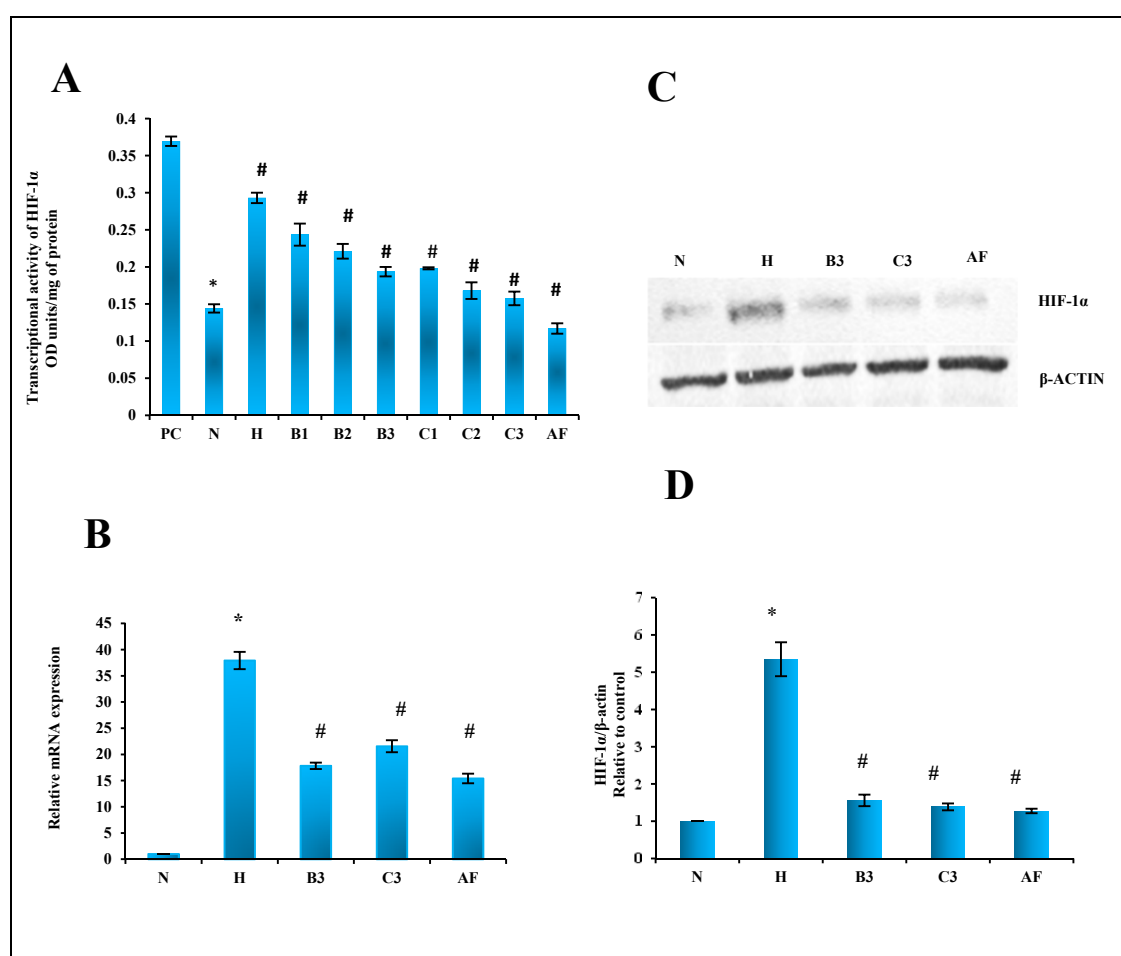
Fig. 2.2 Expression of HIF-1α transcription factor in normoxic and hypoxic groups: A) Determination of HIF-1α transcription factor in nuclear extract B) mRNA expression of Hif1a normalised to β-actin C) Immunoblot analysis of HIF-1α D) Quantification of protein level normalised to β-actin. PC – 150 µL of Dimethyloxaloylglycine (DMOG) stimulated HeLa cell extract provided with kit, N-normoxia, H-hypoxia, , B1-10 µM, B2-20 µM, B3-50 µM of bilobalide, C1-5 µM, C2-10 µM, C3-20 µM of curcumin, and AF-5 µm of acriflavine, treated hypoxic groups. Values are means, with standard deviations represented by vertical bars (n=3).* Mean value are significantly different from the control cells (P≤0.05). # Mean values are significantly different from hypoxia treated cells (P≤0.05).

The expression of HIF-1α, the marker of hypoxia was determined in nuclear extract of normoxic and hypoxic groups. The expression was significantly increased (P≤0.05) by 1.94 fold in hypoxia-treated cells compared with normal cells (Fig. 2.2A). This confirmed the induction of hypoxia in cells. Experiments were also performed to see whether treatment with bilobalide and curcumin could affect the expression of HIF-1α. We found that all the doses of bilobalide (10, 20 and 50 µM) and curcumin (5, 10, and 20 µM) significantly decreased (P≤0.05) the expression of HIF-1α, in hypoxia-treated cells in a dose dependent manner (1.20, 1.32, & 1.51 fold; 1.48, 1.74, & 1.86 fold respectively; Fig. 2.2A). Likewise acriflavine prevented HIF-1α increase in hypoxia treated groups significantly (2.50 fold; Fig. 2.2A). The mRNA and protein level expression of HIF-1α were also checked in normoxic and hypoxic groups. The Hif1a mRNA level was significantly (P≤0.05) increased by 37.8 fold after 24 hrs of hypoxic treatment compared to normoxia. The treatment with bilobalide (50 µM), curcumin (20 µM) and acriflavine significantly (P≤0.05) inhibited hypoxia induced upregulation of Hif1a mRNA level (Fig. 2.2B). Similar results were obtained with western blot analysis. Hypoxic group showed a significant (P≤0.05) increase in protein level of HIF-1α (5.34 fold) compared to normoxia. Bilobalide (50 µM), curcumin (20 µM) and acriflavine (5 µM) significantly reduced the protein level of HIF-1α (Fig. 2.2C & D).

2.3.3 Molecular docking

In order to assess the interaction of these compounds with HIF-1α, docking experiments were performed using Autodock 4.2 and iGEMDOCK v2.1 softwares. Acriflavine, bilobalide and curcumin were made to bind to HIF-1α ligand using Autodock 4.2 software. The free energy binding thus determined were found to be -6.01 kcal/mol, -3.57 kcal/mol and -5.72 kcal/mol (Table 2.2B) for acriflavine, bilobalide and curcumin respectively, showing the high potential binding affinity to the LBD. The docking fitness scores of acriflavine, bilobalide, and curcumin obtained from iGEMDOCKv2 software were found to be -165.72, -64.0106, and -92.5441 kcal/mol (Table. 2.2A) respectively. The best docking pose obtained from Autodock 4.2 and iGEMDOCKv2 was shown in figure 2.3A. The interactions between HIF-1α with bilobalide, curcumin and acriflavine were shown in the interaction table (Table 2.2A) as obtained from iGEMDOCKv2. Since lowest (high negative value) energy of docked molecule indicates high binding affinity with the

target protein/compound, our results showed, bilobalide curcumin and acriflavine exhibited a high binding affinity with LBD of HIF-1α.

Table. 2.2

Compound	Bilobalide	Curcumin	Acriflavine
Energy	**-64**	**-92.5**	**-165.7**
H-S-ASP-126	0	0	-9.54548
H-M-ARG-167	0	0	-3.41931
V-M-THR-124	0	0	-20.2569
V-S-THR-124	0	0	-16.9218
V-S-ASP-126	0	0	-10.3045
V-M-GLN-164	0	0	-6.35545
V-M-ARG-167	0	0	-16.6087
V-S-ARG-167	0	0	-35.8088
V-M-SER-168	0	0	-9.90935
V-S-HIS-191	0	0	-9.26746
V-M-GLY-127	-7.34741	0	0
V-S-TYR-156	-8.13498	0	0
V-S-GLU-160	-7.13907	0	0
V-S-ASP-197	-4.65993	0	0
V-S-ARG-200	-4.6432	0	0
V-M-GLY-33	0	-10.0688	0
V-M-ILE-34	0	-8.84361	0
V-S-ILE-34	0	-6.69121	0
V-S-MET-17	0	-6.87731	0
V-M-TYR-18	0	-7.18374	0
V-S-TYR-18	0	-12.1162	0
V-S-LYS-20	0	-7.55535	0
V-M-ASN-58	0	-10.5363	0

Compound	Energy(kcal/mol)	VDV	H-bond	Electr
Bilobalide	-64.01	-64.01	0	0
Curcumin	-92.5	-92.5	0	0
Acriflavine	-165.72	-150.93	-14.79	0

Fig. 2.3 Docking of bilobalide, curcumin and acriflavine to the LBD of HIF-1α: A) Best binding pose of bilobalide, curcumin and acriflavine with HIF-1α LBD; a, c, e Autodock 4.2 representing best binding pose of bilobalide, curcumin and acriflavine with HIF-1α LBD b, d, f : iGEMDOCK v2.1 representing the best docking pose of bilobalide, curcumin and acriflavine with HIF-1α LBD.

Tab. 2.2 Pharmacological interactions in post-screening analysis: A) Interaction table of bilobalide, curcumin and acriflavine from iGEMDOCK. Energy represents the binding energy (kcal mol^{-1}). B) iGEMDOCK fitness results of bilobalide, curcumin and acriflavine with HIF-1α. VDW- van der Waals interaction; H bond - hydrogen bonding; Elect - electrostatic interaction

2.3.4 Lactate release and PDK1 expression in normoxic and hypoxic adipocytes

In our study, we determined lactate release, the end product of anaerobic glycolysis under normoxic and hypoxic conditions. The hypoxic 3T3-L1 adipocytes were found to secrete significant quantity of lactate into media (2.84 fold P≤0.05) compared with normoxic cells. Like HIF-1α here also bilobalide (1.41, 1.54 & 1.99 fold) curcumin (1.25, 1.4 & 1.57 fold) and acriflavine (2.3 fold) significantly reduced the lactate release in hypoxic groups in a dose dependent manner (P≤0.05; Fig. 2.4A). We also analysed the expression of PDK1 by qRT-PCR and immunoblot analysis. PDK1 is the protein that maintains increased lactate release in hypoxic condition. Result showed an increased expression of PDK1 in protein level as well as mRNA level in hypoxia treated cells compared with normoxic cells. The treatment with bilobalide (50 µM), curcumin (20 µM), and acriflavine (5 µM) significantly (P≤0.05) reduced PDK 1 expression in hypoxic 3T3-L1 adipocytes (Fig. 2.4B & C).
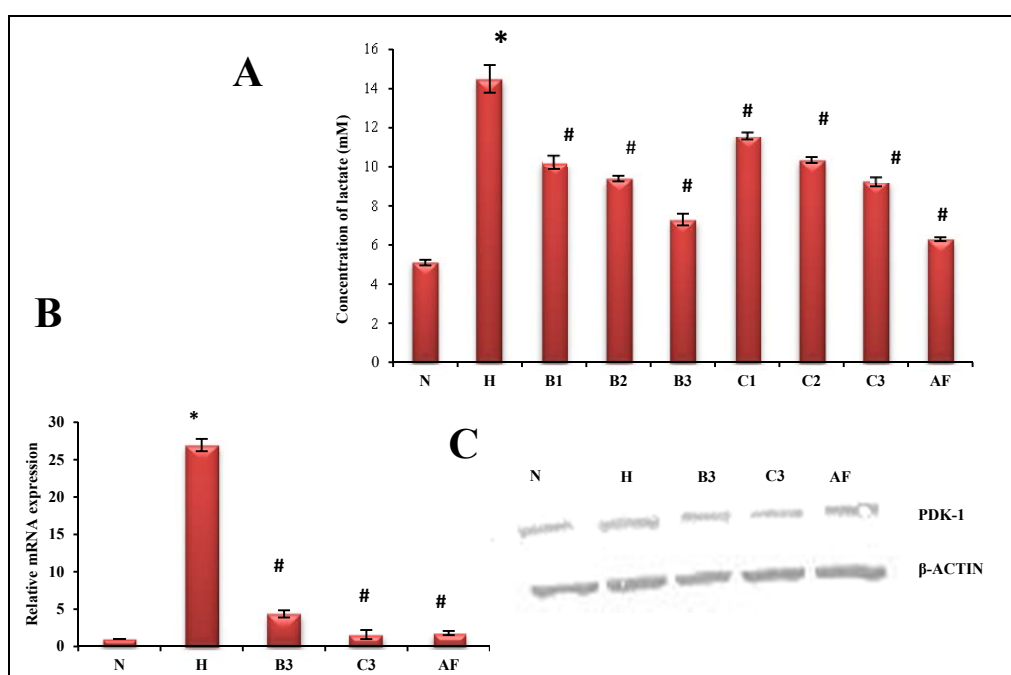
Fig. 2.4 Lactate release and expression of PDK-1 in normoxic and hypoxic adipocytes: A) Estimation of concentration of lactate release by colorimetric assay in different groups. B) mRNA expression of Pdk-1 normalised to β-actin C) Immunoblot analysis of PDK-1. N-normoxia, H-hypoxia, B1-10 µM, B2-20 µM, B3-50 µM of bilobalide, C1-5 µM, C2-10 µM, C3-20 µM of curcumin, and AF-5 µm of acriflavine, treated hypoxic groups. Values are means, with standard deviations represented by vertical bars (n=3).* Mean value are significantly different from the control cells (P≤0.05). # Mean values are significantly different from hypoxia treated cells (P≤0.05).

2.3.5 Intracellular ROS generation in normoxic and hypoxic adipocytes
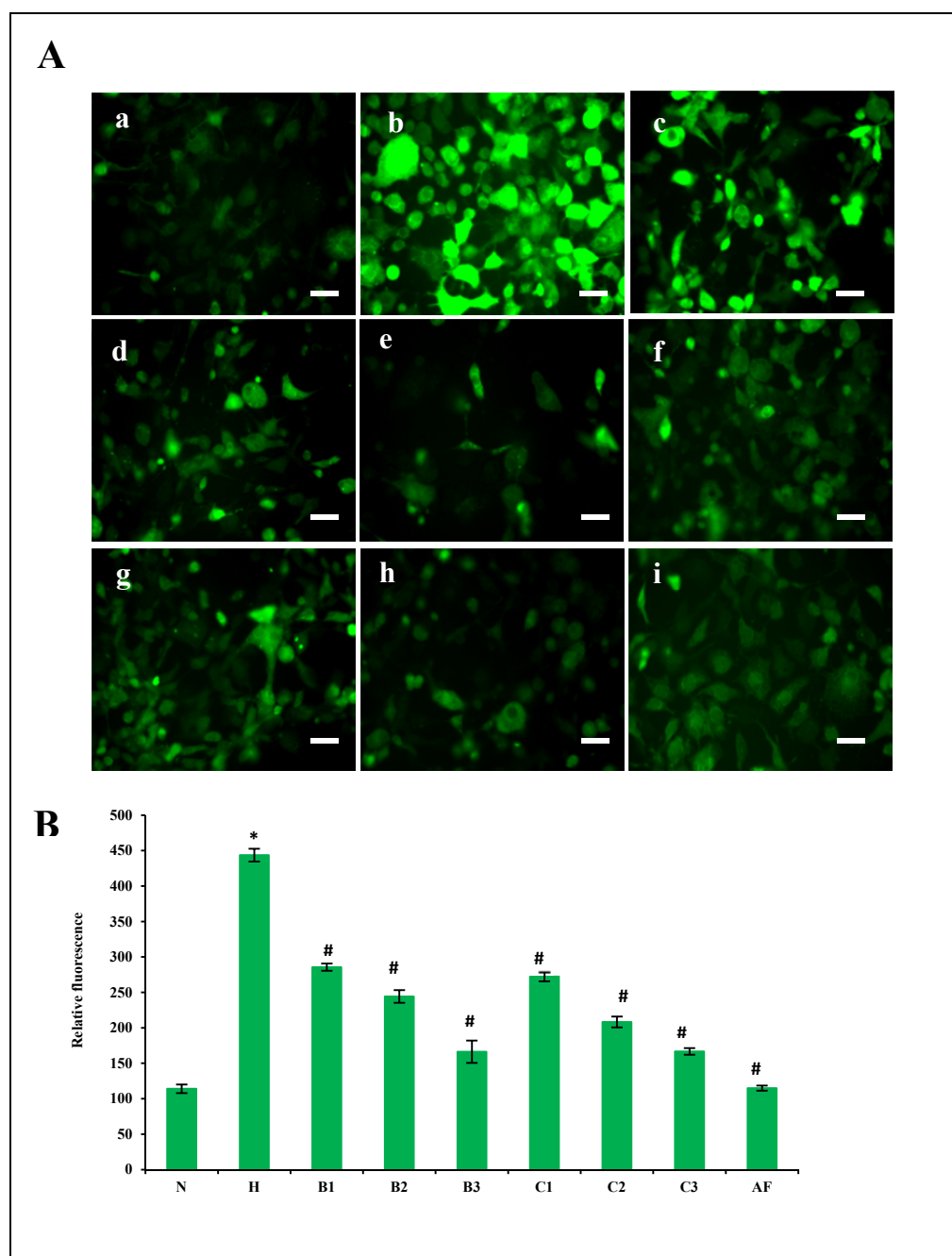
Fig. 2.5 Intracellular ROS generation determined by DCFDA incorporation in normoxic and hypoxic groups: A) The representative images of ROS-induced fluorescence. a-normoxia; b-hypoxia; c, d, e-10, 20 & 50 µM of bilobalide treated hypoxic groups; f, g, h-5, 10 & 20 µM of curcumin treated hypoxic groups; i- acriflavine (5 µM) treated hypoxic group respectively. Scale bar: 100 µm. B) Relative fluorescence intensity of ROS. Values are means, with standard deviations represented by vertical bars (n=6). *Mean value is significantly different from the control cells (P≤0.05). # Mean values are significantly different from hypoxia treated cells (P≤0.05).

Hypoxia caused significant ROS generation compared with normoxia. The ROS production monitored by imaging showed hypoxia caused 3.89 fold increase of ROS generation compared to normoxia (P≤0.05; Fig. 2.5A & B). The different doses of bilobalide (10, 20 and 50 μM) and curcumin (5, 10, and 20 μM) treatment, dose dependently (1.55, 1.81 & 2.67 fold; 1.62, 2.12, & 2.66 fold respectively; P≤0.05) prevented ROS generation in hypoxia. The acriflavine-treated cells also prevented ROS production (3.85 fold) in hypoxic groups (Fig. 2.5A & B).

2.3.6 Endogenous antioxidant status in normoxic and hypoxic adipocytes

Evaluation of endogenous antioxidant status during hypoxia provides an indication of oxidative damage. For this, we measured the concentration of TBARS, protein carbonyl content and the activities of various antioxidant enzymes like catalase, superoxide dismutase, glutathione peroxidase, glutathione reductase, reduced glutathione level and total antioxidant activity in hypoxic and normoxic groups. Hypoxia aggravated lipid peroxidation (4.69 fold) and protein oxidation (5.52 fold) significantly (P≤0.05) compared with normoxia. While different doses of bilobalide (10, 20 and 50 μM) and curcumin (5, 10, and 20 μM) treatment reduced lipid peroxidation (1.41, 1.77, 2.46 & 1.33, 1.67, 2.41 fold respectively) and protein oxidation (1.21, 1.42, 1.63 & 1.21, 1.22, 1.43 fold) in dose dependent manner in hypoxic cells significantly (P≤0.05; Table 2.3). Acriflavine-treated cells showed less oxidation of lipids (4.55 fold) and proteins (1.65 fold) compared to hypoxia. Hypoxia was found to inhibit both SOD (2 fold) and CAT activity (1.64 fold) significantly (P≤0.05; Table 2.3) in 3T3-L1 adipocytes compared to normoxia. Treatment with different concentrations (10, 20 and 50 μM) of bilobalide and (5, 10, and 20 μM) curcumin restored (P≤0.05) SOD (1.61, 1.66, 1.79 & 1.52, 1.64, 1.76 fold respectively) and CAT activity (1.12, 1.20, 1.33 & .97, 1.06, 1.22 fold respectively; Table 2.3). Acriflavine was able to keep the enzyme unaltered in hypoxia.

Table 2.3 Endogenous antioxidant status in normoxic and hypoxic groups

Parameters	Normoxia Mean ± SD	Hypoxia Mean ± SD	Bilobalide (10 µM) Mean ± SD	Bilobalide (20 µM) Mean ± SD	Bilobalide (50 µM) Mean ± SD	Curcumin (5 µM) Mean ± SD	Curcumin (10 µM) Mean ± SD	Curcumin (20 µM) Mean ± SD	Acriflavine (5 µM) Mean ± SD
TBARS (nM MDA/mg protein)	$0.26 \pm .015$	$1.22 \pm .017^{*}$	$0.863 \pm .02^{\#}$	$0.689 \pm .038^{\#}$	$0.496 \pm 0.06^{\#}$	$0.914 \pm .028^{\#}$	$0.7305 \pm .058^{\#}$	$0.506 \pm .043^{\#}$	$0.268 \pm .03^{\#}$
Proteincarbonyls (nmol/ml)	6.52 ± 0.108	$35.98 \pm 4.2^{*}$	$29.55 \pm 2.1^{\#}$	$25.32 \pm 3.11^{\#}$	$22.14 \pm 1.33^{\#}$	$29.55 \pm 3.71^{\#}$	$29.44 \pm 3.81^{\#}$	$25.14 \pm 2.33^{\#}$	$21.85 \pm .036^{\#}$
SOD (Unit/mg protein)	0.5 ± 0.028	$0.26 \pm 0.008^{*}$	$0.41 \pm 0.015^{\#}$	$0.43 \pm 0.008^{\#}$	$0.46 \pm 0.006^{\#}$	$0.39 \pm .005^{\#}$	$0.42 \pm .0095^{\#}$	$0.45 \pm .11^{\#}$	$0.48 \pm 0.0055^{\#}$
Catalase (µmoles of H_2O_2 decomposed/min/ mg protein)	5.17 ± 0.2	$3.14 \pm 0.22^{*}$	$3.5 \pm 0.07^{\#}$	$3.7 \pm 0.1^{\#}$	$4.1 \pm 0.18^{\#}$	$3.24 \pm .051$	$3.34 \pm .089^{\#}$	$3.82 \pm .064^{\#}$	$4.82 \pm 0.13^{\#}$
GPx (Unit/mg protein)	$14.45 \pm .099$	$8.6 \pm .056^{*}$	$9.7 \pm .049^{\#}$	$10.7 \pm .102^{\#}$	$11.6 \pm .020^{\#}$	$9.43 \pm .105^{\#}$	$10.4 \pm .015^{\#}$	$12.4 \pm .170^{\#}$	$11.75 \pm .075^{\#}$
GR (Unit/mg protein)	$10.2 \pm .085$	$3.9 \pm .128^{*}$	$5.4 \pm .317^{\#}$	$6.11 \pm .153^{\#}$	$6.9 \pm .2^{\#}$	$5.3 \pm .076^{\#}$	$7.2 \pm .067^{\#}$	$8.2 \pm .10^{\#}$	$7.22 \pm .105^{\#}$
GSH (nM/mg protein)	$9.62 \pm .05$	$5.66 \pm .28^{*}$	$5.89 \pm .15^{\#}$	$6.26 \pm .27^{\#}$	$7.07 \pm .14^{\#}$	$6.27 \pm .17^{\#}$	$7.38 \pm .24^{\#}$	$7.78 \pm .25^{\#}$	$8.12 \pm .06^{\#}$
Total antioxidant activity (mM of trolox equivalents)	$0.190 \pm .003$	$0.016 \pm .002^{*}$	$0.041 \pm .002^{\#}$	$.059 \pm .0023^{\#}$	$0.13 \pm .0031^{\#}$	$0.13 \pm .0024^{\#}$	$0.17 \pm .0032^{\#}$	$0.18 \pm .0012^{\#}$	$0.18 \pm .0041^{\#}$

TBARS, Thiobarbituric acid-reactive substances; MDA, Malondialdehyde; SOD, Superoxide dismutase; GPx, Glutathione peroxidase; GSH, Reduced glutathione; GR, Glutathione reductase.

Values are means, with standard deviations represented by vertical bars (n=6).* Mean value are significantly different from the control cells ($P \leq 0.05$). # Mean values are significantly different from hypoxia treated cells ($P \leq 0.05$).

Similarly the activities of antioxidant enzymes like GPx, GR and GSH content were reduced in hypoxia treated cell (1.67, 2.60, 1.70 fold respectively; P≤0.05) when compared with normoxic cells. The treatment with different doses of bilobalide and curcumin significantly improved (P≤0.05) antioxidant status in a dose dependant manner (Table 2.3). Acriflavine treatment also improved antioxidant status. There was a significant (P≤0.05) depletion of total antioxidant activity (12.15) fold in hypoxic group compared with normoxia and the activity were restored almost normal level by treatment with bilobalide (2.65, 3.77, & 8.05 fold), curcumin (8.11, 10.75, & 11.23 fold) and acriflavine (11.22 fold) in a dose dependent manner (P≤0.05; Table 2.3). These results validate the potential free radical scavenging effect of bilobalide and curcumin.

2.3.7 Nrf2 and HO-1 expression in normoxic and hypoxic adipocytes

In response to oxidative stress, Nrf2 translocated to the nucleus, where it binds to ARE sequences resulting in transcriptional activation of antioxidant genes, such as HO-1. Here we investigated the effect of hypoxia on expression of Nrf2 and HO-1, the proteins involved in cellular defence against oxidative stress. The analysis of Nrf2 in nuclear and cytosolic fraction of hypoxia treated cells, by ELISA showed an increased protein level expression of Nrf2 in nuclear fraction (1.9 folds; P≤0.05; Fig. 2.6) compared to normoxia. But cytosolic expression of Nrf2 was significantly higher in normoxic groups, relative to nuclear fraction. This clearly depicted the nuclear translocation of Nrf2 during hypoxia.
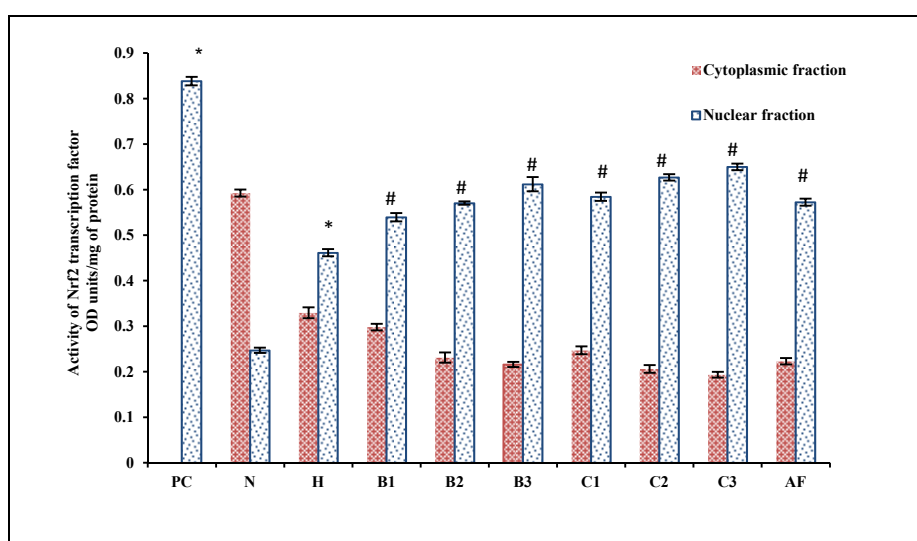
Fig. 2.6 Nrf2 translocation assay in normoxic and hypoxic groups: PC- Nuclear extract of HepG2 cells treated with 90 µM tert-butylhydroquinone, N-normoxia, H-hypoxia, B1-10 µM, B2-

20 μM, B3-50 μM of bilobalide, C1-5 μM, C2-10 μM, C3-20 μM of curcumin and AF-5 μm of acriflavine, treated hypoxic groups. Values are means, with standard deviations represented by vertical bars (n=6).* Mean value are significantly different from the control cells (P ≤0.05). # Mean values are significantly different from hypoxia treated cells (P≤0.05).

Furthermore, expression of HO-1, which is a downstream molecule of Nrf2, was analysed. The mRNA and protein level expression of HO-1 were significantly (P≤0.05) increased (1.38 fold; Fig. 2.7A & B) in hypoxia treated group, indicating increased oxidative stress. The treatment with bilobalide (10, 20 and 50 μM) and curcumin (5, 10 and 20 μM) and acriflavine (5 μM) augmented (P≤0.05) the nuclear translocation of Nrf2 (2.2, 2.3, 2.5 fold; 2.4, 2.5, 2.6 fold; 2.3 fold respectively Fig. 2.6) and expression of HO-1 (1.49, 1.54, 1.58; 1.6, 1.7, 1.8; 1.38 fold respectively, Fig. 2.7A & B), in hypoxia treated groups and hence protected adipocytes from hypoxia induced oxidative stress.
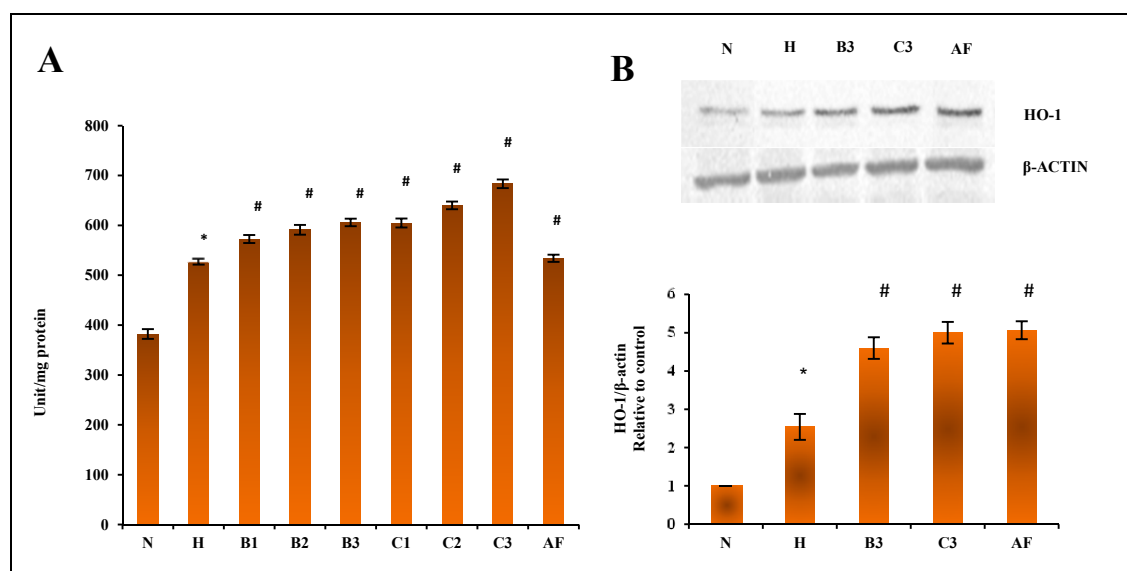
Fig. 2.7 Heme oxygenase-1 activity in normoxic and hypoxic groups: A) Determination of heme oxygenase-1 activity by colorimetric assay B) Immunoblot analysis of HO-1 and quantification of protein level normalized to β-actin. N-normoxia, H-hypoxia, B1-10 μM, B2-20 μM, B3-50 μM of bilobalide, C1-5 μM, C2-10 μM, C3-20 μM of curcumin and AF-5 μm of acriflavine, treated hypoxic groups. Values are means, with standard deviations represented by vertical bars (n=3).* Mean value are significantly different from the control cells (P ≤0.05). # Mean values are significantly different from hypoxia treated cells (P≤0.05).

2.3.8 The expression of ER stress markers in normoxic and hypoxic adipocytes

To examine the effect of hypoxia and hypoxia induced oxidative stress on ER function, the expression of ER stress markers were determined in normoxic and hypoxic 3T3-L1 adipocytes.

We conducted qRT-PCR and immunoblot analysis of expression of molecular chaperone, GRP78/BiP after 24 hrs of hypoxia treatment. The hypoxic group showed a marked elevation (P≤0.05) of the expression of GRP78/BiP compared to control group (Fig 2.8). We also determined the expression levels of other ER stress markers, including ERO1-Lα and PDI, protein involved in disulphide bond formation and ROS production. The expression levels of these ER stress markers were significantly (P≤0.05) up-regulated in hypoxic group compared to normoxia (Fig. 2.9).
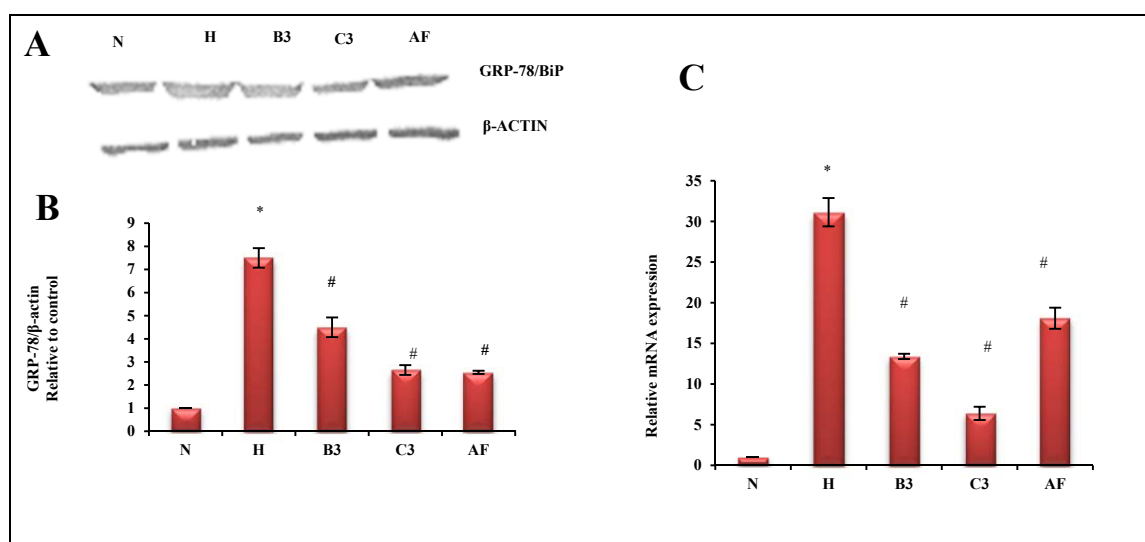
Fig. 2.8 The expression of Grp78/BiP in normoxic and hypoxic adipocytes: A) The immunoblot analysis of GRP78/BiP (B) Quantification of protein level normalized to β-actin (C) Relative mRNA expression of Grp-78 normalized to β-actin.
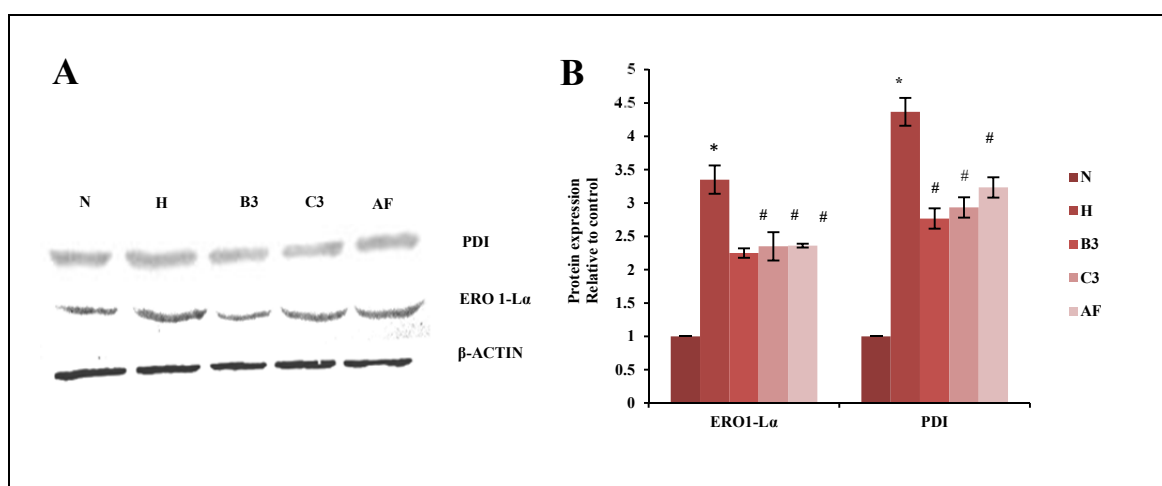
Fig. 2.9 The expression of PDI and ERO1-Lα in normoxic and hypoxic adipocytes: (A) The immunoblot of PDI and ERO1-Lα (B) Quantification of protein level of PDI and ERO1-Lα normalized to β-actin. N-normoxia, H-hypoxia, B3-50 µM of bilobalide, C3-20 µM of curcumin

and AF-5 μm of acriflavine, treated hypoxic groups. Values are means, with standard deviations represented by vertical bars (n=3).* Mean value are significantly different from the control cells (P≤0.05). # Mean values are significantly different from hypoxia treated cells (P≤0.05).

We then focused on downstream events of ER stress and UPR signaling. The expression of UPR sensors IRE-1α, PERK and ATF6, significantly (P≤0.05) upregulated in hypoxic group compared with control indicating the activation of UPR (Fig. 2.10). UPR activation results in a rapid repression of translation of proteins through PERK-mediated eIF-2α phosphorylation. Here we observed an increased (P≤0.05; 3.5 fold; Fig. 2.11) phosphorylation of eIF-2α in hypoxic groups compared with normoxia that clearly suggested ER stress induced activation of UPR after 24hrs of hypoxia treatment in adipocytes.
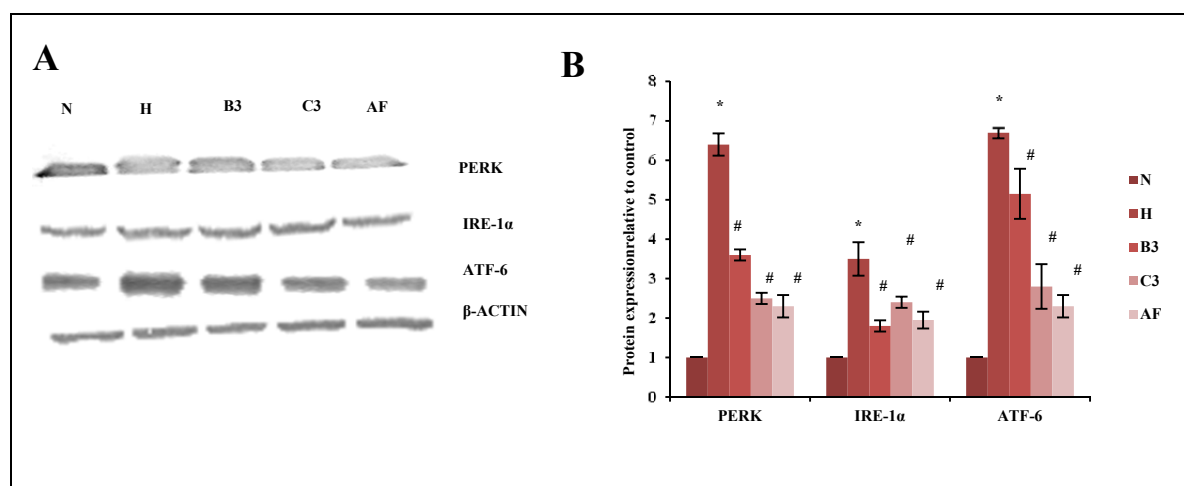
Fig. 2.10 Immunoblot analysis of unfolded protein response markers Lα in normoxic and hypoxic adipocytes (A) The immunoblot of PERK, IRE-1α and ATF-6 (B) Quantification of protein level of PERK, IRE-1α and ATF-6 normalized to β-actin. N-normoxia, H-hypoxia, B3-50 μM of bilobalide, C3-20 μM of curcumin and AF-5 μm of acriflavine, treated hypoxic groups. Values are means, with standard deviations represented by vertical bars (n=3).* Mean value are significantly different from the control cells (P≤0.05). # Mean values are significantly different from hypoxia treated cells (P≤0.05).

Next we studied the expression of CHOP, one of the components of the ER stress-mediated apoptosis pathway. Hypoxia for 24 hrs significantly (P≤0.05) upregulated the expression of CHOP at mRNA and protein level compared with normoxia (Fig. 2.12). Treatment with bilobalide, curcumin and acriflavine significantly (P≤0.05) inhibited hypoxia induced expression of ER stress markers and UPR sensors. Taken together, these results indicate bilobalide and curcumin attenuated hypoxia induced ER stress and UPR signaling pathway in adipocytes.
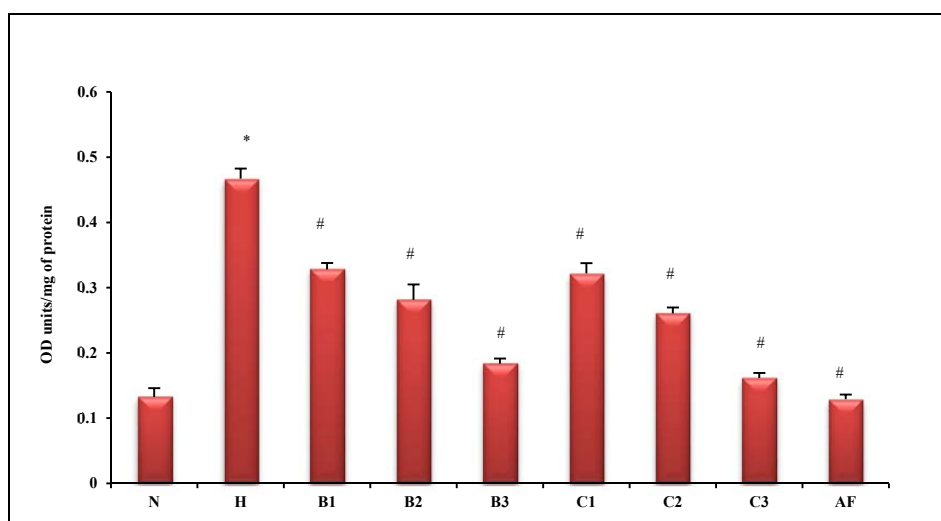
Fig. 2.11 Expression of p-eIF-2α in normoxic and hypoxic groups: N-normoxia, H-hypoxia, B1-10 µM, B2-20 µM, B3-50 µM of bilobalide, C1-5 µM, C2-10 µM, C3-20 µM of curcumin and AF-5 µm of acriflavine, treated hypoxic groups. Values are means, with standard deviations represented by vertical bars (n=6).* Mean value are significantly different from the control cells (P≤0.05). # Mean values are significantly different from hypoxia treated cells (P≤0.05).
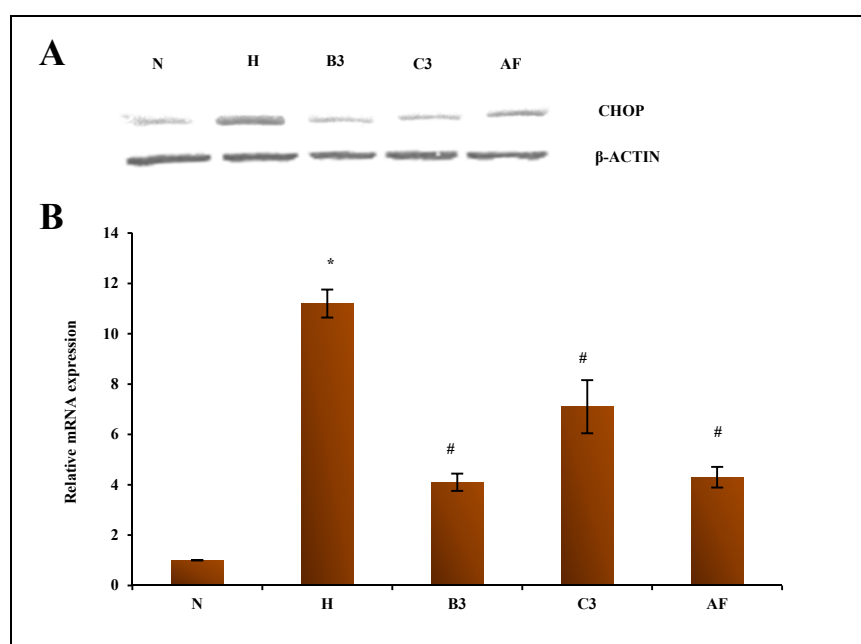
Fig. 2.12 Protein and mRNA level expression of CHOP in normoxic and hypoxic groups: (A) The immunoblot of CHOP (B) mRNA expression of CHOP normalized to β-actin.
N-normoxia, H-hypoxia, B3-50 µM of bilobalide, C3-20 µM of curcumin and AF-5 µm of acriflavine, treated hypoxic groups. Values are means, with standard deviations represented by vertical bars (n=3).* Mean value are significantly different from the control cells (P≤0.05). # Mean values are significantly different from hypoxia treated cells (P≤0.05).

2.4 Discussion

Excessive expansion of adipose tissue is a hallmark of obesity which leads to complications such as type 2 diabetes, cardiovascular diseases, and cancer (Kopelman, 2004). Adipose tissue hypoxia is a major contributor to obesity related dysfunctions in adipocyte. In this investigation, to mimic characteristic features of *in vivo* hypoxia in culture flask (*in vitro*), 3T3-L1 adipocytes were kept at 1% O_2 for 24 hrs. 1% O_2 is equivalent to a PO_2 of 7.6 mm Hg, which is close to the level observed in white adipose tissue of very obese mice (ob/ob) (Trayhurn, 2013). Hypoxia for 24 hrs substantially increased HIF-1α expression, lactate release, oxidative stress, and affected innate antioxidant status severely. We also evaluated the potential of curcumin and bilobalide, against hypoxia induced changes.

Obese individual shows a decreased oxygenation in adipocytes which leads to local hypoxia. It induces inflammatory cytokine secretion and metabolic stress gene transcription in adipose tissue of obese individual (Ye et al., 2007). Large size of adipocytes and a reduction in adipose tissue blood flow may be the factors for reduced oxygenation (Brook et al., 1972). The local hypoxia activates HIF-1 that induces the expression of several other HIF dependent genes which involve in inflammation, angiogenesis, glucose metabolism, apoptosis, cellular stress, and extracellular matrix remodelling. These genes facilitate cell survival in a low oxygen environment, by promoting glycolytic metabolism, angiogenesis, or maintenance of redox status (Bento and Pereira, 2011). But hypoxic conditions in the expanded adipose tissue may also be involved in some of the inflammatory and metabolic complications seen in the obese state (Trayhurn and Wood, 2004).

The induction of hypoxia was confirmed by evaluating the high expression of hypoxic marker, HIF-1α. The treatment with bilobalide and curcumin inhibited the expression of HIF-1α in 3T3- L1 adipocytes. By molecular docking experiment using Autodock 4.2 and iGEMDOCK v2.1, appropriate binding and conformation of bilobalide, curcumin, and acriflavine to the LBD of HIF-1α was found. Bilobalide and curcumin exhibited a high binding affinity with LBD of HIF-1α similar to positive control acriflavine which is a known HIF-1α inhibitor (Morris et al., 2009; Hsu et al., 2011). Unlike other HIF-1 inhibitors, acriflavine binds directly to HIF-1α and HIF-2α and inhibits HIF-1 dimerization and transcriptional activity (Lee et al., 2009). Like acriflavine, bilobalide and

curcumin showed high binding affinity with HIF-1α and also reduced HIF-1α expression in hypoxic adipocytes.

Lactate is an end product of anaerobic respiration. Our study showed an increased release of lactate in hypoxic 3T3-L1 adipocytes. In anaerobic conditions, pyruvate is metabolised to lactate. But in normoxia, pyruvate is converted to acetyl-CoA, by pyruvate dehydrogenase enzyme (PDH). PDH activity is controlled by two regulatory enzymes; pyruvate dehydrogenase kinase (PDK), which phosphorylates and inactivates the enzyme and pyruvate dehydrogenase phosphatase, which dephosphorylates the enzyme to the active form. Recent study identified PDK-1 as a hypoxia responsive protein that regulates the function of the mitochondria under hypoxic conditions (Kim et al., 2006; Papandreou et al., 2006). PDK-1 is up-regulated in hypoxia and contributes substantially to maintaining increased levels of lactate (Wigfield et al., 2008). In our study, PDK-1 expression is substantially increased with an increased lactate production. These finding indicates upregulation of PDK-1 increases lactate release in hypoxic groups, via inhibiting PDH, the enzyme that convert pyruvate to acetyl CoA.

Reactive oxygen species are associated with obesity related chronic inflammation, adiponectin reduction, and other metabolic dysfunctions (Furukawa et al., 2004). Hypoxia induces ROS production in almost all cell types. Previous studies revealed that hypoxia significantly increased oxidative stress in adipocytes and treatment with antioxidants N-acetyl cysteine (NCA) and CAT significantly abolished hypoxia induced ROS production (Chen et al., 2006). This study also showed a significant production of ROS after 24 hrs of hypoxia. Treatment with different doses of bilobalide and curcumin reduced the ROS production significantly. Surplus ROS can also oxidize lipids, proteins and DNAs which leads to many diseases. Most general indicator used as a marker of protein oxidation is protein carbonyl content. There are reports on aggravated level of lipid and protein oxidation in hypobaric hypoxia in lung tissues of rodents (Arya et al., 2013). Similarly, we observed an increase in the lipid peroxidation and protein oxidation in hypoxic cells and bilobalide and curcumin treatment significantly reduced oxidation of lipids and proteins.

In order to protect against oxidative stress, cells have developed antioxidant enzymes and non-enzymatic antioxidants. These act as a first line of defence against oxidative stress in the cell. The activity levels of these enzymes have been used to quantify oxidative stress in cells. Among the various antioxidant enzymes, SOD catalyses

the dismutation of the superoxide anion to H_2O_2 and molecular O_2. H_2O_2 is decomposed to H_2O by catalase and GPx. In the reaction catalysed by GPx, GSH is oxidised to oxidised glutathione, which can be subsequently reduced back to GSH by glutathione reductase. GSH is one of the major non-enzymatic antioxidant and depletion of GSH leads to the impairment of cellular defence against ROS and may lead to oxidative injury (Yu, 1994). In present study, we observed reduction in the activities of innate antioxidant system (SOD, CAT, GPx, GSH and GR) in hypoxia-treated cells. Previous study by Karar et al. (2007) on hypobaric hypoxia in murine heart supports depletion of antioxidant defense system under hypoxia. These enzymes were increased on treatment with different concentrations of bilobalide and curcumin. This may be due to potent antioxidant properties of these phytochemicals.

HO-1 is a stress-inducible enzyme that catalyses the degradation of heme to biliverdin, iron, and carbon monoxide (Foresti et al., 1997). In hypoxia, HIF-1 mediates transcriptional activation of the HO-1 (Lee et al., 1997). Another factor that regulates HO-1 gene expression is the Nrf2/ARE pathway, and induction of this enzyme protects cells against oxidative stress-induced cell death and tissue injury (Chapple et al., 2012; Jeong et al., 2006). Nrf2 plays a central role in inducible expression of many cytoprotective genes in response to oxidative and electrophilic stresses. Under unstressed conditions, Nrf2 is constantly degraded via the ubiquitin–proteasome pathway in a Keap1-dependent manner. When oxidative inactivates Keap1, Nrf2 is stabilized and translocated into nuclei, where it heterodimerizes with small Maf proteins and activates target genes for cytoprotection through antioxidant response element (ARE). Therefore, activation of Nrf2 is critical for cellular rescue pathways against oxidative stress (Cho et al., 2006; Lee et al., 2014). In our study, we found increased expression of HO-1 at mRNA and protein level after 24 hrs of hypoxia induction, along with increased nuclear translocation of Nrf2. Several studies have revealed increased expression of HO-1 in hypoxic cells of different origin (Gong et al., 2001; Neubauer and Sunderram, 2012). This indicated the increased production of ROS during hypoxia and subsequent activation of Nrf2/HO-1 in order to protect cells from hypoxic injury (Kolamunne et al., 2013). The treatment with curcumin and bilobalide augmented nuclear translocation of Nrf2 and expression of HO-1, and protected the cells from oxidative stress injury during hypoxia. Phytochemicals are known to activate Nrf2, resulting in the induction of some cytoprotective proteins including HO-1 and protecting

the cells from oxidative injury (Lee et al., 2014; Cho et al., 2006; Huang et al., 2014; Zhang et al., 2012). There are reports on the up regulated expression of HO-1 by curcumin (Yang, 2009) and bilobalide (Shah et al., 2011) in order to protect cells from oxidative stress.

Recent evidence reveals that hypoxia-induced excessive generation of ROS and ROS-based ER stress are major pathological complications associated with various diseases (Chhunchha et al., 2013). In ATH, in addition to oxidative stress, hypoxia itself up-regulate the induction of unfolded protein response. We found an increased expression of ERO 1-Lα and protein disulfide isomerases (PDI) in hypoxia treated adipocytes. ERO 1-Lα oxidizes the active-site cysteines of certain PDIs, which in turn introduce disulfide bonds into newly synthesized proteins. The final electron acceptor downstream of ERO1 is molecular oxygen. ERO 1 is transcriptionally induced by HIF during hypoxia, but in the absence of oxygen, it cannot fold the protein properly (Gess et al., 2003). This can result in protein misfolding and thereby turn on the unfolded protein response (UPR) in adipocytes. In addition, hypoxia induced ROS also induce ER stress by oxidizing proteins and disrupting calcium homeostasis. PERK, IRE1α, and ATF6 constitute the three UPR transducers that are activated upon ER stress (Walter and Ron, 2011). 24 hrs of hypoxia in 3T3-L1 adipocytes induced ER stress which is evident from increased expression of GRP78/BiP at mRNA and protein level. In addition, hypoxia also augmented the expression of proximal UPR transducers, PERK, IRE1α and ATF-6 in 3T3-L1 adipocytes. CHOP is another ER stress marker, also known as growth arrest and DNA damage-inducible gene 153, and involved in ER stress mediated apoptotic pathway (Tsang et al., 2010). Hypoxia also induced CHOP expression at mRNA and protein level. The treatment with bilobalide and curcumin attenuated hypoxia induced oxidative stress and ER stress. The antioxidant potential of bilobalide and curcumin reduced oxidative stress and oxidative stress induced ER stress. Zhou and Zhu (2000), have reported that bilobalide could attenuate ROS-induced apoptosis, suggesting that bilobalide might be working as a free-radical scavenger. Recent report suggests the protective role of curcumin on hypoxia induced oxidative stress based ER stress in mouse hippocampal cells (Chhunchha et al., 2013). Curcumin is also known to downregulate the expression of HIF-1 (Choi et al., 2006) and thus protects cells from hypoxia induced oxidative stress and subsequent complications.

Overall result showed that hypoxia induced the expression of HIF-1α, lactate release and PDK1 expression, oxidative stress, Nrf2/HO-1 expression and ER stress in 3T3-L1 adipocytes. The treatment with bilobalide and curcumin protected the adipocytes from hypoxia induced dysfunctions via scavenging reactive oxygen species and downregulating the expression of HIF-1α.
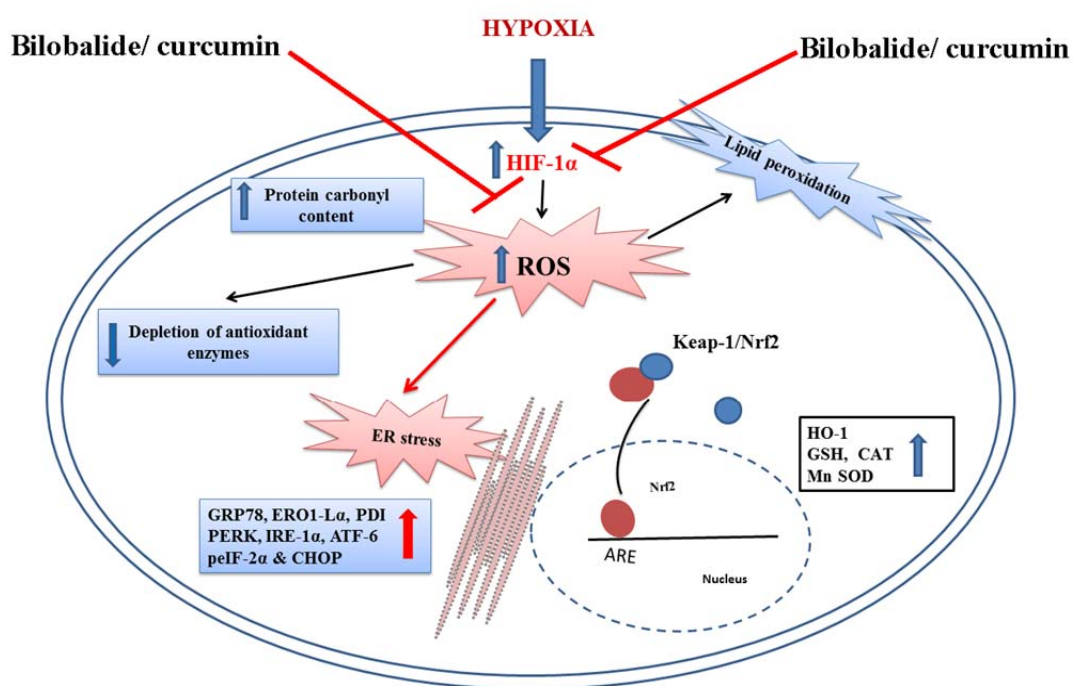
Fig. 2.13 Schematic representation - Summary of chapter 2: Hypoxia induced expression of HIF-1α, lactate release, oxidative stress and ER stress in 3T3-L1 adipocytes while treatment with bilobalide and curcumin reduced increased oxidative stress and ER stress via downregulating HIF-1α expression and scavenging ROS.

References

Arya A, Sethy NK, Singh SK, Das M, Bhargava K. (2013). Cerium oxide nanoparticles protect rodent lungs from hypobaric hypoxia-induced oxidative stress and inflammation. *Int J Nanomed*, 8: 4507-4520.

Bento CF, Pereira P. (2011). Regulation of hypoxia-inducible factor 1and the loss of the cellular response to hypoxia in diabetes. *Diabetologia*, 54: 1946-1956.

Bergman RN, Van Citters GW, Mittelman SD, Dea MK, Hamilton-Wessler M, Kim SP, Ellmerer M. (2001). Central role of the adipocyte in the metabolic syndrome. *J Investig Med*, 49: 119-126.

Bianchini F, Kaaks R, Vainio H. (2002). Overweight, obesity, and cancer risk. *Lancet Oncol*, 3: 565-574.

Brook CG, Lloyd JK, Wolf OH. (1972). Relation between age of onset of obesity and size and number of adipose cells. *Br Med J*, 2: 25-27.

Chapple SJ, Siow RC, Mann GE. (2012). Crosstalk between Nrf2 and the proteasome: Therapeutic potential of Nrf2 inducers in vascular disease and aging. *Int J Biochem Cell Bio,* 44: 1315-1320.

Chen B, Lam KS, Wang Y, Wu D, Lam MC, Shen J, Wong L, Hoo RL, Zhang J, Xu A. (2006). Hypoxia dysregulates the production of adiponectin and plasminogen activator inhibitor-1 independent of reactive oxygen species in adipocytes. *Biochem Biophys Res Commun*, 341: 549-556.

Cheng X, Siow RC, Mann GE. (2011). Impaired redox signaling and antioxidant gene expression in endothelial cells in diabetes: a role for mitochondria and the nuclear factor-E2-related factor 2-Kelch-like ECH-associated protein 1 defense pathway. *Antioxid Redox Signal*, 14: 469-487.

Chhunchha B, Fatma N, Kubo E, Rai P, Singh SP, Singh DP. (2013). Curcumin abates hypoxia-induced oxidative stress based-ER stress mediated cell death in mouse hippocampal cells (HT22) by controlling Prdx6 and NF-κB regulation. *Am J Physiol Cell Physiol*, 304: C636-C655.

Chiang CK, Inagi R. (2010). Glomerular diseases: genetic causes and future therapeutics. *Nat Rev Nephrol*, 6: 539-554.

Cho HY, Reddy SP, Kleeberger SR. (2006). Nrf2 defends the lung from oxidative stress. *Antioxid Redox Signal*, 8: 76-87.

Choi H, Chun YS, Kim SW, Kim MS, Park JW. (2006). Curcumin inhibits hypoxia-inducible factor-1 by degrading aryl hydrocarbon receptor nuclear translocator: a mechanism of tumor growth inhibition. *Mol Pharmacol*, 70: 1664-1671.

Cohen G, Dembiec D, Marcus J. (1970). Measurement of catalase activity in tissue extract. *Anal Biochem*, 34: 30-37.

David M, Richard JS. (1983). In: Methods of enzymatic analysis, Bergmeyer, J and Grab M. (Eds), Verlag Chemie Wenhein Deer Field, Beach Floride, pp 358.

Engvall E, Perlman P. (1971). Enzyme-linked immunosorbent assay (ELISA): Quantitative assay of immunoglobulin G. *Immunochemistry*, 8: 871-874.

Foresti R, Clark JE, Green CJ, Motterlini R. (1997). Thiol compounds interact with nitric oxide in regulating heme oxygenase-1 induction in endothelial cells. Involvement of superoxide and peroxynitrite anions. *J Biol Chem*, 272: 18411-18417.

Furukawa S, Fujita T, Shimabukuro M, Iwaki M, Yamada Y, Nakajima Y, Nakayama O, Makishima M, Matsuda M, Shimomura I. (2004). Increased oxidative stress in obesity and its impact on metabolic syndrome. *J Clin Invest*, 114: 1752-1756.

Gess B, Hofbauer KH, Wenger RH, Lohaus C, Meyer HE, Kurtz A. (2003). The cellular oxygen tension regulates expression of the endoplasmic oxidoreductase ERO1-L alpha. *Eur J Biochem*, 270: 2228-2235.

Gong P, Hu B, Stewart D, Ellerbe M, Figueroa YG, Blank V, Beckman BS, Alam J. (2001). Cobalt induces heme oxygenase-1 expression by a hypoxia-inducible factor-independent mechanism in Chinese hamster ovary cells: regulation by Nrf2 and MafG transcription factors. *J Biol Chem,* 276: 27018-27025.

Gunzler WA, Kramers H, Flohe L. (1974). An improved coupled test procedure for glutathione peroxidase. *Z Klin Chem Klin Biochem*, 12: 444-448.

Guzy RD, Hoyos B, Robin E, Chen H, Liu L, Mansfield KD, Simon MC, Hammerling U, Schumacker PT. (2005). Mitochondrial complex III is required for hypoxia-induced ROS production and cellular oxygen sensing. *Cell Metab*, 1: 401-408.

He M, Pan H, Chang RC, So KF, Brecha NC, Pu M. (2014). Activation of the Nrf2/HO-1 antioxidant pathway contributes to the protective effects of Lycium barbarum

polysaccharides in the rodent retina after ischemia-reperfusion-induced damage. *PLoS ONE*, 9: e84800. doi: 10.1371/journal.pone.0084800.

Hsu KC, Chen YF, Lin SR, Yang JM. (2011). iGEMDOCK: a graphical environment of enhancing iGEMDOCK using pharmacological interactions and post-screening analysis. *BMC Bioinformatics*, 12: S33.

Huang XS, Chen HP, Yu HH, Yan YF, Liao ZP, Huang, QR. (2014). Nrf2-dependent upregulation of antioxidative enzymes: A novel pathway for hypoxic preconditioning-mediated delayed cardioprotection. *Mol Cell Biochem,* 385: 33-41.

Inagi R, Shoji K, Nangaku M. (2013). Oxidative and Endoplasmic Reticulum (ER) Stress in Tissue Fibrosis. *Curr Pathobiol Rep,* 1: 283-289.

Jeong WS, Jun M, Kong AN. (2006). Nrf2: a potential molecular target for cancer chemoprevention by natural compounds. *Antioxid Redox Signal*, 8: 99-106.

Jiang C, Kim JH, Li F, Qu A, Gavrilova O, Shah YM, Gonzalez FJ. (2013). Hypoxia-inducible Factor 1 α regulates a Socs3- Stat3-adiponectin signal transduction pathway in adipocytes. *J Biol Chem*, 288: 3844-3845.

Jiang C, Qu A, Matsubara T, Chanturiya T, Jou W, Gavrilova O, Shah YM, Gonzale FJ. (2011). Disruption of hypoxia-inducible factor 1 in adipocytes improves insulin sensitivity and decreases adiposity in high-fat diet-fed mice. *Diabetes*, 60: 2484-2495.

Kakkar P, Das B, Viswanathan PN. (1984). A modified spectrophotometric assay of superoxide dismutase. *Indian J Biochem Biophys*, 21: 130-132.

Karar J, Dolt KS, Mishra MK, Arif E, Javed S, Pasha MA. (2007). Expression and functional activity of pro-oxidants and antioxidants in murine heart exposed to acute hypobaric hypoxia. *FEBS Lett*, 581: 4577-4582.

Kim JW, Tchernyshyov I, Semenza GL, Dang CV. (2006). HIF-1-mediated expression of pyruvate dehydrogenase kinase: a metabolic switch required for cellular adaptation to hypoxia. *Cell Metab*, 3: 177-185.

Kolamunne RT, Dias IH, Vernallis AB, Grant MM, Griffiths HR. (2013). Nrf2 activation supports cell survival during hypoxia and hypoxia/reoxygenation in cardiomyoblasts; the roles of reactive oxygen and nitrogen species. *Redox Biol*, 22: 418-426.

Kopelman PG. (2004). Obesity as a medical problem. *Nature*, 404: 635-643.

Koukourakis MI, Giatromanolaki A, Simopoulos C, Polychronidis A, Sivridis E. (2005). Lactate dehydrogenase 5 (LDH5) relates to up-regulated hypoxia inducible factor pathway and metastasis in colorectal cancer. *Clin Exp Metastasis*, 22: 25-30.

Lee HS, Lee GS, Kim SH, Kim HK, Suk DH, Lee DS. (2014). Anti-oxidizing effect of the dichloromethane and hexane fractions from *Orostachys japonicus* in LPS-stimulated RAW 264.7 cells via upregulation of Nrf2 expression and activation of MAPK signaling pathway. *BMB Rep*, 47: 98-103.

Lee K, Zhang H, Qian DZ, Rey S, Liu JO, Semenza GL. (2009). Acriflavine inhibits HIF-1 dimerization, tumor growth, and vascularization. *Proc Natl Acad Sci,* 106: 17910-17915.

Lee PJ, Jiang BH, Chin BY, Iyer NV, Alam J, Semenza GL, Choi AM. (1997). Hypoxia-inducible factor-1 mediates transcriptional activation of the heme oxygenase-1 gene in response to hypoxia. *J Biol Chem*, 272: 5375-5381.

Malhotra JD, Kaufman RJ. (2007). Endoplasmic reticulum stress and oxidative stress: avicious cycle or a double-edged sword? *Antioxid Redox Signal*, 9: 2277-2293.

Maxwell PH, Dachs GU, Gleadle JM, Nicholls LG, Harris AL, Stratford IJ, Hankinson O, Pugh CW, Ratcliffe PJ. (1997). Hypoxia-inducible factor-1 modulates gene expression in solid tumors and influences both angiogenesis and tumor growth. *Proc Natl Acad Sci*, 94: 8104-8109.

Millar TM, Phan V, Tibbles LA. (2007). ROS generation in endothelial hypoxia and reoxygenation stimulates MAP kinase signaling and kinase-dependent neutrophil recruitment. *Free Radic Biol Med*, 42: 1165-1175.

Moran MS, Defierre JW, Mannervik B. (1979). Levels of glutathione, glutathione reductase and glutathione s transferase activities in rat lung and liver. *Biochem Boiphys Acta*, 582: 67-68.

Morris GM, Huey R, Lindstrom W, Sanner MF, Belew RK, Goodsell DS, Olson AJ. (2009). AutoDock4 and Autodock Tools 4: Automated docking with selective receptor flexibility. *J Comput Chem*, 30: 2785-2791.

Neubauer JA, Sunderram J. (2012). Heme oxygenase-1 and chronic hypoxia. *Respir Physiol Neurobiol*, 184: 178-185.

Niehius WG, Samuelsson D. (1968). Formation of Malondialdehyde from phospholipid arachidonate during microsomal lipid peroxidation. *Eur J Biochem*, 6: 126-130.

Papandreou I, Cairns RA, Fontana L, Lim AL, Denko NC. (2006). HIF-1 mediates adaptation to hypoxia by actively downregulating mitochondrial oxygen consumption. *Cell Metab*, 3: 187-197.

Prabhakar NR, Kumar GK, Nanduri J, Semenza GL. (2007). ROS signaling in systemic and cellular responses to chronic intermittent hypoxia. *Antioxid Redox Signal*, 9: 1397-1403.

Rocha S. (2007). Gene regulation under low oxygen: holding your breath for transcription. *Trends Biochem Sci*, 32: 389-397.

Semenza GL. (2004). Hydroxylation of HIF-1: oxygen sensing at the molecular level. *Physiology (Bethesda)*, 19: 176-182.

Shah ZA, Nada SE, Dore S. (2011). Heme oxygenase-1, beneficial role in permanent ischemic stroke and in Ginkgo biloba (EGb 761) neuroprotection. *Neuroscience*, 180: 248-255.

Trayhurn P, Wood IS. (2004). Adipokines: inflammation and the pleiotropic role of white adipose tissue. *Br J Nutr*, 92: 347-355.

Trayhurn P. (2013). Hypoxia and adipose tissue functions and dysfunctions in adipocytes. *Physiol Rev*, 93: 1-21.

Tsang KY, Chan D, Bateman JF, Cheah KS. (2010). *In vivo* cellular adaptation to ER stress: survival strategies with double-edged consequences. *J Cell Sci*, 123: 2145-2154.

Walter P, Ron D. (2011). The unfolded protein response. From stress pathway to homeostatic regulation. *Science*, 334: 1081-1086.

Wang H, Joseph JA. (1999). Quantifying cellular oxidative stress by dichlorofluorescein assay using microplate reader. *Free Radic Biol Med*, 27: 612-616.

Weisberg SP, McCann D, Desai M, Rosenbaum M, Leibel RL, Ferrante AW Jr. (2003). Obesity is associated with macrophage accumulation in adipose tissue. *J Clin Inves*, 112: 1796-1808.

Wigfield SM, Winter SC, Giatromanolaki A, Taylor J, Koukourakis ML, Harris AL. (2008). PDK-1 regulates lactate production in hypoxia and is associated with poor prognosis in head and neck squamous cancer. *Br J Cancer*, 98: 1975-1984.

Yang C, Zhang X, Fan H, Liu Y. (2009). Curcumin upregulates transcription factor Nrf2, HO-1 expression and protects rat brains against focal ischemia. *Brain Res*, 1282: 133-141.

Ye J, Gao Z, Yin J, He Q. (2007). Hypoxia is a potential risk factor for chronic inflammation and adiponectin reduction in adipose tissue of ob/ob and dietary obese mice. *Am J Physiol Endocrinol Metab*, 293: 1118-1128.

Yu BP. (1994). Cellular defense against damage from reactive oxygen species. *Physiol Rev*, 74: 139-162.

Zhang S, Zhao Y, Xu M, Yu L, Zhao Y, Chen J, Yuan Y, Zheng Q, Niu X. (2013). FoxO3a modulates hypoxia stress induced oxidative stress and apoptosis in cardiac microvascular endothelial cells. *PLoS ONE*, 8: e80342. doi: 10.1371/journal.pone.0080342.

Zhang Z, Cui W, Li G, Yuan S, Xu D, Hoi MP, Lin Z, Dou J, Han Y, Lee SM. (2012). Baicalein protects against 6-OHDA-induced neurotoxicity through activation of Keap1/Nrf2/HO-1 and involving PKCα and PI3K/AKT signaling pathways. *J Agric Food Chem*, 60: 8171-8182.

Zhou LJ, Zhu XZ. (2000). Reactive oxygen species-induced apoptosis in PC12 cells and protective effect of bilobalide. *J Pharmacol Exp Ther*, 293: 982-988.

CHAPTER 3

EFFECT OF HYPOXIA ON MITOCHONDRIAL FUNCTIONS IN 3T3-L1 ADIPOCYTES AND POSSIBLE AMELIORATION WITH BILOBALIDE AND CURCUMIN

3.1 Introduction

Mitochondria are key organelles as their main function is to synthesize most of the cell's ATP via the oxidative phosphorylation (OXPHOS) system. Mitochondrial defects associated with hypoxia has been invoked in many diverse complex disorders, such as type 2 diabetes (Catrina et al., 2004), Alzheimer's disease (Peers et al., 2007), cardiac ischemia/reperfusion injury (Solaini and Harris, 2005), tissue inflammation (Nizet and Johnson, 2009), and cancer (Denko, 2008). This is due to mitochondria's central role in energy production, reactive oxygen species homeostasis, and cellular respiration. These processes are interdependent and may occur under various stress conditions, among which hypoxia are certainly prominent.

The number of mitochondria in white adipose tissue (WAT) is less compared to brown adipose tissue. But WAT represent 10% of total body weight in lean adults and >50% in obese subjects (Kusminski and Scherer, 2012), therefore any obesity-induced changes in WAT mitochondria can substantially disrupt whole-body energy homeostasis. In obese condition, mitochondrial number and function may be decreased gradually in adipose tissue. HIF-1α is a major mediator of the hypoxia signal involved in the adipocyte dysfunction. It has been reported that HIF-1α also functions as a negative regulator of mitochondrial biogenesis, respiration and oxygen utilization (Jang et al., 2013). Other factors which induce mitochondrial dysfunctions include ER stress and oxidative stress, both of this can be initiated by hypoxia.

Mitochondria are dynamic organelles whose morphology is regulated by fusion and fission processes. A growing body of evidence suggests the relevance of this process in the control of mitochondrial activity and cell metabolism (Liesa et al., 2009; Zorzano, 2009; Lee et al., 2004). Several genes encoding mitochondrial fusion and fission proteins have been recently identified. Mammalian proteins involved in mitochondrial fission are Fission 1 homologue protein (Fis1) and Dynamin-related protein 1 (DRP1). Similarly, Mitofusin 1 (MFN1), Mitofusin 2 (MFN2) and Optic Atrophy gene 1 (OPA1) are proteins

that participate in mitochondrial fusion in mammals (Cipolat et al., 2004; Frank et al., 2001). Recent study reports that peroxisome-proliferator–activated receptor coactivator 1-α (PGC-1-α) and HIF-1-α also provide transcriptional control of fission and fusion (Zorzano et al., 2009; Rehman et al., 2012). Since HIF-1α plays a key role in hypoxia induced mitochondrial dysfunction, the detrimental effects of hypoxia can be ameliorated by inhibiting HIF-1α expression.

In this chapter, we evaluated the effect of hypoxia on adipocyte mitochondria emphasising on intracellular reactive oxygen species (ROS) levels, mitochondrial superoxide production, aconitase activity, mitochondrial membrane potential ($\Delta\psi$) and mitochondrial transition pore opening (mPTP opening), ATP production and oxygen consumption, proteins involved in oxidative phosphorylation, mitochondrial mass and mitochondrial DNA (mtDNA) copy number, expression of genes and proteins involved in mitochondrial biogenesis and proteins involved in mitochondrial structural dynamics and possible protection with bilobalide and curcumin.

3.2 Materials and methods

3.2.1 Chemicals and cell culture reagents

Curcumin, bilobalide, acriflavine, 3-isobutyl-1-methylxanthine (IBMX), dexamethasone, insulin, dimethyl sulfoxide (DMSO) cobalt chloride hexahydrate, JC1 and Dulbecco's Modified Eagle's Medium (DMEM) were purchased from Sigma Aldrich (St. Louis, MO, USA). Calcein AM, was from Invitrogen (Carlsbad, CA, USA). Foetal calf serum (FCS) was from Gibco (Langley, OK, USA) and FBS and supplements were from Hi-media Pvt Ltd. India. All other chemicals used were of analytical grade.

3.2.2 Cell culture

3T3-L1 preadipocytes (ATCC) were maintained in DMEM (4.5 g/L high glucose) supplemented with 10% FBS, antibiotic (100 U penicillin/mL, and 100 μg streptomycin/mL) and incubated at 5% CO_2 and 37^oC. To induce differentiation, 2-days post confluent 3T3-L1 preadipocytes were stimulated for 48 hrs with 0.5 mM isobutyl methyl xanthine, 0.25 mM dexamethasone, and 1 μg/ml insulin in DMEM. Then differentiated adipocytes were maintained in and refed every 2 days with DMEM containing 1 μg/ml insulin.

3.2.3 Hypoxia induction and treatment

In order to induce hypoxia, differentiated 3T3-L1 adipocytes at 9th day were incubated in a hypoxic chamber (Galaxy 48R, New Brunswick, Eppendorf, Germany) at an atmosphere of 1% O_2, 94% N_2, 5% CO_2, and at 37^oC for 24 hrs. The control cells were incubated in an atmosphere of 21% O_2 and 5% CO_2 at 37^oC. The cells were treated with different concentrations (10, 20 & 50 µM) of bilobalide or (5, 10, 20 µM) of curcumin or acriflavine (5 µM; positive control) during hypoxic period (24 hrs). For mRNA expression and protein expression studies, only higher doses of test materials were used. Acriflavine was used as positive control.

3.2.4 Detection of intracellular reactive oxygen species (ROS) and mitochondrial superoxide production

Intracellular ROS levels were measured using flow cytometry technique with fluorescent 2', 7' dichloro dihydrofluorescein diacetate (DCFH-DA). DCFH-DA is cleaved intracellularly by non-specific esterase and turn to high fluorescent upon oxidation by ROS, which were analysed with FACS Aria II (BD Bioscience, San Jose, USA).

The generation of mitochondrial superoxide was evaluated using MitoSOX^{TM} dye. For this, the cells were treated with 5 µM stain in serum-free media for 30 mins at 37^oC. The stain was washed off with HBSS/Ca/Mg solution. Images of the cells were collected using spinning disk microscope (BD Pathway^{TM} Bioimager System, BD Biosciences) and fluorescence intensity was measured using multimode reader (Biotek Synergy 4, Winooski, VT, USA) at excitation and emission wavelengths of 510 nm and 580 nm, respectively.

3.2.5 Determination of aconitase activity

Aconitase activity was assayed in normoxic and hypoxic groups using kit purchased from Cayman chemicals (Cayman Chemical Company, Ann Arbor, USA) as per manufacturer's instructions. After respective treatments, cells were washed with cold PBS (pH 7.4). Then fresh PBS was added to cover the cells and centrifuged the cells at 800×g for 10 mins at 4°C. Then supernatant was discarded and the resuspended the cell pellet in 1 ml of homogenization buffer. The cell suspension was sonicated for 5 seconds and centrifuged the cell suspension at 20,000×g for 10 mins at 4°C. This supernatant was used for the assay of aconitase. 50 µl of the sample was added to 5 µl of assay buffer, 50 µl NADP+ reagent, 50 µl of isocitric dehydrogenase and 50 µl of aconitase substrate solution

and incubated for 15 mins at 37°C. The absorbance was taken once in every min at 340 nm for 10 mins.

3.2.6 Assay for mitochondrial membrane potential ($\Delta\psi$)

Changes in $\Delta\psi$ were measured using JC-1 mitochondrial staining kit, (Sigma) and images were visualized under spinning disk microscope (BD Pathway^{TM} Bioimager System, BD Biosciences) using JC-1, a cationic fluorescent dye. Simultaneously fluorescence intensity was measured in multiwell plate reader (Biotek Synergy 4, Winooski, VT, USA). For JC-1 monomers, the fluorimeter was set at 490 nm excitation and 530 nm emission wavelengths, and for J-aggregates, the fluorimeter was set at 525 nm excitation and 590 nm emission wavelengths. Valinomycin (1 µg/mL) was used as positive control.

3.2.7 Mitochondrial permeability transition pore opening

Mitochondrial permeability transition pore (mPTP) opening was examined by loading the cells with 0.25 mM calcein-AM in the presence of 8 mM cobalt chloride for 30 mins. Images of cells were collected using spinning disk fluorescent microscope at excitation and emission wavelengths of 488 nm and 525 nm, respectively.

3.2.8 Determination of the activity of mitochondrial respiratory complexes

For determining the activity of mitochondrial respiratory complexes after normoxic and hypoxic treatments, mitochondria were isolated using mitochondria isolation kit (Sigma-Aldrich, USA) The isolated mitochondria was then dissolved in CelLytic M, cell lysis reagent with protease inhibitor Cocktail [1:100 (v/v)] for further analysis.

The effect of hypoxia on complex I mediated electron transfer (NADH dehydrogenase) was studied using NADH as the substrate and menadione as electron acceptor. The reaction mixture containing 200 µM menadione and 150 µM NADH was prepared in phosphate buffer (0.1 M, pH 8.0). To this, mitochondria (100 µg) was added, mixed immediately and observed quickly for change in the absorbance at 340 nm for 8 mins (UV-2450 PC; Shimadzu, Kyoto, Japan) (Paul et al., 2008). Rotenone (10 µM) was used to inhibit the complex I.

Complex II mediated activity (succinate dehydrogenase) was measured spectrophotometrically at 600 nm using dichlorophenolindophenol (DCPIP) as an artificial

electron acceptor and succinate as substrate. The extent of decrease of absorbance (ΔOD) was considered as the measure of the electron transfer activity of complex II (Paul et al., 2008). The reaction mixture was prepared in 0.1 M phosphate buffer (pH 7.4) containing 10 mM EDTA, 50 μM DCPIP, 20 mM succinate and mitochondria (50 μg). The change in absorbance was observed immediately for 8 mins at 30°C. Malonate (25 μM) was used to inhibit the complex II.

Complex III (Ubiquinol-cytochrome C reductase) activity was determined as per the method described previously (Sudheesh et al., 2009). In brief, mitochondrial protein (50 μg) was mixed with 100 μM EDTA, 2 mg BSA, 3 mM sodium azide, 60 μM ferricytochrome C, decylubiquinol (1.3 mM) and phosphate buffer (50 mM, pH 8.0) in a final volume of 1 ml. The reaction was started by the addition of decylubiquinol and monitored for 2 mins at 550 nm and again after the addition of 1 μmol/l of antimycin A. The activity was calculated from the linear part of absorption-time curve, which was not less than 30 seconds. Activity of complex III was expressed as μmoles of ferricytochrome C reduced/minute/mg protein. Antimycin A (10 μM) was used as standard inhibitor of complex III.

Complex IV activity of mitochondria was assayed using kit from Sigma Aldrich chemicals (USA) as per manufacturer's instructions. Briefly, 950 μl of 1X assay buffer was added to a cuvette and then 10 μg of mitochondrial suspension was added and brought the reaction volume to 1.05 ml with 1X enzyme dilution buffer. The reaction was initiated by the addition of 50 μl of ferrocytochrome c substrate solution. Absorbance was read at 550/min.

3.2.9 Oxygen consumption rate assay

The rate of oxygen consumption in the cells was determined using oxygen consumption rate (OCR) assay kit from Cayman in accordance with the manufacturer's protocol. The phosphorescence of MitoXpress-Xtra, a phosphorescent oxygen probe, is quenched by oxygen and the phosphorescent signal is inversely proportional to the amount of oxygen present. The OCR was calculated from the change in MitoXpress probe signal over time (excitation: 380 nm; emission: 650 nm).

3.2.10 ATP determination assay

The ATP content was measured using a luciferase-based bioluminescence assay kit (ATP Determination Kit, Molecular Probes, Invitrogen). The cells, after treatment were homogenized in an ice-cold ATP releasing buffer (100 mM potassium phosphate pH-7.8, 2mM EDTA, 1 mM DDT, 1% Triton X 100). Then 90 µl of standard reaction mixture (8.9 ml distilled water, 0.5 ml 20X reaction buffer, 0.1 ml 0.1 M DTT, 0.5 ml of 10 mM D-luciferin, 2.5 µl of 5 mg/ml firefly luciferase) and 10 µl samples were gently mixed and the luminescence was read at 560 nm in a multiplate reader (Tecan Infinite 200PRO, Tecan, Austria). Using ATP standard provided with kit, ATP concentrations were determined and then normalized to protein concentrations.

3.2.11 Mitochondrial mass measurement

Mitochondrial mass was determined using Mitotracker Deep Red FM (Molecular Probe, Invitrogen). Briefly, the cells were treated with 5 µM stain in serum-free media for 30 mins at 37ºC. The stain was washed off with PBS and examined under spinning disk microscope (BD Pathway^{TM}, BD Biosciences) and fluorescence intensity was measured using multimode reader (Biotek Synergy 4, Winooski, VT, USA) at excitation and emission wavelengths of 644 nm and 665 nm, respectively.

3.2.12 Determination of mitochondrial biogenesis

Mitochondrial biogenesis was analysed with MitoBiogenesis™ In-Cell ELISA Kit (ABCAM, MA, USA) in all normoxic and hypoxic groups according to manufacturer's procedure. In brief, the cells after treatment were fixed with 4% paraformaldehyde. Cells were then washed with PBS and followed by the addition of 100 µL of freshly prepared 0.5% acetic acid for 5 mins to block endogenous alkaline phosphatase activity. Cells were washed again with PBS and permeabilized with 0.1% Triton X-100 for 30 mins and followed by the addition of 200 µL of 1X Blocking Solution for 2 hrs. These cells were then incubated with primary antibodies specifically against mtDNA encoded COX-I (subunit I of Complex IV, cytochrome c oxidase-1), and nuclear-DNA encoded SDH-A (a subunit of complex II, succinate dehydrogenase) proteins overnight at 4ºC. Cells were washed with a washing buffer and incubated with AP for SDH-A and HRP for COX-I secondary antibodies for 1 hr. After thorough washing, AP Substrate was added and colour development was measured at 405 nm for SDH-A. Then the wells were emptied and added

HRP Substrate. The colour developed was measured at 600 nm for COX-I. COX-I signal and SDH-A signal was then plotted independently for analysing the data.

3.2.13 Quantitative real-time PCR

Total RNA from 3T3-L1 adipocytes was extracted using Trizol reagent (Invitrogen, Carlsbad, CA). 2 µg of total RNA was reverse transcribed using Super Script III reverse transcriptase and random hexamers (Life technologies, Invitrogen, USA). The gene expression levels were analysed by quantitative real-time RT-PCR, conducted using the CFX96 Real Time PCR system (Bio-rad, USA) using the following conditions: an initial denaturation for 10 mins at 95ºC, followed by 39 cycles of 15s denaturation at 95ºC, 30s annealing at the optimal primer temperature and 10s extension at 72ºC. Each sample was assayed in triplicate in a 20 µL reaction volume containing 1 µL cDNA, 10 µL SYBR Green master mix (Power SYBR® Green PCR Master Mix, life technologies, Invitrogen, USA), 5.81 µL DEPC water and 1.6 µL of appropriate primer. Negative controls (no template) were run as well to ensure the absence of contamination. Analysis was performed according to the ΔΔCt method using β-actin as the housekeeping gene. Specific primers for each gene were designed to amplify a single product, as confirmed by dissociation curve analysis after the real-time PCR run.

$$\text{Fold change} = 2^{-\Delta(\Delta CT)}$$

where ΔCT = CT, target - CT, β-actin and ΔΔCT = ΔCT, stimulated- ΔCT, control

CT is the intersection between an amplification curve and a threshold line.

Table. 3.1 Nucleotide sequence of qRT-PCR primers.

mRNA		Primer sequence
Tfam	Forward	5'-GGAATGTGGAGCGTCCTAAAA-3'
	Reverse	5'-TGCTGGAAAAACACTTCGGAATA-3'
Pgc1a	Forward	5'-CGGAAATCATATCCAACCAG-3'
	Reverse	5'-TGAGGACCGCTAGCAAGTTTG-3'
Nrf1	Forward	5'-TGGTCCAGAGAGTGCTTGTG-3'
	Reverse	5'-TTCCTGGGAAGGGAGAAGAT-3'
MtDNA	Forward	5'-CCACTTCATCTTACCATTTA-3'
	Reverse	5'-ATCTGCATCTGAGTTTAATC-3'
Cyt B	Forward	5'-TTTTATCTGCATCTGAGTTTAATCCTG-3'
	Reverse	5'-CCACTTCATCTTACCATTTATTATCGC-3'
β-Actin	Forward	5'-AGTACCCCATTGAACGC-3'
	Reverse	5'-TGTCAGCAATGCCTGGGTAC-3'

3.2.14 Western blot analysis

Treated cells were washed with ice-cold PBS and lysed in RIPA buffer containing protease inhibitors. The cell suspensions were centrifuged at 12000 rpm for 15 mins at 4°C, and the supernatants was collected. Proteins were quantified using the bicinchoninic acid protein assay kit (BCA kit; Pierce, Rockford, IL, USA) in accordance with the manufacturer's instructions. Equal amount of proteins (50 μg) were separated by 10% SDS-PAGE and transferred to PVDF membranes using turbo transblot apparatus (BD Bioscience). The membranes were blocked with 5% BSA in TBST (50 mM Tris, pH 7.5, 150 mM NaCl, 0.01% Tween-20) for 1 hr at room temperature. The membrane was washed 3 times with TBST for 10 mins each. The membrane was incubated at 4ºC overnight in 5% BSA in TBST containing primary antibodies to one of the following:, OPA1 1:500 , MFN2 1:500, DRP 1:500, FIS 1:500 or β-ACTIN 1:1000. After washing with TBST, the membrane was incubated with peroxidase-conjugated corresponding secondary antibodies for 1 hr at room temperature. After washing, membranes were developed using 3, 3'-diaminobenzidine tablets (DAB) (Sigma Aldrich, St Louis, MO, USA) and H_2O_2. The immunoblot results were analysed in quantity one software using Gel doc (BD Bioscience, USA).

3.2.15 Statistical analysis

Results are expressed as means ± standard deviations. Data were subjected to one-way ANOVA and the significance of differences between means were calculated by Duncan's multiple range tests using SPSS for Windows, standard version 7.5.1 (SPSS), and significance was accepted at P≤0.05.

3.3 Results

3.3.1 Intracellular ROS generation and mitochondrial superoxide production

Flow cytometry analysis was performed to monitor intracellular ROS generation in normoxic and hypoxic adipocytes. 44.2% of hypoxic population showed significant ($P \leq 0.05$) ROS production compared with normoxia (8.2%; Fig. 3.1). Treatment with different concentration of bilobalide (10, 20, 50 µM), curcumin (5, 10, 20 µM), and acriflavine (5 µM) significantly reduced ($P \leq 0.05$) ROS production in hypoxia treated cells (Fig. 3.1).
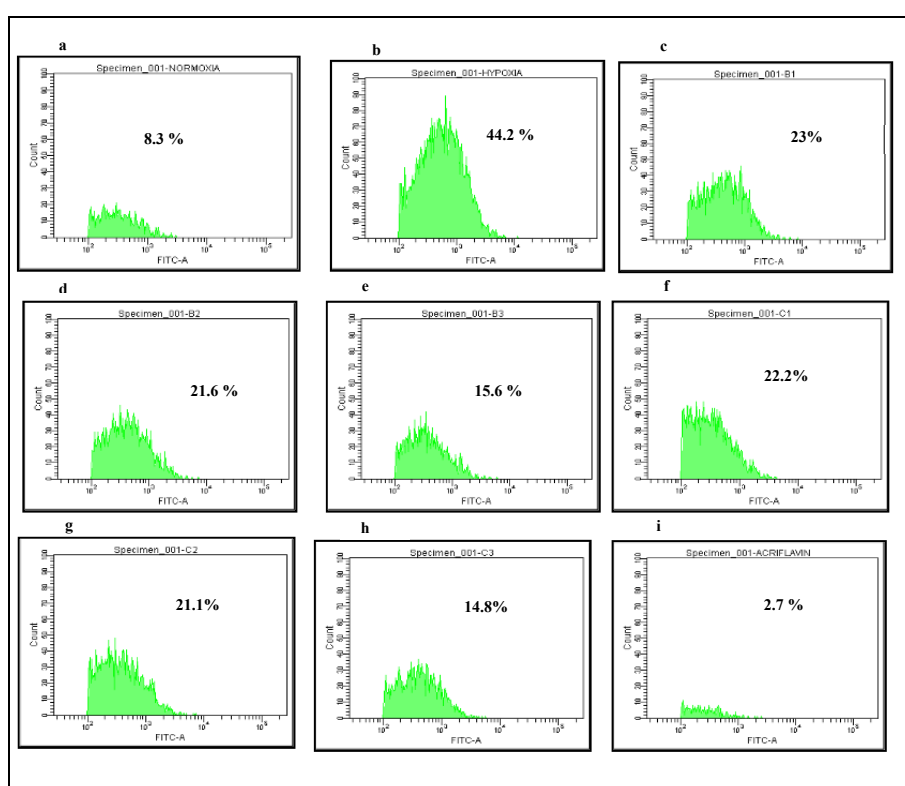
Fig. 3.1 Intracellular ROS generation in normoxic and hypoxic groups: a-normoxia; b-hypoxia, c-hypoxia + 10 µM bilobalide; d-hypoxia + 20 µM bilobalide; e-hypoxia + 50 µM bilobalide; f-hypoxia + 5 µM curcumin; g-hypoxia + 10 µM curcumin; h-hypoxia + 20 µM curcumin; i-hypoxia + 5 µM acriflavine.

The mitochondrial superoxide production was monitored in these cells and found that hypoxia caused significant superoxide production (4.47 fold) compared to normoxia. Bilobalide (10, 20, 50 µM) and curcumin (5, 10, 20 µM) treated group showed less fluorescence, suggesting protective effect of these compounds against superoxide

production in hypoxic cells. Acriflavine also showed limited superoxide production (Fig. 3.2A & B).
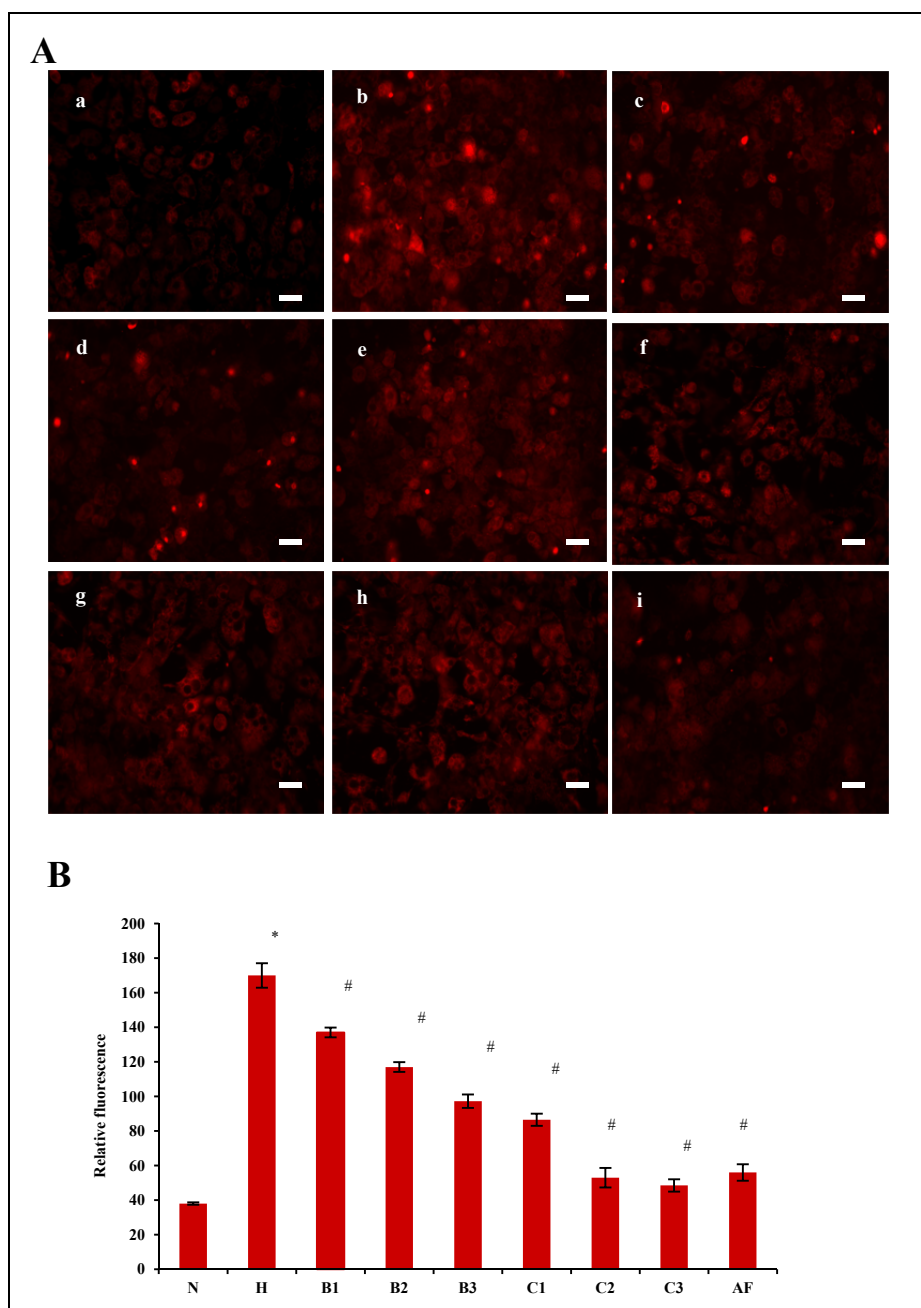
Fig. 3.2 Mitochondrial superoxide production determined by mitoSOX^{TM}: A) Fluorescent microscopic images of 3T3-L1 cells stained with mitoSOX^{TM} in normoxic and hypoxic groups. a-normoxia; b-hypoxia, c-hypoxia + 10 µM bilobalide; d-hypoxia + 20 µM bilobalide; e-hypoxia + 50 µM bilobalide; f-hypoxia + 5 µM curcumin; g-hypoxia + 10 µM curcumin; h-hypoxia + 20 µM curcumin; i-hypoxia + 5 µM acriflavine. Scale bar: 100 µm. B) Relative fluorescent intensity of mitochondrial superoxide production.
N-normoxia, H-hypoxia, B1-10 µM, B2-20 µM, B3-50 µM of bilobalide, C1-5 µM, C2-10 µM, C3-20 µM of curcumin and AF-5 µM of acriflavine, treated hypoxic groups. Values are means,

with standard deviations represented by vertical bars (n=6).* Mean value are significantly different from the control cells (P≤0.05). # Mean values are significantly different from hypoxia treated cells (P≤0.05).

3.3.2 Aconitase activity

The activity of this enzyme is sensitive to oxidative stress and superoxide radicals (Gardner et al., 1994; Gardner et al., 1995). In this study, aconitase activity was significantly (P≤0.05) reduced in hypoxic group (4.54 fold) when compared with control cells. Bilobalide (10, 20, 50 µM) and curcumin (5, 10, 20 µM) treatment dose dependently improved (1.47, 1.99, 3.69 & 2.28, 3.74, 4.12 fold) the activity significantly (P≤0.05) and brought back the activity near to normal. Acriflavine also improved aconitase activity (3.24 fold; Fig. 3.3). Thus, inhibition of aconitase activity in hypoxia indicates elevated level of mitochondria generated ROS.
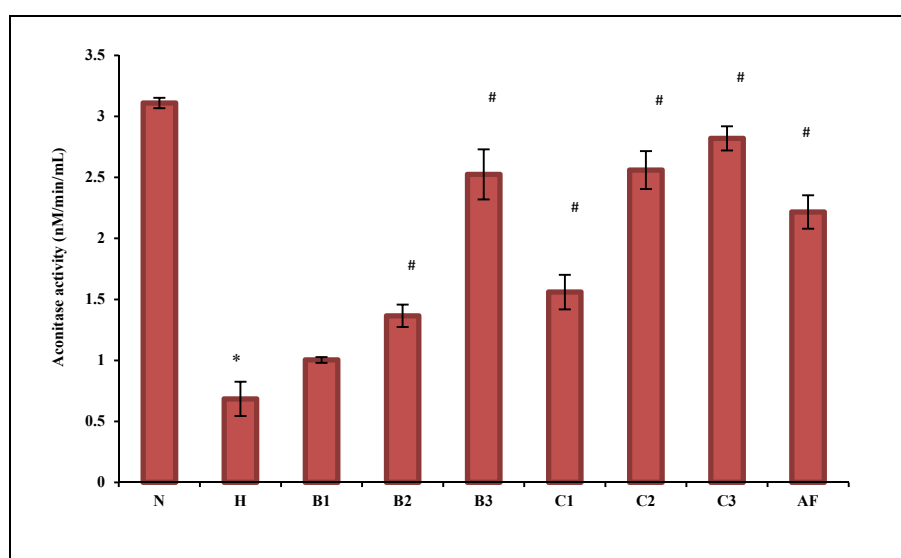
Fig. 3.3 Aconitase activity in normoxic and hypoxic groups: N-normoxia, H-hypoxia, B1-10 µM, B2-20 µM, B3-50 µM of bilobalide, C1-5 µM, C2-10 µM, C3-20 µM of curcumin and AF-5 µM of acriflavine, treated hypoxic groups. Values are means, with standard deviations represented by vertical bars (n=6).* Mean value are significantly different from the control cells (P≤0.05). # Mean values are significantly different from hypoxia treated cells (P≤0.05).

3.3.3 Alterations in mitochondrial transmembrane potential (Δψm) and mitochondrial permeability transition pore (mPTP)

Fig. 3.3 shows the mitochondrial transmembrane potential of normoxic and hypoxic cells.
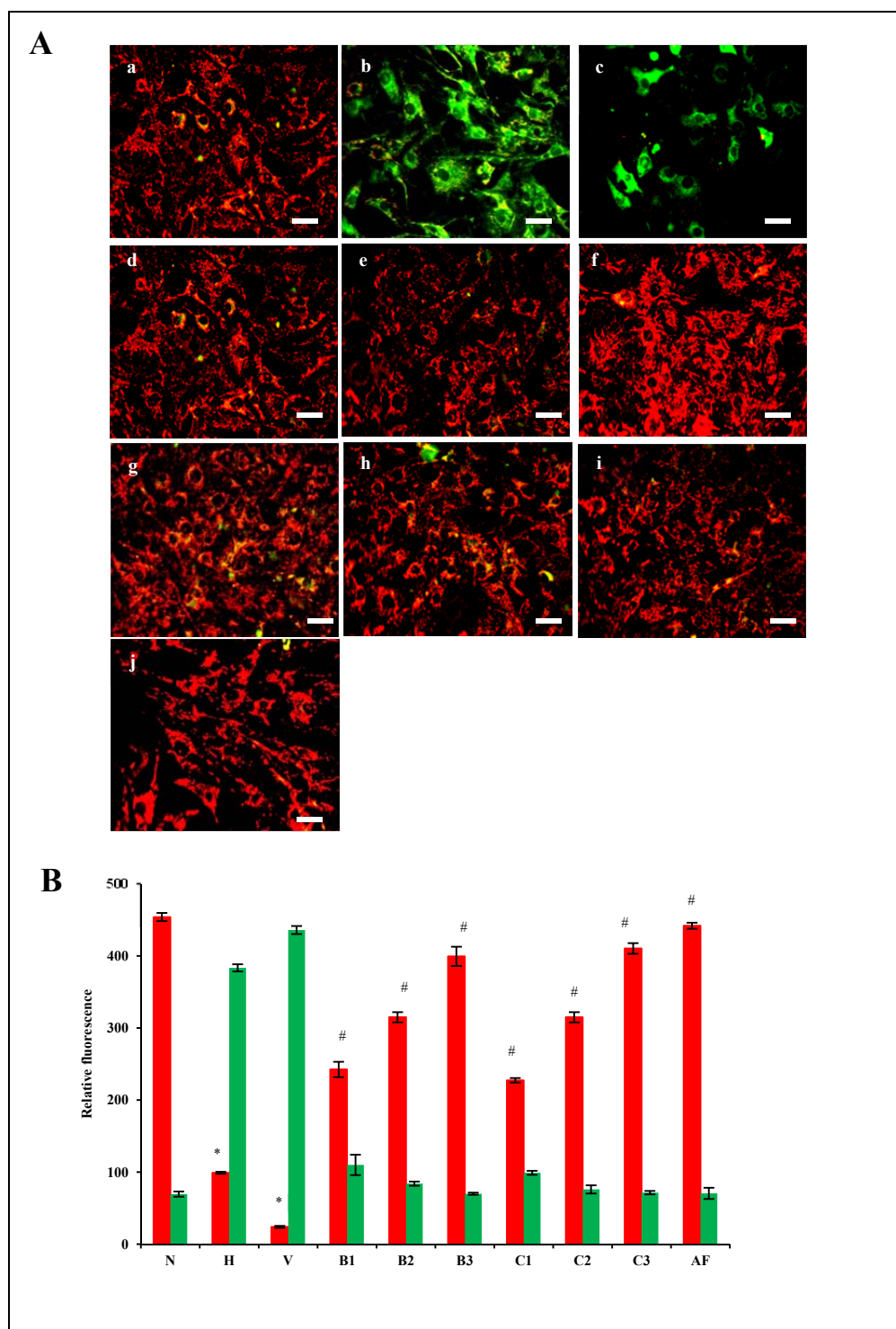
Fig. 3.4 Mitochondrial transmembrane potential changes with normoxic and hypoxic groups:
A) Fluorescent microscopic merged images of 3T3 L1 adipocytes; a-normoxia; b-hypoxia; c-valinomycine, d, e, f - 10, 20 & 50 µM of bilobalide treated hypoxic groups; g, h, i- 5, 10 & 20 µM of curcumin treated hypoxic groups; j- acriflavine (5 µM) treated hypoxic group respectively. Scale bar: 100 µm. B) Relative fluorescence intensity of mitochondrial transmembrane potential ($\Delta\psi$m) change. N-normoxia, H-hypoxia, V-1 µg/mL valinomycin, B1-10 µM, B2-20 µM, B3-50

µM of bilobalide, C1-5 µM, C2-10 µM, C3-20 µM of curcumin and AF-5 µM of acriflavine, treated hypoxic groups. Values are means, with standard deviations represented by vertical bars (n=6).* Mean value are significantly different from the control cells (P ≤0.05). # Mean values are significantly different from hypoxia treated cells (P≤0.05).

The JC-1 dye concentrates in mitochondrial matrix and form red fluorescent aggregates in normal cells due to the existence of electrochemical potential gradient. Alteration of $\Delta\psi$m prevents the accumulation of JC-1 in the mitochondrial matrix and gets dispersed throughout the cells, leading to a shift from red (JC-1 aggregates) to green fluorescence (JC-1 monomers). It was found from the fluorimetric and imaging data that in hypoxia treated group, JC-1 green monomers formed were significantly more in comparison with normoxic cells, whereas red aggregates were significantly less. This indicated dissipation $\Delta\psi$m in hypoxic group. A similar pattern was observed in valinomycin-treated cells. The treatment with different doses of bilobalide, curcumin and acriflavine showed more red aggregates and less green monomers, providing a significant improvement in impairment of mitochondrial $\Delta\psi$m due to hypoxia. Acriflavine also showed better result (Fig. 3.4)

Integrity of permeability transition pore was checked by calcein-cobalt loading. In normoxic and acriflavine-treated cells, calcein fluorescence was highly compartmentalized, corresponding to the mitochondrial space. On hypoxia induction, a decompartmentalization of calcein fluorescence was observed, indicating mPTP opening (Fig. 3.5). The loss of cobalt concentration in the cytosol by entering within the mitochondria leads to the dequenching of calcein fluorescence throughout the cells. However, in bilobalide and curcumin treated hypoxic cells, no calcein decompartmentalization was observed, and the cells appeared with punctiform fluorescence that was comparable with cells under normoxia and acriflavine treated group (Fig. 3.5). This suggested that hypoxia-induced mPTP opening in 3T3-L1 adipocytes was modestly reduced by bilobalide and curcumin.
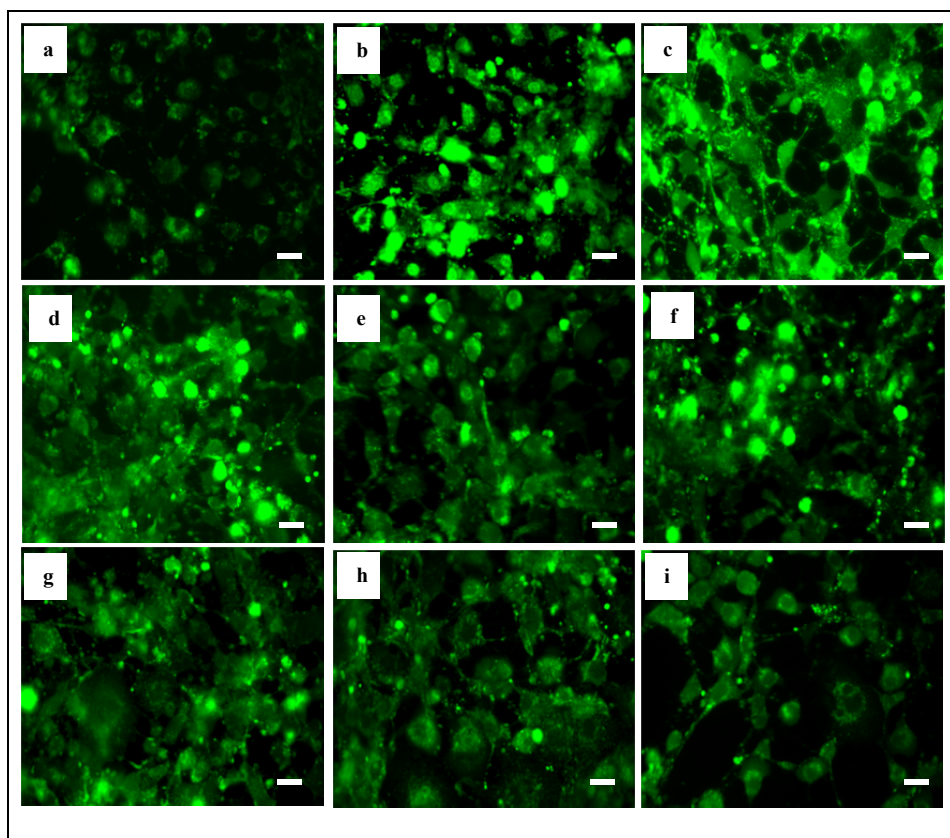
Fig. 3.5 Integrity of permeability transition visualized by calcein and cobalt coloading in hypoxic and normoxic groups: a normoxia; b hypoxia; c, d, e-10, 20 & 50 µM of bilobalide treated hypoxic groups; f, g, h-5, 10 & 20 µM of curcumin treated hypoxic groups; i- acriflavine (5 µM) treated hypoxic group respectively. Scale bar: 100 µm.

3.3.4 Activities of mitochondrial respiratory chain complexes

Table. 3.2 shows the activities of mitochondrial respiratory complexes in normoxic and hypoxic groups. The activities of respiratory chain complexes such as complexes I, III and IV were significantly decreased (2.05, 2.35 & 2.9 fold; Table. 3.2) in hypoxic adipocytes (P≤0.05) compared to normal cells. Bilobalide (50 µM), curcumin (20 µM) and acriflavine (10 µM) treatment prevented the reduction (1.31, 1.36, 1.28 fold; 1.80, 1.89, 1.45 fold; 1.4, 1.6, 1.3 folds respectively; Table. 3.2) of respiratory chain complexes activities in hypoxic 3T3-L1 adipocytes (P≤0.05). Standard compounds like rotenone, inhibited complex I activity by 3.87 fold, malonate inhibited complex II activity by 3.40 fold, antimycin A inhibited complex III activity by 2.44 fold and KCN inhibited complex IV activity by 7.45 fold. There were no significant changes in complex II activity in normoxic and hypoxic groups.

Table 3.2 Activities of mitochondrial respiratory chain complexes

	Complex I (NADH:ubiquinone oxidoreductase) (ΔOD 340 nm)	Complex II (Succinate-CoQ reductase) (ΔOD 600 nm)	Complex III (Cytochrome c reductase) (µM of ferricytochrome C reduced/min/mg protein)	Complex IV (Cytochrome c oxidase) (µM of ferrocytochrome C oxidized/min/mg protein)
N	0.391±0.006	0.245±0.008	5.14±1.015	6.11±0.18
H	0.191±.003*	0.239±0.01	2.19±0.16*	2.90±0.25*
B3	0.251±0.015#	0.237±0.016	3.95±0.41#	4.11±.029#
C3	0.260±0.007#	0.251±0.008	4.15±.72#	4.52±0.61#
AF	0.245.011#	0.249±0.012	3.18±.52#	3.88±0.41#
Rotenone	0.101±0.008*			
Malonate		0.072±0.021*		
Antimycin A			2.11±0.24*	
KCN				0.82±0.52*

N-normoxia, H-hypoxia, B3-50 µM of bilobalide & C3-20 µM of curcumin and AF-5 µm of acriflavine, treated hypoxic groups. Values are means, with standard deviations represented by vertical bars (n=6).* Mean value are significantly different from the control cells (P≤0.05). # Mean values are significantly different from hypoxia treated cells (P≤0.05).

3.3.5 Oxygen consumption rate and ATP content

The oxygen consumption rate (OCR) was analysed using Cayman's O_2 consumption assay kit. The kit utilizes a phosphorescent probe MitoXpress®, signal of which is quenched by oxygen and resulting in a signal that is inversely proportional to the amount of oxygen present. Adipocytes under hypoxia showed a significant (P≤0.05) decrease in OCR (2.23 fold) compared with the normoxic cells (Fig. 3.6). However, co-treatment with bilobalide, curcumin and acriflavine dose dependently promoted oxygen consumption rate under hypoxia. 10, 20, 50 µM of bilobalide significantly accelerated 1.11, 1.37, & 1.67 fold oxygen consumption rate respectively in hypoxic adipocytes. Similarly, 5 10, 20 µM curcumin also significantly improved 1.18, 1.85, & 1.92 fold oxygen consumption rate in hypoxic adipocytes (P≤0.05; Fig.3.6). Acriflavine (5 µM) also increased (P≤0.05) oxygen consumption rate (2.09 fold) in hypoxic adipocytes, indicating

protection against the defect in oxygen consumption.
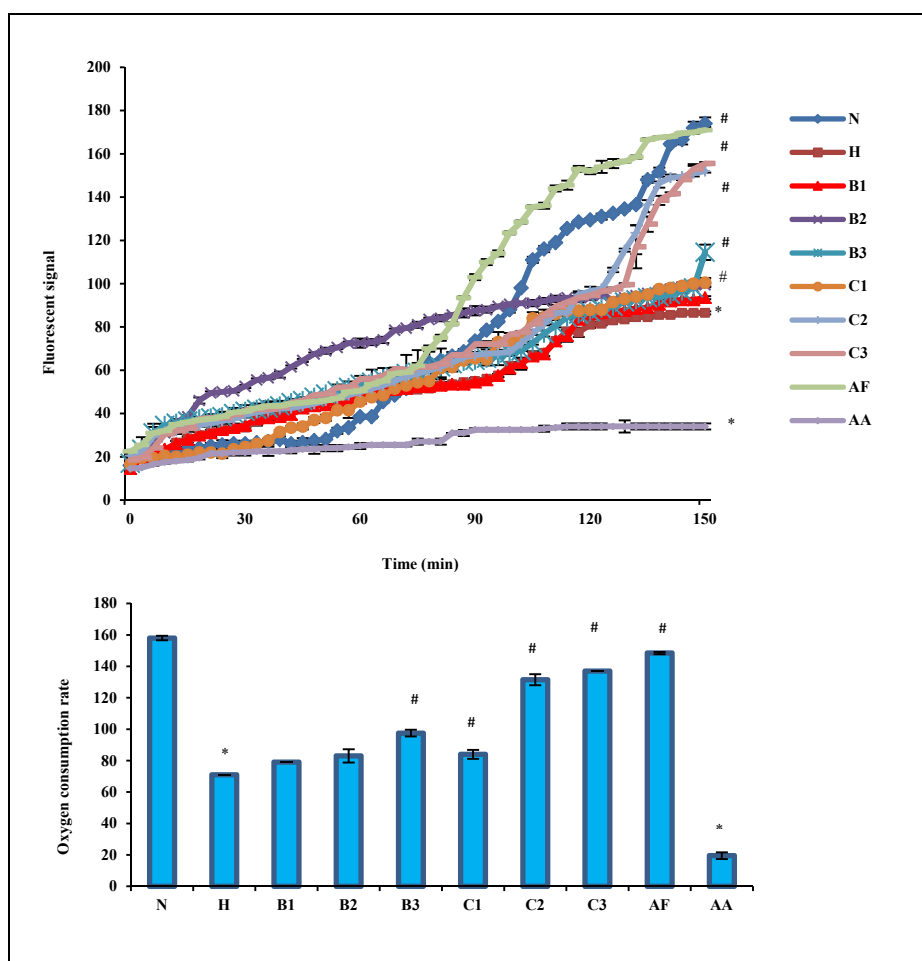
Fig. 3.6 Changes in oxygen consumption in normoxic and hypoxic groups: Hypoxia significantly reduced the oxygen consumption rate compared with the control group. Bilobalide, curcumin and acriflavine co-treatment partly restored the oxygen consumption rate. N-normoxia, H-hypoxia, B1-10 µM, B2-20 µM, B3-50 µM of bilobalide, C1-5 µM, C2-10 µM & C3-20 µM of curcumin, AF-5 µm of acriflavine treated hypoxic groups, and AA-antimycin A treated group. Values are means, with standard deviations represented by vertical bars (n=6).* Mean value are significantly different from the control cells (P≤0.05). # Mean values are significantly different from hypoxia treated cells (P≤0.05).

ATP content in hypoxic group was significantly (P≤0.05) reduced (4.32 fold) when compared to normoxia (Fig. 3.7). Treatment with bilobalide, curcumin and acriflavine restored (2, 2.34, & 3.08; 2.21, 2.93 & 3.24; 3.55 fold respectively; P≤0.05; Fig. 3.7). ATP content, further confirms the protective effect of these compounds against alterations in mitochondrial function.
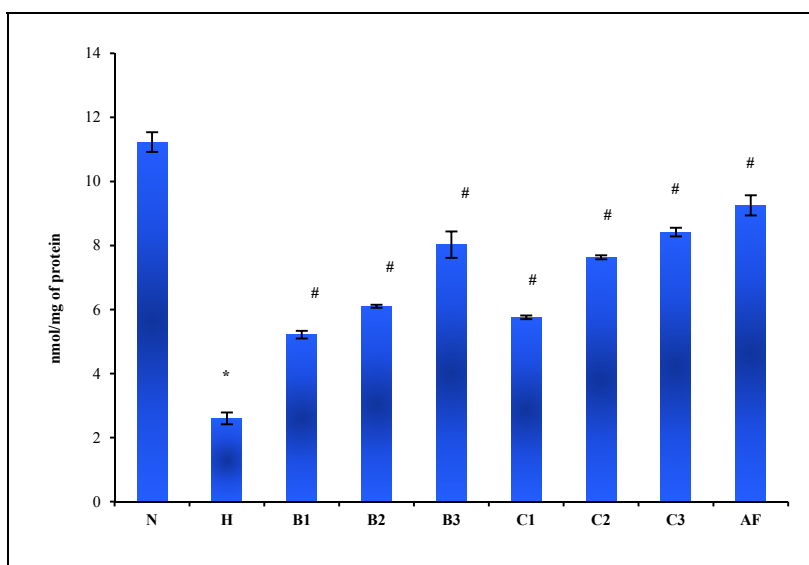
Fig. 3.7 Determination of ATP content in normoxic and hypoxic group: Hypoxia significantly reduced ATP content compared with the normoxic group. Bilobalide, curcumin and acriflavine co-treatment partly restored ATP content in hypoxic groups. N-normoxia, H-hypoxia, B1-10 µM, B2-20 µM, B3-50 µM of bilobalide, C1-5 µM, C2-10 µM, C3-20 µM of curcumin and AF-5 µM of acriflavine, treated hypoxic groups. Values are means, with standard deviations represented by vertical bars (n=6).* Mean value are significantly different from the control cells (P ≤0.05). # Mean values are significantly different from hypoxia treated cells (P≤0.05).

3.3.6 Mitochondrial mass

The mass of mitochondria in normoxia and hypoxia treated cells were assessed with mitotracker red. MitoTracker is a fluorescent dye that enters into the mitochondrial matrix independent of the mitochondrial membrane potential and forms covalent bonds with free thiol groups of cysteine residues of mitochondrial proteins. Fluorescence intensity was related to mitochondrial number. Here the hypoxic cells showed less (P≤0.05) fluorescence compared with normoxic condition (5.04 fold) indicating the loss of mitochondria. The treatment with bilobalide and curcumin dose dependently increased (2, 2.63, 3.24 fold; 2.04, 2.83, 3.25 fold; 3.73 fold; P≤0.05; Fig. 3.8)   the fluorescence indicating more number of functional mitochondria. Acriflavine showed high fluorescence indicating the presence of functional mitochondria (Fig. 3.8). This is an indication of protection by bilobalide and acriflavine against mitochondrial alterations in hypoxia.
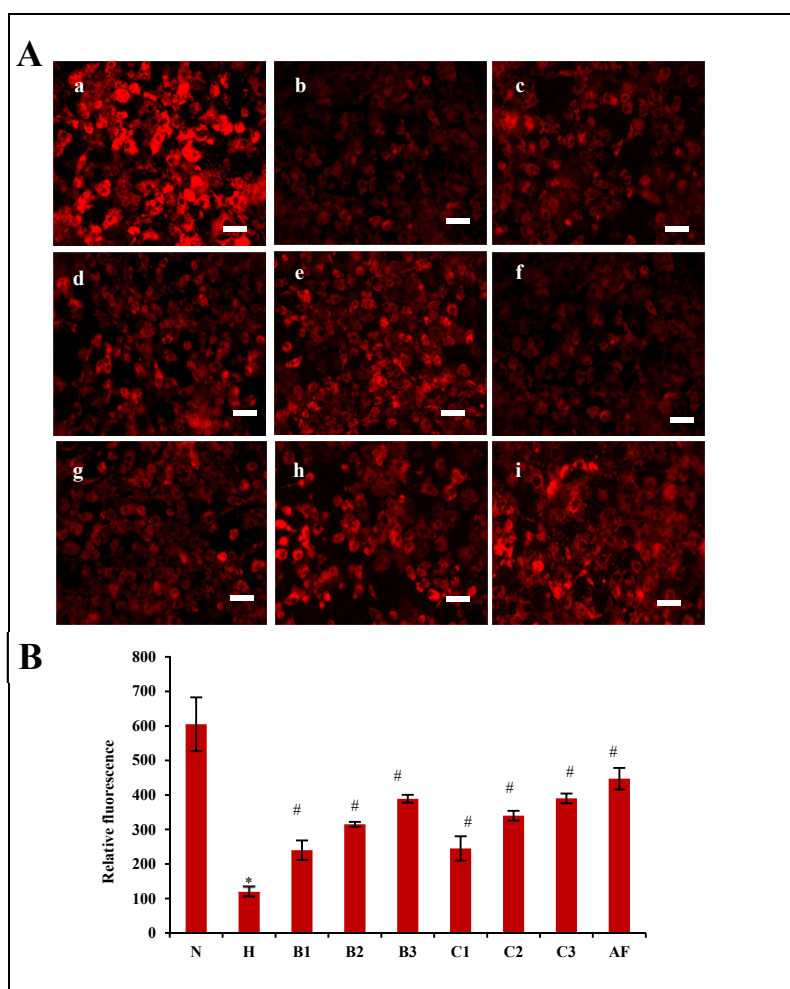
Fig. 3.8 Studies on alteration in mitochondrial mass in normoxic and hypoxic groups: (A) Fluorescent microscopic images of 3T3 L1 cells stained with mitotracker red. a-normoxia; b-hypoxia; c, d, e-10, 20 & 50 µM of bilobalide treated hypoxic groups; f, g, h-5, 10 & 20 µM of curcumin treated hypoxic groups; i- acriflavine (5 µM) treated hypoxic group respectively. Scale bar: 100µm. (B) Relative fluorescence intensity of mitochondrial mass. N-normoxia, H-hypoxia, B1-10 µM, B2-20 µM, B3-50 µM of bilobalide, C1-5 µM, C2-10 µM, C3-20 µM of curcumin and AF-5 µM of acriflavine, treated hypoxic groups. Values are means, with standard deviations represented by vertical bars (n=6).* Mean value are significantly different from the control cells (P≤0.05). # Mean values are significantly different from hypoxia treated cells (P≤0.05).

3.3.7 Mitochondrial biogenesis

The mitobiogenesis in cell ELISA assay measures the specific activities of two mitochondrial proteins, the subunit I of Complex IV (cytochrome c oxidase- 1, COX-1), which is mtDNA encoded, and a subunit of Complex II (succinate dehydrogenase-A, SDH-A), which is nuclear DNA-encoded.
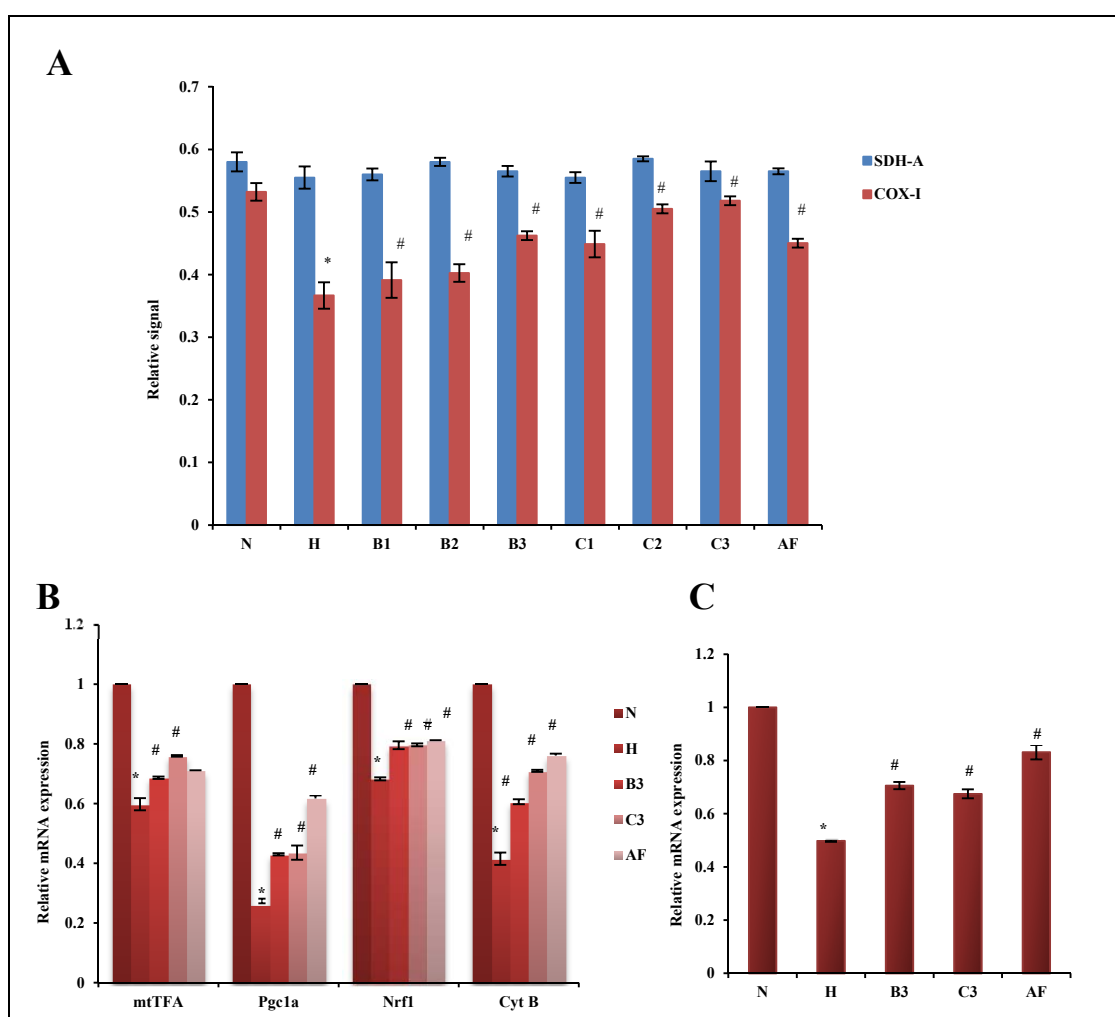
Fig. 3.9 Studies on mitochondrial biogenesis in normoxic and hypoxic groups: A) Mitochondrial biogenesis in normoxic and hypoxic group based on the specific activities of Subunit I of complex IV (COX-1), which is mtDNA encoded, and Subunit of Complex II (SDH-A), which is encoded in nuclear DNA. B) The relative expression of genes involved in mitochondrial biogenesis in normoxic and hypoxic groups. C) Mitochondrial DNA copy number in normoxic and hypoxic groups determined by qRT PCR.
N-normoxia, H-hypoxia, B1-10 μM, B2-20 μM, B3-50 μM of bilobalide, C1-5 μM, C2-10 μM, C3-20 μM of curcumin and AF-5 μM of acriflavine, treated hypoxic groups. Values are means, with standard deviations represented by vertical bars (n=6).* Mean value are significantly different from the control cells (P≤0.05). # Mean values are significantly different from hypoxia treated cells (P≤0.05).

The specific activity of mtDNA encoded COX-1 was significantly (P≤0.05) depleted (1.45 fold) in hypoxic group compared with normoxia indicating, loss of mitochondrial biogenesis. The treatment with bilobalide (10, 20, 50 μM), curcumin (5, 10, 20 μM) and acriflavine (5 μM) significantly (P≤0.05) restored COX-1 activity (1.07, 1.10, 1.26 fold; 1.22, 1.38, 1.41 fold; 1.23 fold; Fig. 3.9A) in a dose dependent manner, showing protection from loss of mitochondrial biogenesis. But there was no significant changes in

the activity of SDH-A, the nuclear DNA encoded protein in normoxic and hypoxic groups. These results strongly support hypoxia induced mitochondrial dysfunctions in adipocytes.

3.3.8. Mitochondrial biogenesis marker expression and mtDNA copy number

Next, we examined the mRNA level expression of the mitochondrial biogenesis related factors, Pgc1a, Nrf1, mtTFA and Cyt b in normoxic and hypoxic adipocytes. The results showed that the gene level expression of Pgc-1a, Nrf1, mtTFA and Cyt b were drastically (P≤0.05) decreased after hypoxia treatment with respect to normoxia (Fig. 3.9B). Similarly qRT PCR analysis of mtDNA copy number also found to be significantly decreased in hypoxic group (Fig. 3.9C). The treatment with bilobalide (50 µM), curcumin (20 µM) and acriflavine (5 µM) significantly (P≤0.05) restored mitochondrial biogenesis related proteins and mtDNA copy number almost to normal level in hypoxia treated groups (Fig. 3.9B & C).

3.3.9. Alterations in proteins involved in mitochondrial structural dynamics
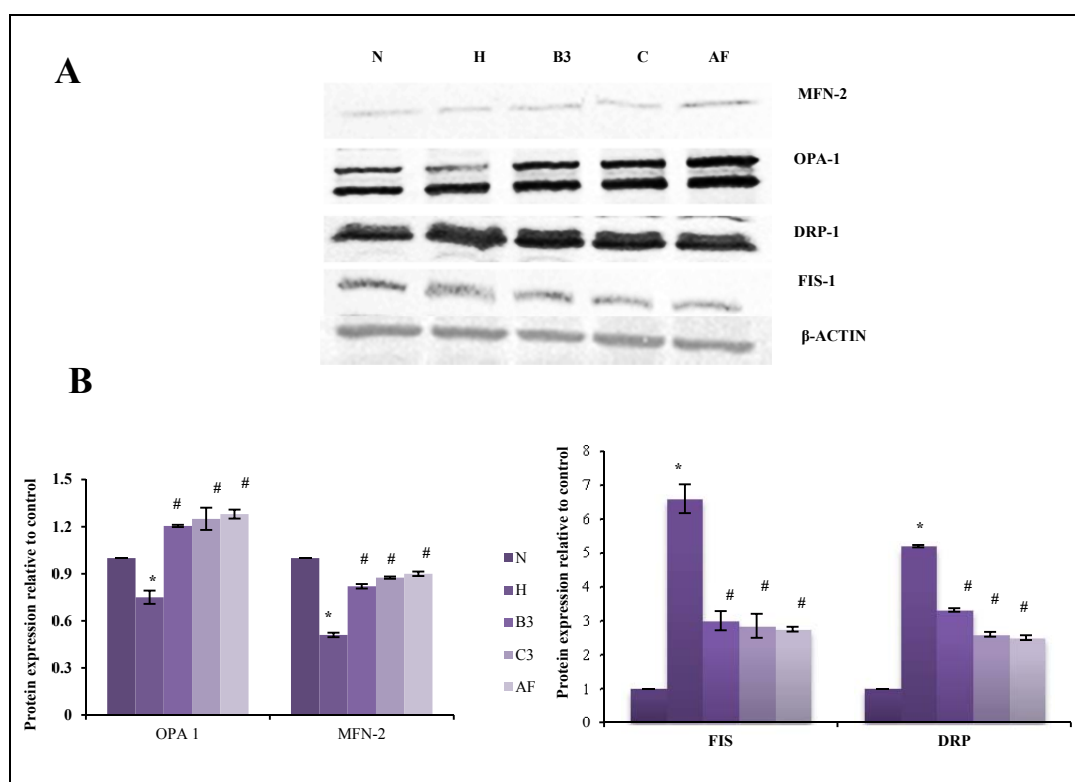
Fig. 3.10 Studies on mitochondrial structural dynamics in normoxic and hypoxic groups: A) Immunoblot analysis of proteins involved in mitochondrial fusion (MFN-2 & OPA-1) and fission (DRP-1 & FIS-1). B) Quantification of protein level normalized to β-actin. N-normoxia, H-

hypoxia, B3-50 μM of bilobalide, C3-20 μM of curcumin and AF-5 μm of acriflavine, treated hypoxic groups.
Values are means, with standard deviations represented by vertical bars (n=3).* Mean value are significantly different from the control cells (P≤0.05). # Mean values are significantly different from hypoxia treated cells (P≤0.05).

An important factor mediating mitochondrial function is mitochondrial dynamics. An appropriate balance in mitochondrial fusion and fission is essential for cells to maintain normal function. We therefore investigated expression of the fusion proteins, MFN2 and OPA1, and fission proteins, DRP1 and FIS1 in hypoxic and normoxic cells by immunoblot analysis. The results showed a significant (P≤0.05) decrease in MFN2 & OPA1 (fusion proteins) expression and significant increase in DRP1 & FIS1 (fission proteins) in hypoxic adipocytes indicating impaired mitochondrial function. The treatment with bilobalide (50 μM), curcumin (20 μM) and acriflavine (5 μM) restored the fusion and fission proteins in normal range (Fig. 3.10A & B).

3.4. Discussion

Mitochondria are considered as "powerhouse" of the cell, where tricarboxylic acid (TCA) cycle and β-oxidation take place and chemical energy is converted into ATP (Goldenthal and Marin-Garcia, 2004). Mitochondrial impairment is emerging as a contributing factor to pathogenesis of obesity. The mitochondrial content in white adipose tissue is significantly less compared with brown adipose tissue. But more than 95% of cellular ATP required by adipocytes for triglyceride and adipokines synthesis and secretion, is produced by mitochondria. It also plays an essential role in many different pathways in the adipocyte, including differentiation and maturation (De Pauw et al., 2009). So any alterations in mitochondrial activity may lead to malfunctions in adipocytes (Keijer and van Schothorst, 2008). Key contributors to mitochondrial dysfunction in obesity include ROS, ER stress, inflammation and all of this could be initiated by hypoxia and that ultimately leads to insulin resistance in adipocytes. Hypoxia inducible factor 1α (HIF-1α) is a major mediator of the hypoxia signal in the inhibition of mitochondrial function (Zhang et al., 2010; Jang et al., 2013). Mitochondria are crucial oxygen sensors. Therefore, in present study, mitochondrial function under normoxia and hypoxia were analysed.

The mitochondrial ETC is a major site of ROS production in adipocytes. Oxidative stress has been described in WAT of many mouse models of obesity, such as the KKAy, diet-induced obesity (DIO), and db/db mice (Curtis et al., 2010; Houstis et al.,

2006; Furukawa et al., 2004). In our study, we found an increased level of ROS along with surplus generation of mitochondrial superoxide radicals in hypoxic cells. Studies support mitochondria as a primary source of ROS production during hypoxic stress. Mitochondrial ROS generated at Complex III, causes stabilisation of HIF-1α during hypoxia (Chandel et al., 2000; Chhunchha et al., 2013). Mitochondrial aconitase is an enzyme that plays a central role in carbohydrate and energy metabolism and is responsible for the interconversion of citrate to isocitrate as part of the citric acid cycle (Tsui et al., 2013). The activity of this enzyme is sensitive to oxidative stress and superoxide radicals (Gardner et al., 1995 Gardner et al., 1994). Inhibition of mitochondrial aconitase is used as a marker for superoxide detection. Thus, the assay for aconitase activity is a sensitive marker of mitochondrial-generated ROS level (Gardner, 2002). In accordance with several other reports (Magalhaes et al., 2005; Regazzetti et al., 2009), the present study confirmed the paradoxical phenomenon of hypoxia-induced oxidative stress and damage in 3T3-L1 adipocytes. This leads to reduction in aconitase activity. This supports the role of mitochondria as a potential ROS source and also as a target under severe hypoxic conditions. Bilobalide and curcumin protected mitochondria from ROS as well as superoxide production in hypoxic cells which is evident from decreased production of ROS, superoxide production and increased aconitase enzyme activity. Bilobalide could attenuate ROS in different cells and act as a free radical scavenger (Zhou and Zhu, 2000). Curcumin is known to restore the activity and expression levels of many antioxidant genes (Aggarwal and Sung, 2009). Curcumin also enhance the cellular antioxidant defense system and thereby protect cells against oxidative stress (Onder et al., 2012).

Increased mitochondrial superoxide production and oxidative stress is associated with a dissipation of Δψm (Prathapan et al., 2014). Δψm represents an important marker of mitochondrial integrity, and its dissipation is a critical event in cell pathology. Δψm is highly negative, approximately -180 mV, due to the chemiosmotic gradient of protons across the inner mitochondrial membrane, the energy of which is used for ATP synthesis by the respiratory chain. Maintenance of Δψm is fundamental for the normal performance and survival of cells (Mathur et al., 2000). This study also showed a dissipation of Δψm in hypoxia-treated cells. Bilobalide and curcumin was found effective to prevent mitochondrial membrane potential dissipation. Conversely, Gao et al. and Chen et al. (2010) reported loss of Δψm in 3T3-L1 adipocytes on treatment with TNF α, high glucose

and free fatty acids. All these confirm impairment of $\Delta\psi$m in adipocyte mitochondria of obese individuals via hypoxia.

ROS, low membrane potential, and oxidized pyridine nucleotides all may lead to opening of the mitochondrial permeability transition pore (Scheffler, 1999). Alteration in $\Delta\psi$m may lead to the uncoupling of respiratory chain, and this accompanies mPTP opening (Javadov and Karmazyn, 2007). Under normal physiological conditions, the mitochondrial inner membrane is impermeable to almost all metabolites and ions. The compounds that enter or leave the mitochondria are generally transported via specific and controlled carriers. mPTP opening dramatically changes the properties of the inner membrane, making it unspecifically permeable to molecules smaller than 1,500 Da (Zoratti and Szabo, 1995). We observed mPTP opening in hypoxia-treated cells along with dissipation in $\Delta\psi$m, and these effects were modestly attenuated by bilobalide and curcumin.

A reduction in mitochondrial oxygen consumption rate as well as intracellular ATP content after 24 hrs of hypoxia treatment in 3T3-L1 adipocytes had been observed. It is known that hypoxia is associated with disturbances of ATP synthesis resulting from depressed functions of electron transport and oxidative phosphorylation in the respiratory chain (Lukyanova, 2013). The mitochondrial membrane potential provides the driving force for ATP synthesis. In this study we found a dissipation of $\Delta\psi$m which ultimately leads to disruption of ETC, ATP synthesis and oxygen consumption. Mitochondrial oxygen consumption and ATP synthesis can be regulated by PDK1 expression (Papandreou et al., 2006). It is a direct target of HIF-1, which phosphorylates and inactivates the TCA cycle enzyme pyruvate dehydrogenase (PDH) enzyme complex that converts pyruvate to acetyl-coenzyme A. Thereby it inhibits pyruvate metabolism via the tricarboxylic acid (TCA) cycle (Sugden and Holness, 2002). Since TCA cycle is coupled to electron transport, regulation of the PDH complex by PDK-1 is critical for mitochondrial respiration and ROS production (Kim et al., 2006). We found an increased PDK-1 expression in hypoxia and treatment with bilobalide and curcumin restored its expression to normal level in the first chapter. So by regulating $\Delta\psi$m and PDK-1 expression, bilobalide and curcumin maintained ATP synthesis and oxygen consumption rates to normal level under hypoxia.

Many factors including age, obesity, and T2DM could reduce mitochondrial content in white adipocytes (Choo et al., 2006; Schöttl and Klingenspor, 2013). Recent

studies also reported that transgenic as well as high fat diet obese mice have less mitochondrial density compared to lean control. This may be an indication of less mitochondrial biogenesis (Rong et al., 2007) in obese. Obesity induced alterations in mitochondrial biogenesis substantially impair white adipocyte metabolism. In our study we analysed, how hypoxia affects the major factors involved in mitochondrial biogenesis. Of several regulatory factors involved in biogenesis, peroxisome proliferator activated receptor (PPAR) gamma coactivator-1 (PGC-1α and PGC-1β) and nuclear respiratory factors (NRF1 and NRF2) are master regulators (Liu et al., 2009). We found a reduction in the expression of PGC-1α in hypoxia treated 3T3-L1 adipocytes. NRF1 and mtTFA are two key transcription factors for mitochondrial biogenesis and all targets of PGC-1α. NRF1 can stimulate the transcription of many nuclear-encoded mitochondrial genes, such as OXPHOS genes and respiratory complexes. mtTFA can also bind to the D loop of the mitochondrial genome and promote transcription of mitochondrial genes and replication of mitochondrial DNA (Scarpulla et al., 2012). There were significant reductions in NRF1, mtTFA expression and mtDNA copy number after hypoxia induction, which was consistent with the decreased expression of PGC-1α. Our study also showed that bilobalide and curcumin prevented downregulation of mitochondrial biogenesis influencing factors under hypoxic condition. Bilobalide and curcumin improved the expression of PGC-1α and all other PGC-1α regulated downstream factors of biogenesis. Previous study by Krishnan et al. (2012) reported that HIF-1α inactivation promotes mitochondrial biogenesis specifically in white adipocytes. We have already found bilobalide and curcumin inhibit HIF-1α at mRNA and protein level, and thus protected hypoxic cells from mitochondrial biogenesis impairment.

Another important factor mediating mitochondrial function is mitochondrial dynamics. An appropriate balance in mitochondrial fusion and fission is essential for cells to maintain metabolic states and homeostasis. Although opposing, the fusion and fission processes work in concert to maintain mitochondrial morphology, size, and number (Chan, 2012). Key mediators of mitochondrial fission/fusion include the DRP1 and FIS which are essential for fission, and OPA1, MFN1 and MFN2 which mediate fusion. Recent study by Liu et al., (2014) found that proteins controlling mitochondrial fusion MFN1 and MFN 2 but not OPA1 were decreased and proteins governing mitochondrial fission FIS1 and DRP1 were increased in skeletal muscle of HFD-fed mice when compared to normal diet

fed mice. Our study has exhibited significantly lower expression of MFN2 and OPA1 in hypoxic condition, when compared with normoxic group. Previous report described, PGC-1α acts as mediator of mitochondrial biogenesis and transcriptional coactivator of MFN-2, a protein involved in fusion (Zorzano et al., 2009). Hence this lower expression of MFN-2 could be attributed to reduced expression of PGC-1α in hypoxic condition. We also observed an increased expression of fission proteins DRP1 and Fis1 in hypoxic adipocytes. It is already reported in cancer studies that HIF-1α promotes mitochondrial fission by upregulation of DRP1 and Fis proteins (Chiang et al., 2009). From this study, we concluded that, obesity related hypoxia in adipocytes promotes mitochondrial fission by overexpression of proteins DRP-1 and Fis which down regulate mitochondrial biogenesis, oxygen consumption, OXPHOS, and ATP synthesis. Bilobalide and curcumin treatment restored the expression of proteins DRP-1 and Fis to normal level, and protected the cells from enhanced mitochondrial fission by inhibiting HIF-1 activation as well as by improving PGC-1α expression.

Overall results of this chapter provide a new insight into hypoxia induced impairment of mitochondrial function in 3T3-L1 adipocytes and possible recovery with bilobalide and curcumin. Hypoxia for 24 hrs substantially increased ROS, and mitochondrial superoxide production. Surplus ROS impaired mitochondrial membrane potential, finally led to transition pore opening. Hypoxia also reduced mitochondrial biogenesis, oxygen consumption, ATP synthesis, and proteins involved in oxidative phosphorylation. Hypoxia also impaired fusion/fission balance in adipocytes. HIF-1α is considered as main culprit of all these mitochondrial dysfunctions. Bilobalide and curcumin protected the 3T3-L1 adipocytes from adverse effects of hypoxia by enhancing mitochondrial biogenesis, mitochondrial functional performance and by controlling mitochondrial dynamics, via downregulating HIF-1α expression and scavenging ROS. In conclusion hypoxia impaired mitochondria functions in differentiated 3T3-L1 cells. However, phytochemical treatment that downregulate the expression of HIF-1α, partially recovered the hypoxia mediated mitochondrial dysfunction, suggesting that HIF-1α could be used as a therapeutic target for adipocyte hypoxia-mediated mitochondrial dysfunctions in obesity.
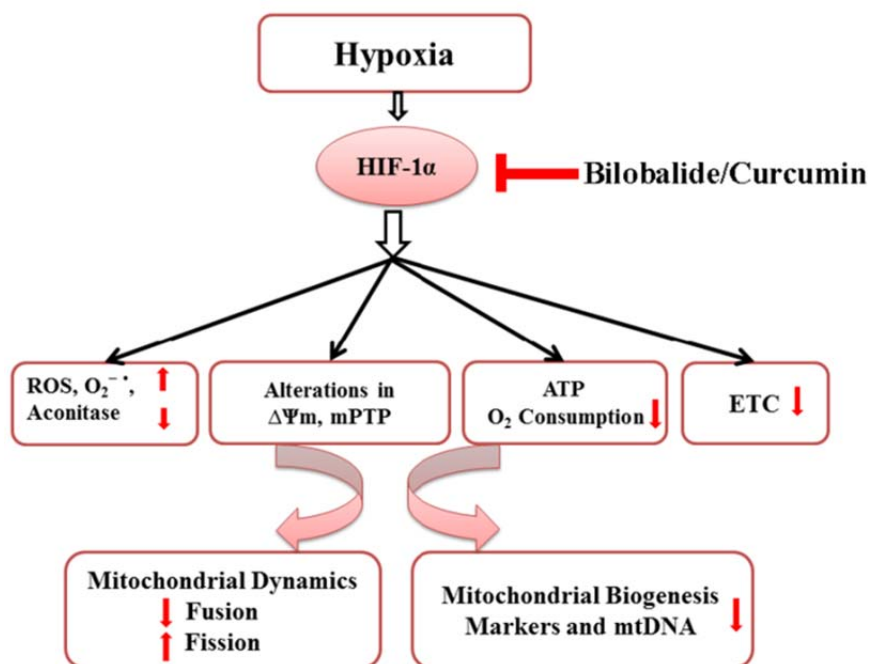
Fig. 3.11 Schematic representation: Summary of chapter 3 – Hypoxia impaired mitochondrial functions in 3T3-L1 adipocytes while bilobalide and curcumin protected adipocytes from mitochondrial disfunctions by enhancing mitochondrial biogenesis, mitochondrial functional performance and by controlling mitochondrial dynamics, via downregulating HIF-1α expression and scavenging ROS.

References

Aggarwal BB, Sung B. (2009). Pharmacological basis for the role of curcumin in chronic diseases: an age-old spice with modern targets. *Trends Pharmacol Sci*, 30: 85-94.

Catrina SB, Okamoto K, Pereira T, Brismar K, Poellinger L. (2004). Hyperglycemia regulates hypoxia-inducible factor-1alpha protein stability and function. *Diabetes*, 53: 3226-3232.

Chan DC. (2012). Fusion and fission: interlinked processes critical for mitochondrial health. *Annu Rev Genet*, 46: 265-287.

Chandel NS, McClintock DS, Feliciano CE, Wood TM, Melendez JA, Rodriguez AM, Schumacker PT. (2000). Reactive oxygen species generated at mitochondrial complex III stabilize hypoxia-inducible factor-1alpha during hypoxia: a mechanism of O_2 sensing. *J Biol Chem*, 275: 25130-25138.

Chen XH, Zhao YP, Xue M, Ji CB, Gao CL, Zhu JG, Qin DN, Kou CZ, Qin XH, Tong ML, Guo XR. (2010). TNF-α induces mitochondrial dysfunction in 3T3-L1 adipocytes. *Mol Cell Endocrinol*, 328: 63-69.

Chhunchha B, Fatma N, Kubo E, Rai P, Singh SP, Singh DP. (2013). Curcumin abates hypoxia-induced oxidative stress based-ER stress-mediated cell death in mouse hippocampal cells (HT22) by controlling Prdx6 and NF-κB regulation. *Am J Physiol Cell Physiol,* 304: C636-C655.

Chiang YY, Chen SL, Hsiao YT, Huang CH, Lin TY, Chiang IP, Hsu WH, Chow KC. (2009). Nuclear expression of dynamin-related protein 1 in lung adenocarcinomas. *Mod Pathol*, 22: 1139-1150.

Choo HJ, Kim JH, Kwon OB, Lee CS, Mun JY, Han SS, Yoon YS, Yoon G, Choi KM, Ko YG. (2006). Mitochondria are impaired in the adipocytes of type 2 diabetic mice. *Diabetologia*, 49: 784-791.

Cipolat S, Martins de Brito O, Dal Zilio B, Scorrano L. (2004). OPA1 requires mitofusin 1 to promote mitochondrial fusion. *Proc Natl Acad Sci U S A,* 101: 15927-15932.

Curtis JM, Grimsrud PA, Wright WS, Xu X, Foncea RE, Graham DW, Brestoff JR, Wiczer BM, Ilkayeva O, Cianflone K, Muoio DE, Arriaga EA, Bernlohr DA. (2010). Downregulation of adipose glutathione s-transferase a4 leads to increased

protein carbonylation, oxidative stress, and mitochondrial dysfunction. *Diabetes*, 59: 1132-1142.

De Pauw A, Tejerina S, Raes M, Keijer J, Arnould T. (2009). Mitochondrial (dys)function in adipocyte (de)differentiation and systemic metabolic alterations. *Am J Pathol*, 175: 927-939.

Denko NC. (2008). Hypoxia, HIF1 and glucose metabolism in the solid tumour. *Nat Rev Cancer*, 8: 705-713.

Frank S, Gaume B, Bergmann-Leitner ES, Leitner WW, Robert EG, Catez F, Smith CL, Youle RJ. (2001). The role of dynamin-related protein 1, a mediator of mitochondrial fission, in apoptosis. *Dev Cell*, 1: 515-525.

Furukawa S, Fujita T, Shimabukuro M, Iwaki M, Yamada Y, Nakajima Y, Nakayama O, Makishima M, Matsuda M, Shimomura I. (2004). Increased oxidative stress in obesity and its impact on metabolic syndrome. *J Clin Invest,* 114: 1752-1761.

Gao CL, Zhu C, Zhao YP, Chen XH, Ji CB, Zhang CM, Zhu JG, Xia ZK, Tong ML, Guo XR. (2010). Mitochondrial dysfunction is induced by high levels of glucose and free fatty acids in 3T3-L1 adipocytes. *Mol Cell Endocrinol*, 320: 25-33.

Gardner PR, Nguyen DH, White CW. (1994). Aconitase is a sensitive and critical target of oxygen poisoning in cultured mammalian cells and in rat lungs. *Proc Natl Acad Sci*, 91: 12248-12252.

Gardner PR, Raineri I, Epstein LB, White CW. (1995). Superoxide radical and iron modulate aconitase activity in mammalian cells. *J Biol Chem*, 270: 13399-13405.

Gardner PR. (2002). Aconitase: sensitive target and measure of superoxide. *Methods Enzymol*, 349: 9-23.

Goldenthal MJ, Marín-García J. (2004). Mitochondrial signaling pathways: a receiver/integrator organelle. *Mol Cell Biochem*, 262: 1-16.

Houstis N, Rosen ED, Lander ES. (2006). Reactive oxygen species have a causal role in multiple forms of insulin resistance. *Nature*, 440: 944-948.

Jang MK, Son Y, Jung MH. (2013). ATF3 plays a role in adipocyte hypoxia-mediated mitochondria dysfunction in obesity. *Biochem Biophys Res Commun*, 431: 421-427.

Javadov S, Karmazyn M. (2007). Mitochondrial permeability transition pore opening as an endpoint to initiate cell death and as a putative target for cardioprotection. *Cell Physiol Biochem*, 20: 1-22.

Keijer J, van Schothorst EM. (2008). Adipose tissue failure and mitochondria as a possible target for improvement by bioactive food components. *Curr Opin Lipidol*, 9: 4-10.

Kim JW, Tchernyshyov I, Semenza GL, Dang CV. (2006). HIF-1-mediated expression of pyruvate dehydrogenase kinase: a metabolic switch required for cellular adaptation to hypoxia. *Cell Metab*, 3: 177-185.

Krishnan J, Danzer C, Simka T, Ukropec J, Walter KM, Kumpf S, Mirtschink P, Ukropcova B, Gasperikova D, Pedrazzini T and Krek W. (2012). Dietary obesity-associated Hif1α activation in adipocytes restricts fatty acid oxidation and energy expenditure via suppression of the Sirt2-NAD+ system. *Genes Dev*, 26: 259-270.

Kusminski CM, Scherer PE. (2012). Mitochondrial Dysfunction in White Adipose Tissue. *Trends Endocrinol Metab,* 23: 435-443.

Lee YJ, Jeong SY, Karbowski M, Smith CL, Youle RJ. (2004). Roles of the mammalian mitochondrial fission and fusion mediators Fis1, Drp1, and Opa1 in apoptosis. *Mol Biol Cell,* 15: 5001-5011.

Liesa M, Palacín M, Zorzano A. (2009). Mitochondrial dynamics in mammalian health and disease. *Physiol Rev*, 89: 799-845.

Liu J, Shen W, Zhao B, Wang Y, Wertz K, Weber P, Zhang P. (2009). Targeting mitochondrial biogenesis for preventing and treating insulin resistance in diabetes and obesity: Hope from natural mitochondrial nutrients. *Adv Drug Deliv Rev*, 61: 1343-1352.

Liu R, Jin P, Yu L, Wang Y, Han L, Shi T, Li X. (2014). Impaired Mitochondrial Dynamics and Bioenergetics in Diabetic Skeletal Muscle. *PLoS ONE,* 9: e92810. doi:10.1371/journal.pone.0092810

Lukyanova LD. (2013). Mitochondrial Signaling in Hypoxia. *Open J Endocr Metab Dis*, 3: 20-32.

Magalhaes J, Ascensao A, Soares JM, Neuparth MJ, Ferreira R, Oliveira J, Amado F, Duarte JA. (2004). Acute and severe hypobaric hypoxia-induced muscle oxidative stress in mice: the role of glutathione against oxidative damage. *Eur J Appl Physiol*, 91: 185-191.

Mathur A, Hong Y, Kemp BK, Barrientos AA, Erusalimsky JD. (2000). Evaluation of fluorescent dyes for the detection of mitochondrial membrane potential changes in cultured cardiomyocytes. *Cardiovasc Res*, 46: 126-138.

Nizet V, Johnson RS. (2009). Interdependence of hypoxic and innate immune responses. *Nat Rev Immunol*, 9: 609-617.

Onder A, Kapan M, Gumus M, Yuksel H, Boyuk A, Alp H, Basarili MK, Firat U. (2012). The protective effects of curcumin on intestine and remote organs against mesenteric ischemia/reperfusion injury. *Turk J Gastroenterol,* 23: 141-147.

Papandreou I, Cairns RA, Fontana L, Lim AL, Denko NC. (2006). HIF-1 mediates adaptation to hypoxia by actively downregulating mitochondrial oxygen consumption. *Cell Metab,* 3: 187-197.

Paul MK, Kumar R, Mukhopadhyay AK. (2008). Dithiothreitol abrogates the effect of arsenic trioxide on normal rat liver mitochondria and human hepatocellular carcinoma cells. *Toxicol Appl Pharmacol*, 226: 140-152.

Peers C, Pearson HA, Boyle JP. (2007). Hypoxia and Alzheimer's disease. *Essays Biochem*, 43: 153-164.

Prathapan A, Vineetha VP, Raghu KG. (2014). Protective effect of boerhaavia diffusa l. against mitochondrial dysfunction in angiotensin ii induced hypertrophy in h9c2 cardiomyoblast cells. *PLoS ONE,* 9: e96220. doi: 10.1371/journal.pone.0096220.

Regazzetti C, Peraldi P, Grémeaux T, Najem-Lendom R, Ben-Sahra I, Cormont M, Bost F, Le Marchand-Brustel Y, Tanti JF, Giorgetti-Peraldi S. (2009). Hypoxia decreases insulin signaling pathways in adipocytes. *Diabetes*, 58: 95-103.

Rehman J, Zhang HJ, Toth PT, Zhang Y, Marsboom G, Hong Z, Salgia R, Husain AN, Wietholt C, Archer SL. (2012). Inhibition of mitochondrial fission prevents cell cycle progression in lung cancer. *FASEB J*, 26: 2175-2186.

Rong JX, Qiu Y, Hansen MK, Zhu L, Zhang V, Xie M, Okamoto Y, Mattie MD, Higashiyama H, Asano S, Strum JC, Ryan TE. (2007). Adipose mitochondrial biogenesis is suppressed in db/db and high-fat diet-fed mice and improved by rosiglitazone. *Diabete*s, 56: 1751-1760.

Scarpulla RC, Vega RB, Kelly DP. (2012). Transcriptional integration of mitochondrial biogenesis. *Trends Endocrinol Metab*, 23: 459-466.

Scheffler I. (1999). Mitochondria, Mitochondrial electron transport and oxidative phosphorylation, New York: Wiley-Liss, pp. 141-245.

Schöttl T, Klingenspor M. (2013). Boosting mitochondrial biogenesis in white adipocytes: A route towards improved insulin sensitivity? *Mol Metabol,* 2: 128-129.

Solaini G, Harris DA. (2005). Biochemical dysfunction in heart mitochondria exposed to ischaemia and reperfusion. *Biochem J*, 390: 377-394.

Sudheesh NP, Ajith T, Janardhanan KK. (2009). Ganoderma lucidum (Fr.) P. Karst enhances activities of heart mitochondrial enzymes and respiratory chain complexes in the aged rat. *Biogerontology*, 10: 627-636.

Sugden MC, Holness MJ. (2002). Therapeutic potential of the mammalian pyruvate dehydrogenase kinases in the prevention of hyperglycaemia. *Curr Drug Targets Immune Endocr Metabol Disord*, 2: 151-165.

Tsui KH, Chung LC, Wang SW, Feng TH, Chang PL, Juang HH. (2013). Hypoxia upregulates the gene expression of mitochondrial aconitase in prostate carcinoma cells. *J Mol Endocrinol,* 51: 131-141.

Zhang X , Lam KS , Ye H , Chung SK , Zhou M , Wang Y , Xu A. (2010). Adipose tissue-specific inhibition of hypoxia-inducible factor 1 α induces obesity and glucose intolerance by impeding energy expenditure in mice. *J Biol Chem*, 285: 32869-32877.

Zhou LJ, Zhu XZ. (2000). Reactive oxygen species-induced apoptosis in PC12 cells and protective effect of bilobalide. *J Pharmacol Exp Ther*, 293: 982-988.

Zoratti M, and Szabo I. (1995). The mitochondrial permeability transition. *Biochim Biophys Acta*, 1241: 139-176.

Zorzano A, Liesa M, Palacín M. (2009). Role of mitochondrial dynamics proteins in the pathophysiology of obesity and type 2 diabetes. *Int J Biochem Cell Biol*, 41: 1846-1854.

Zorzano A. (2009). Regulation of mitofusin-2 expression in skeletal muscle. *Appl Physiol Nutr Metab*, 34: 433-439.

CHAPTER 4

HYPOXIA INDUCED INFLAMMATION AND INSULIN RESISTANCE IN 3T3-L1 ADIPOCYTES AND POSSIBLE ATTENUATION WITH BILOBALIDE AND CURCUMIN

4.1 Introduction

Adipose tissue inflammation is a key event in the pathogenesis of obesity related metabolic syndrome. However the factors that trigger and sustain the inflammatory state remain unclear, but suggestions include involvement of free fatty acid, endoplasmic reticulum stress, oxidative stress, and hypoxia (Ye, 2009; Wang et al., 2007). Recent studies strongly support, adipose tissue hypoxia contribute to this chronic low grade inflammation in obesity (Trayhurn and Wood, 2004; Trayhurn et al., 2008; Wang et al., 2007). Adipocyte hypoxia modulates the production of several inflammation-related adipokines, increasing IL-6, leptin, IL-1β, MCP-1 and decreasing adiponectin secretion (Guilherme et al., 2008; Ye et al., 2007).

HIF-1, the major mediator of the hypoxia response in adipose tissue, is almost undetectable in lean mice but significantly increased in obese mice (Jiang et al., 2011). Hypoxia also activates nuclear factor-κB (NF-κB) inflammatory signal in an HIF-1 dependent manner (Tacchini et al., 2008). Furthermore, hypoxic adipocytes release more saturated FFAs which can bind to macrophage TLR4 receptors resulting in NF-κB activation (Ye, 2009; Schaeffler et al., 2009). NF-κB controls transcription of many pro-inflammatory cytokines or inflammatory mediators. Of the proinflammatory cytokines, TNF-α, IL-6 and IL-1β reduce insulin sensitivity and impair the homeostasis of lipid and glucose metabolism (McArdle et al., 2013; Regazzetti et al., 2009; Hammarstedt et al., 2012). These findings provide strong evidence for a central role for adipose tissue hypoxia induced inflammation in the induction of insulin resistance.

Adiponectin is an adipocyte specific protein, plasma levels of which negatively correlate with adiposity, and insulin resistance, in both mice and humans (Jung and Choi, 2014). Its expression was reduced by hypoxia, and contributes to insulin resistance in obesity (Hammarstedt et al., 2012). The expansion of white adipose tissue (WAT) associated with weight gain requires high rates of angiogenesis to support the expanding tissue mass (Christiaens and Lijnen, 2010; Goossens et al., 2011). ATH leads to an

induction of leptin and VEGF expression in these adipocytes that stimulate angiogenesis in adipose tissue through the HIF-1 pathway (Lolmède et al., 2003). Pharmacological manipulation of adipose tissue hypoxia therefore offers a novel therapeutic option for the treatment of obesity and related metabolic disorders.

In this chapter, we mainly focus on the crosstalk between hypoxia induced inflammation, and insulin resistance and, and also secretion of proangiogenic factors in 3T3-L1 adipocytes and possible reversal with bilobalide and curcumin.

4.2 Materials and methods

4.2.1 Chemicals and cell culture reagents

DMEM, bovine serum albumin, insulin, dexamethasone, IBMX, curcumin and bilobalide were from Sigma–Aldrich Chemicals (St. Louis, MO, USA). 2-(7-Nitrobenz-2-oxa-1,3-diazol-4-yl) amino-2-deoxy-D-glucose (2-NBDG) was purchased from Molecular Probe (Invitrogen Life Technologies, Carlsbad, CA, USA). All antibodies and HRP conjugated secondary antibodies were from Santa Cruz Biotechnology (Texas, USA). All other chemicals used were of standard analytical grade.

4.2.2 Hypoxia induction and treatment

In order to induce hypoxia, differentiated 3T3-L1 adipocytes at 9th day were incubated in a hypoxic chamber (Galaxy 48R, New Brunswick, Eppendorf, Germany) at an atmosphere of 1% O_2, 94% N_2, 5% CO_2, and at $37^{o}C$ for 24 hrs. The control cells were incubated in an atmosphere of 21% O_2 and 5% CO_2 at $37^{o}C$. The cells were treated with different concentrations (10, 20 & 50 µM) of bilobalide or (5, 10, & 20 µM) of curcumin or acriflavine (5 µM; positive control) during hypoxic period (24 hrs). For mRNA expression and protein expression studies, only higher doses of test materials were used.

4.2.3 Estimation of inflammatory cytokines

Inflammatory cytokines (TNF-α, IL-6, IL-1β, MCP-1 and IFN-γ) were estimated in conditioned media, using ELISA kits (BD Bioscience, USA). For performing these assays, 100 µl diluted capture antibody were added to the wells and incubated overnight at 4°C. The supernatant was then aspirated and the wells were washed with wash buffer for 3 times. 200 µl blocking buffer were added to each wells and incubated for 1 hr at room temperature. After washing, 100 µl of conditioned media from respective treatment, were

added to the wells and incubated for 2 hrs at room temperature. After incubation, washing steps were repeated. 100 µl working detector were added to all the wells and incubated for 1 hr at room temperature. After washing, 100 µl of substrate solution was added and incubated for 30 mins in dark. The reaction was then stopped by addition of stop solution and the absorbance was read at 450 nm.

4.2.4 Quantification of adiponectin secretion

Adiponectin was estimated in the conditioned medium using a mouse adiponectin enzyme immunoassay (EIA) kit (SPI Bio, Cayman Chemicals, Ann Arbor, USA). This EIA is based on a double-antibody sandwich technique. The conditioned media after respective treatment were added to wells coated with a monoclonal antibody specific of mouse adiponectin. After one-hour incubation, the wells were washed and added biotin-labelled polyclonal anti-mouse adiponectin antibody and incubated for one hour. After a thorough wash, streptavidin-horseradish peroxidase (HRP) tracer was added and incubated for 30 mins. The concentrations of the adiponectin were then determined by measuring the enzymatic activity of the HRP using the hydrogen peroxide/TMB solution.

4.2.5 Quantification of leptin secretion

The secretion of leptin was quantified in conditioned media using leptin ELISA kit (Merck Millipore, USA). This assay is a sandwich ELISA based method, sequentially, leptin in the sample was bound by a pre-titered antiserum and resulting complexes were immobilized in the wells of the microtiter plate. After washing, purified biotinylated detection antibody was added to the immobilized leptin. Then horseradish peroxidase enzyme solution was added to the immobilized biotinylated antibodies. The concentration of leptin was determined by measuring the enzymatic activity of the HRP using the hydrogen peroxide/TMB solution. The enzyme activity was measured spectrophotometrically at 450 nm and 590 nm within 5 mins.

4.2.6 NF-κB p65 translocation assay

NF-κB p65 transcription factor activity was determined using a kit purchased from Cayman Chemicals (Ann Arbor, USA) as per manufacturer's instructions. The method is sensitive for detecting specific transcription factor DNA binding activity in nuclear extracts. The method is based on ELISA technique and a specific double stranded

DNA sequence containing NF-κB response elements immobilized on the bottom of microplate wells. After respective treatment, the cytoplasmic and nuclear extracts were added to these coated wells and NF-κB present in the extract specifically bound to the NF-κB response elements. NF-κB p65 was then detected by the addition of specific primary antibody. Secondary antibody conjugated with HRP was added to provide a sensitive colorimetric reading at 405 nm.

4.2.7 Glucose uptake activity using 2-NBDG

Fully differentiated 3T3-L1 adipocytes were incubated under normoxia or hypoxia in serum-free, low-glucose (1 g/L) DMEM with 0.5% BSA. Following incubation with phytochemicals and induction of hypoxia, culture medium was removed from each well and replaced with fresh culture medium in the absence or presence of 10 mM fluorescent 2-NBDG (Molecular Probes-Invitrogen, USA), and incubated for 30 mins. The cells were then washed twice with cold phosphate-buffered saline (PBS) and the fluorescence intensity of 2-NBDG in the cells was recorded using a FACS Aria II flow cytometer (BD Biosciences, USA).

4.2.8 Quantification of angiopoietin like protein- 4 (angptl4)

Angiopoietin like protein-4 was estimated using mouse angiopoietin like protein-4 ELISA kit (My Biosource, USA). This assay is a sandwich ELISA based method. The samples after respective treatment were added to plates coated with purified mouse angptl4 antibody. After incubation, HRP conjugated secondary antibody was added to each wells. The concentration of angptl4 was determined by measuring the enzymatic activity of HRP using the hydrogen peroxide/TMB solution. The reaction was terminated by the addition of sulphuric acid solution and the colour change was measured spectrophotometrically at a wavelength of 450 nm. The concentration of angptl4 in the samples was then determined by comparing the OD of the samples to the standard curve.

4.2.9 Quantitative real-time PCR

Total RNA from adipocytes was extracted using Trizol reagent (Invitrogen, Carlsbad, CA). Two micrograms of total RNA was reverse transcribed using Super Script III reverse transcriptase and random hexamers (Life technologies). The gene expression levels were analysed by quantitative real-time RT-PCR, conducted using the CFX96 Real

Time PCR system (Bio-rad, USA) using the following conditions: an initial denaturation for 10 mins at 95ºC, followed by 39 cycles of 15s denaturation at 95ºC, 30s annealing at the optimal primer and 10s extension at 72ºC. Each sample was assayed in triplicate in a 20 µL reaction volume containing 1 µL cDNA, 10 µL SYBR Green master mix (Power SYBR® Green PCR Master Mix, life technologies, Invitrogen, USA), 5.81 µL DEPC water and 1.6 µL of each primer. Analysis was performed according to the ΔΔCt method using β-actin as the housekeeping gene. Specific primers for `each gene were designed to amplify a single product, as confirmed by dissociation curve analysis after the real-time PCR run.

$$\text{Fold change} = 2^{-\Delta(\Delta CT)}$$

where ΔCT = CT, target - CT, β-actin and ΔΔCT = ΔCT, stimulated- ΔCT, control

CT (threshold cycle) is the intersection between an amplification curve and a threshold line.

Table. 4.1 Nucleotide sequence of qRT-PCR primers

mRNA		Primer sequence
Adiponectin	Forward	5'-GTTGCAAGCTCTCCTGTTCC-3'
	Reverse	5'-CTTGCCAGTGCTGTTGTCAT-3'
Resistin	Forward	5'-TCATTTCCCCTCCTTTTCCTTT-3'
	Reverse	5'-TGGGACACAGTGGCATGCT-3'
Tlr4	Forward	5'-CGCCCTTTAAGCTGTGTCTC-3'
	Reverse	5'-CAAAGAGCCTGAAGTGGGAG-3'
Glut-1	Forward	5'-AGGCTTGCTTGTAGAGTGAC-3'
	Reverse	5'- TAAGGATGCCAACGACGATTC-3'
Glut-4	Forward	5'-CAACGTGGCTGGGTAGGC-3'
	Reverse	5'-ACACATCAGCCCAGCCGGT-3'
PPAR-γ2	Forward	5'-GCTGTTATGGGTGAAACTCTG-3'
	Reverse	5'-ATAAGGTGGAGATGCAGGTTC-3'
β - Actin	Forward	5'-AGTACCCCATTGAACGC-3'
	Reverse	5'- TGTCAGCAATGCCTGGGTAC-3'

4.2.10 Western blot analysis

Treated cells were washed with ice-cold PBS and lysed in RIPA buffer containing protease inhibitors. The cell suspensions were centrifuged at 12000 rpm for 15 min at 4°C, and the supernatants were collected. Proteins were quantified using the bicinchoninic acid protein assay kit (BCA kit; Pierce, Rockford, IL, USA) in accordance with the

manufacturer's instructions. Equal amount of proteins (50 μg) were separated by 10% SDS-PAGE and transferred to PVDF membranes using turbo transblot apparatus (BD Bioscience). The membranes were blocked with 5% BSA in TBST (50 mM Tris, pH 7.5, 150 mM NaCl, 0.01% Tween-20) for 1 hr at room temperature. The membrane was washed 3 times with TBST for 10 mins each. The membrane was incubated at 4°C overnight in 5% BSA in TBST containing primary antibodies to one of the following: JNK 1:500, p-JNK 1:500, Ser307p-IRS-1 1:500, IRS-2 1:500, GLUT1 1: 500, GLUT4 1:500, PPAR-γ 1: 500 VEGF, 1:500; MMP2 1: 500, MMP9 1: 500 or β-ACTIN 1:1000. After washing with TBST, the membrane was incubated with peroxidase-conjugated corresponding secondary antibodies for 1hr at room temperature. After washing, membranes were developed using 3, 3'-diaminobenzidine tablets (DAB) (Sigma Aldrich, St Louis, MO, USA) and H_2O_2. The immunoblot results were analysed in quantity one software using Gel doc (BD Bioscience).

4.2.11 Statistical analysis

Results are expressed as means ± standard deviations. Data were subjected to one-way ANOVA and the significance of differences between means were calculated by Duncan's multiple range tests using SPSS for Windows, standard version 7.5.1 (SPSS), and significance was accepted at $P \leq 0.05$.

4.3 Results

4.3.1 Hypoxia induces the secretion of cytokines from 3T3-L1 adipocytes

To assess how hypoxia affects the secretion of cytokines from 3T3-L1 adipocytes, the accumulation of adiponectin, leptin, resistin, TNF-α, IL-6, IL-1β, IFN-γ, and MCP-1 were measured in supernatant. Hypoxia caused significant ($P \leq 0.05$) increase in the level of inflammatory cytokines like TNF- α, IL-6, IL-1β, IFN-γ, and MCP-1, compared with normoxia. Bilobalide (10, 20, and 50 μM) and curcumin (5, 10, and 20 μM) was found to reduce ($P \leq 0.05$) the level of inflammatory markers in stressed cells in a dose-dependent manner compared with the normoxic group.

Table. 4.2 Concentration of inflammatory cytokines in normoxic and hypoxic groups

	IL-6 (pg/mL)	TNF-α (pg/mL)	IL-1β (pg/mL)	MCP-1 (pg/mL)	IFN-γ (pg/mL)
N	760.4±28.3	51.2±1.6	65.7±1.5	287±2.3	170.8±8.3
H	1367±26.9*	194±15.6*	169.7±12.1*	1319±4.3*	348.7±41.2*
B1	1050±70.7#	189.5±.7#	149.7±7.7#	707±3.3#	301±15.5#
B2	888.5±13.4#	159±12.7#	105.1±6.9#	587±3.8#	219.9±8.6#
B3	836.5±19.1#	104±8.4#	75.2±3.7#	413.3±5.2#	192.1±11.1#
C1	978.5±7.8#	141.8±15.5#	114.2±7.7#	673±3.3#	226.7±5.5#
C2	894.5±21.9#	92.2±5.7#	84.4±6.9#	473.3±4.4#	216.5±3.6#
C3	790±2.8#	62.3±9.1#	75.3±3.7#	384.3±2.4#	190.2±8.5#
AF	783±8.4#	36.2±11.7#	74.6±2.7#	376±3.7#	180±2.8#

N-normoxia, H-hypoxia, B1-10 µM, B2-20 µM, B3-50 µM of bilobalide & C1-5 µM, C2-10 µM & C3-20 µM of curcumin and AF-5 µm of acriflavine, treated hypoxic groups. Values are means, with standard deviations represented by vertical bars (n=6).* Mean value are significantly different from the control cells (P≤0.05). # Mean values are significantly different from hypoxia treated cells (P≤0.05).

TNF-α level was increased (P≤0.05; Table. 4.2) significantly in hypoxia (3.8 fold), but treatment with bilobalide and curcumin significantly reduced (1.03, 1.22, 1.87; 1.37, 2.1, 3.11 fold respectively; P≤0.05) the TNF-α levels. IL-6 levels were increased significantly (P≤0.05) in hypoxia-induced cells (1.79 fold) and bilobalide and curcumin treatment caused a significant (P≤0.05) decrease in the cytokine levels (1.30, 1.54, 1.63; 1.40, 1.53, 1.73 fold, respectively; Table. 4.2). There was a significant increase in IFN-γ levels (2.04 fold) during hypoxia, while treatment with bilobalide and curcumin lowered the levels significantly (1.16, 1.64, 1.81; 1.54, 1.61, 1.83 fold, respectively). IL-1β was elevated significantly (P≤0.05) upon induction of stress (2.58 fold) and was significantly reduced (1.13, 1.61, 2.25; 1.49, 2.01, 2.25 fold respectively) on treatment with bilobalide

and curcumin respectively. The level of MCP-1 was increased significantly (P≤0.05) during hypoxia (4.59 fold), which was significantly reduced by bilobalide and curcumin treatment (1.87, 2.25, 3.19; 1.96, 2.79, 3.43 fold, respectively; Table. 4.2). Acriflavine also reduced the over secretion all these adipokines in hypoxic adipocytes (Table. 4.2).
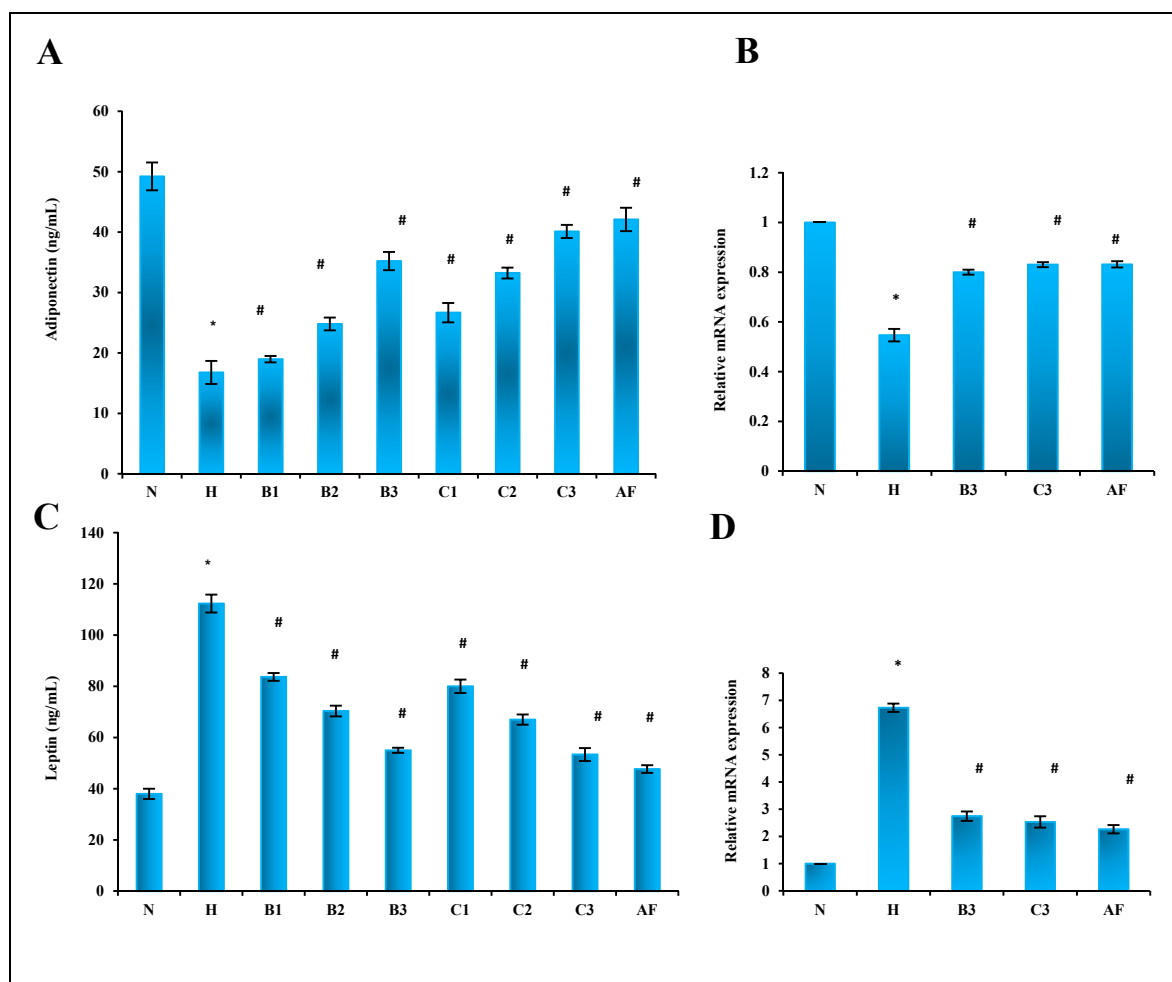
Fig. 4.1 Adiponectin, leptin and resistin levels in normoxic and hypoxic groups: A) Estimation of adiponectin level in conditioned media by ELISA B) Relative mRNA level expression of adiponectin normalised to β-actin C) Leptin level in conditioned media by ELISA D) Relative mRNA level expression of resistin normalised to β-actin.
N-normoxia, H-hypoxia, B1-10 μM, B2-20 μM, B3-50 μM of bilobalide, C1-5 μM, C2-10 μM, C3-20 μM of curcumin and AF-5 μM of acriflavine, treated hypoxic groups. Values are means, with standard deviations represented by vertical bars (n=6).* Mean value are significantly different from the control cells (P≤0.05). # Mean values are significantly different from hypoxia treated cells (P≤0.05)

Next we analysed the level of beneficial adipokine, adiponectin in normoxic and hypoxic groups. The results revealed that hypoxia significantly (P≤0.05) lowered (2.93 fold; Fig. 4.1A) the secretion of adiponectin into the conditioned media compared to

normoxia. The treatment with bilobalide and curcumin significantly (P≤0.05) improved adiponectin secretion at protein (1.13, 1.48, 2.10; 1.59, 1.98, 2.39 fold respectively; Fig 4A) and mRNA level in hypoxic adipocytes (Fig 4B). In addition we monitored the expression of resistin and leptin in hypoxic adipocytes. The secretion of leptin was significantly (P≤0.05) increased (2.96 fold) in hypoxic group, compared to normoxic group. The treatment with bilobalide (10, 20, and 50 μM) and curcumin (5, 10, and 20 μM) caused a significant reduction (1.34, 1.60, 2.04; 1.40, 1.68, 2.11 fold respectively; P≤0.05) in leptin secretion in hypoxic adipocytes in a dose dependent manner (Fig. 4.1C). Acriflavine also lowered leptin secretion in hypoxic adipocytes. The mRNA level of resistin was upregulated (P≤0.05) in hypoxic adipocytes and treatment with bilobalide (50 μM), curcumin (20 μM), and acriflavine (5 μM) significantly restored resistin mRNA level to normal control group (Fig. 4.1D).

4.3.2 Hypoxia induces glycerol release and Tlr 4 expression in adipocytes

The glycerol release from 3T3-L1 adipocytes during hypoxic and normoxic condition were examined. It was significantly (P≤0.05) increased (1.33 fold) in hypoxia cell compared with normal cells. Bilobalide (10, 20 and 50 μM), curcumin (5, 10, and 20 μM) and acriflavine (5 μM) significantly (P≤0.05) prevented the glycerol release (1.14, 1.19, 1.29; 1.13, 1.14, 1.3 fold respectively; Fig. 4.2A). Increased glycerol release is an indication of increased lipolysis and free fatty acid release.

Hypoxia increased (P≤0.05) mRNA levels (8.8 fold) of TLR4 receptors, the key mediator of the activation of NF-κB and JNK pathway. The treatment with bilobalide (50 μM), curcumin (20 μM) and acriflavine (5 μM) significantly reduced (3.27, 3.4 and 2.8 fold respectively; P≤0.05) mRNA level expression of TLR4 receptors in hypoxic adipocytes (Fig. 4.2B).
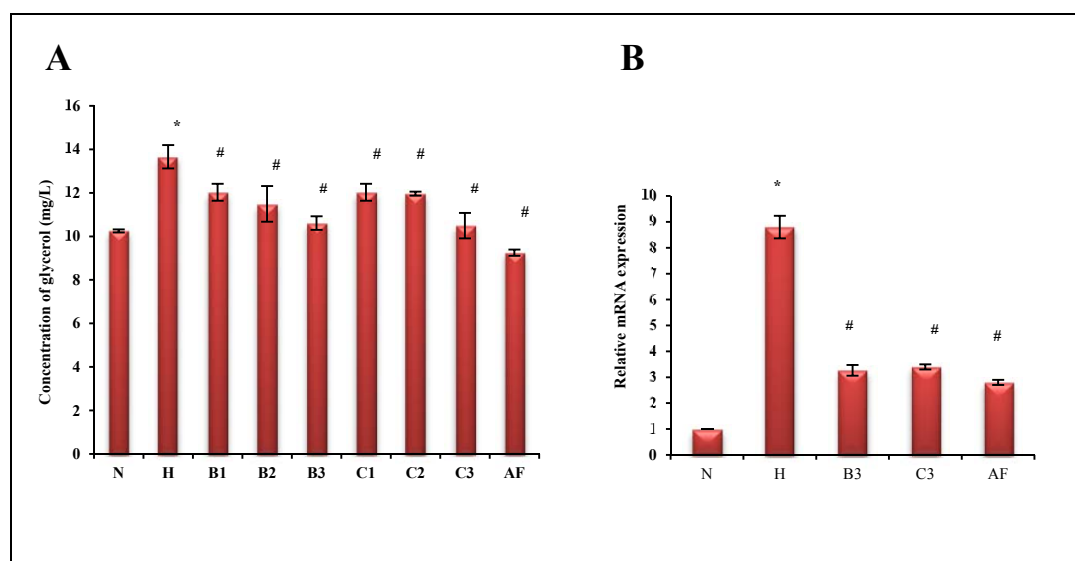
Fig. 4.2 Glycerol release and Tlr-4 expression in normoxic and hypoxic groups: A) Estimation of glycerol release in normoxic and hypoxic groups. B) mRNA expression of Tlr-4 normalised to β-Actin. N-normoxia, H-hypoxia, B1-10 μM, B2-20 μM, B3-50 μM of bilobalide, C1-5 μM, C2-10 μM, C3-20 μM of curcumin and AF-5 μM of acriflavine, treated hypoxic groups. Values are means, with standard deviations represented by vertical bars (n=6).* Mean value are significantly different from the control cells (P≤0.05). # Mean values are significantly different from hypoxia treated cells (P≤0.05).

4.3.3 Hypoxia induces NF-κB p65 translocation in adipocytes
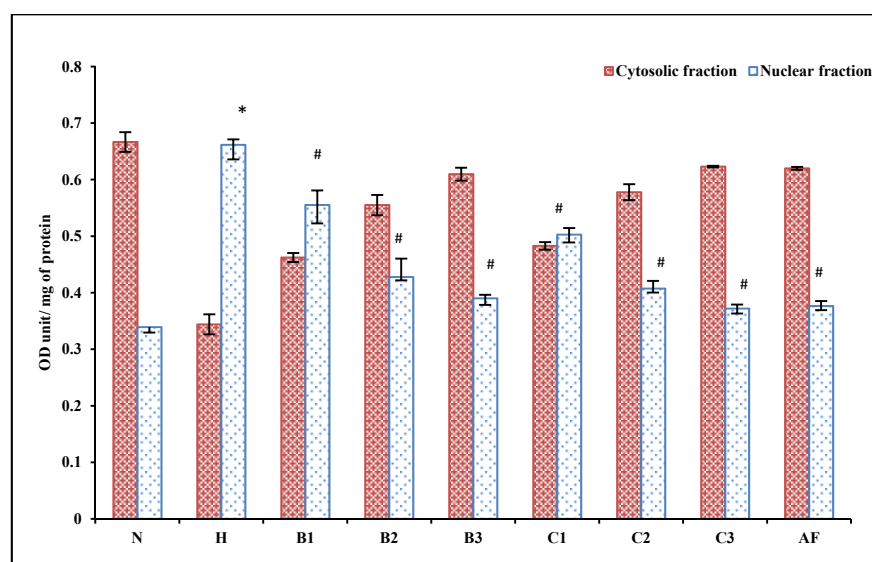
Fig. 4.3 Activity of NF-κB p65 transcription factor in normoxic and hypoxic groups: N-normoxia, H-hypoxia, B1-10 μM, B2-20 μM, B3-50 μM of bilobalide, C1-5 μM, C2-10 μM, C3-20 μM of curcumin and AF-5 μM of acriflavine, treated hypoxic groups. Values are means, with standard deviations represented by vertical bars (n=6).* Mean value are significantly different from the control cells (P≤0.05). # Mean values are significantly different from hypoxia treated cells (P≤0.05).

NF-κB p65 translocation to the nucleus was examined by performing ELISA assay of the cytosolic and nuclear fractions of normoxic and hypoxic groups. Hypoxia for 24 hrs caused significant (P≤0.05) increase (1.9 fold) in nuclear fraction of p65 subunit compared to normoxic group (Fig. 4.3). The treatment with bilobalide (5, 10 and 20 μM) curcumin (5, 10 and 20 μM),   and acriflavine (5 μM) significantly (P≤0.05) prevented (1.19, 1.55, 1.69; 1.32, 1.62, 1.77; 1.76 fold respectively) hypoxia induced nuclear translocation of p65 subunit adipocytes (Fig. 4.3).

4.3.4 Hypoxia induces JNK activation and insulin resistance in adipocytes
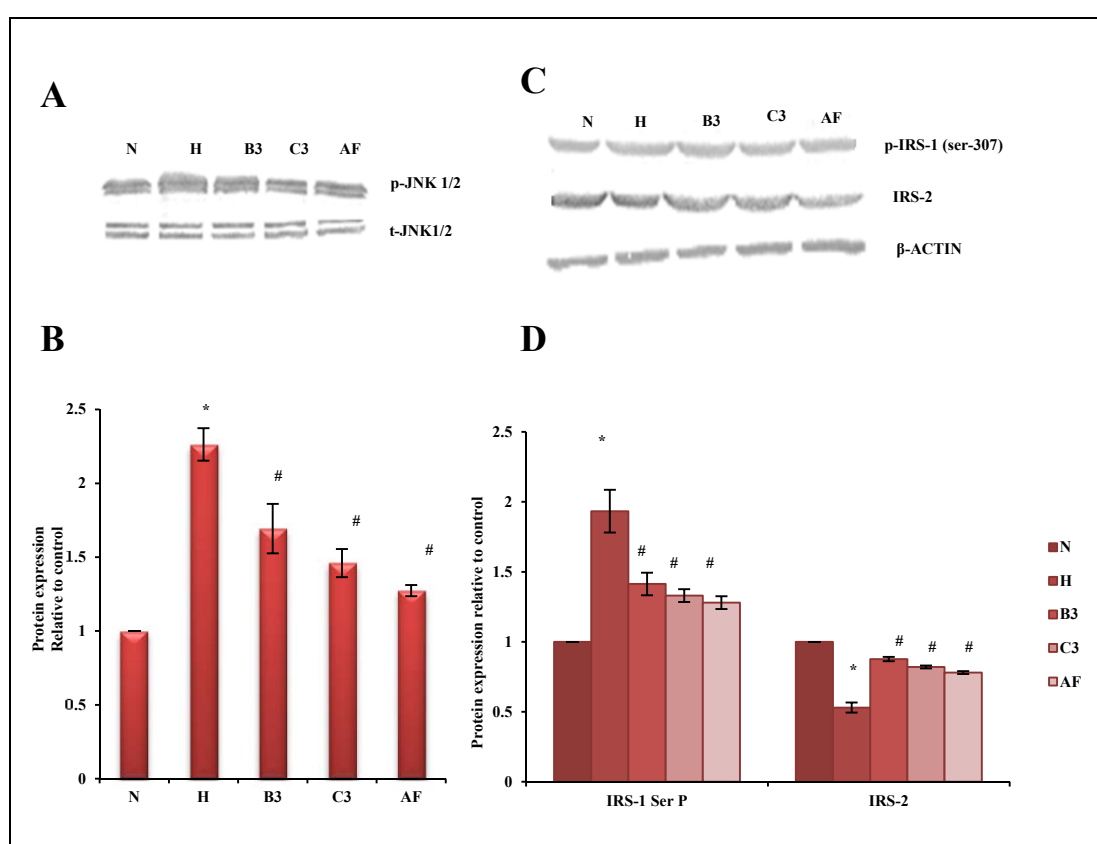
Fig. 4.4 Studies on JNK activation and insulin resistance: A) Immunoblot analysis of p-JNK and JNK in normoxic and hypoxic groups B) Quantification of protein level expression of p-JNK relative to JNK C) Immunoblot analysis of p-IRS-1 (ser-307) and IRS-2 in normoxic and hypoxic groups D) Quantification of protein level expression p-IRS-1 (ser-307) and IRS-2 relative to β-ACTIN. N-normoxia, H-hypoxia, B3-50 μM of bilobalide, C3-20 μM of curcumin and AF-5 μm of acriflavine, treated hypoxic groups. Values are means, with standard deviations represented by vertical bars (n=3).* Mean value are significantly different from the control cells (P≤0.05). # Mean values are significantly different from hypoxia treated cells (P≤0.05).

Immunoblot studies showed increased (P≤0.05) phosphorylation and subsequent activation of JNK, in hypoxic group compared with normoxia (Fig. 4.4A & B). We further investigated the effects of JNK and NF-κB activation on insulin signaling receptors. Western blot analysis showed increased (P≤0.05) serine 307 phosphorylation of IRS-1 and decreased expression of IRS-2 in hypoxic group showing hypoxia induced impairment in insulin signaling (Fig. 4.4C & D). But treatment with bilobalide (50 µM), curcumin (20 µM) and acriflavine (5 µM) significantly (P≤0.05) lowered phosphorylation of JNK, and serine phosphorylation of IRS-1, and also increased the expression of IRS-2 showing protection from hypoxia induced impairment in insulin signaling pathway (Fig.4.4C & D).

4.3.5 Hypoxia induces increased basal glucose uptake and GLUT-1 expression in adipocytes
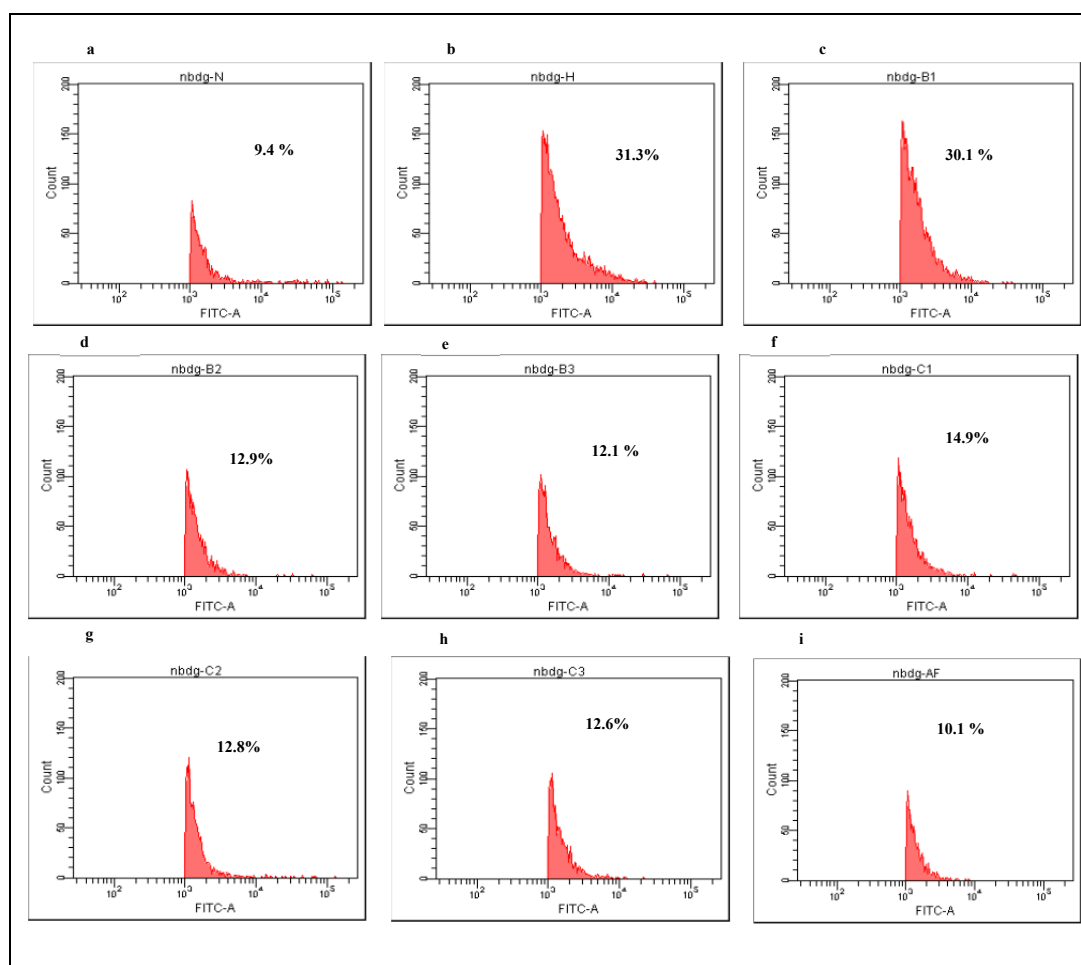

Fig. 4.5 Flow cytometric analysis of basal glucose uptake using 2-NBDG in normoxic and hypoxic groups: The representative histogram shows % cells with fluorescent intensity, which

indicates the glucose uptake activity. a-normoxia; b-hypoxia, c-hypoxia + 10 µM bilobalide; d-hypoxia + 20 µM bilobalide; e-hypoxia + 50 µM bilobalide; f-hypoxia + 5 µM curcumin; g-hypoxia + 10 µM curcumin; h-hypoxia + 20 µM curcumin; i-hypoxia + 5 µM acriflavine.

Flow cytometry was performed to examine glucose uptake in normoxic and hypoxic adipocytes by detecting the fluorescence of 2-NBDG within the cells. The results indicated that hypoxia significantly ($P \leq 0.05$) increased basal glucose uptake in adipocytes. In the 2-NBDG uptake assay, glucose uptake was found to be 31.3% in hypoxic adipocytes, but in normoxic cells only 9.4% of the adipocytes population showed 2-NBDG uptake. Treatment with bilobalide, curcumin and acriflavine resulted in a decreased ($P \leq 0.05$) basal glucose uptake in hypoxic adipocytes (Fig. 4.5).

We further analysed the expression of glucose transporters, GLUT1 and GLUT4 in normoxic and hypoxic groups. GLUT1 expression at mRNA and protein level was significantly ($P \leq 0.05$) upregulated in hypoxic adipocytes, but there was no significant difference in the expression of GLUT4 after 24 hrs of hypoxia compared with normoxia. Bilobalide (50 µM), curcumin (10 µM) and acriflavine (5 µM) treatment significantly ($P \leq 0.05$) restored GLUT1 expression to normal level (Fig. 4.6A & B)
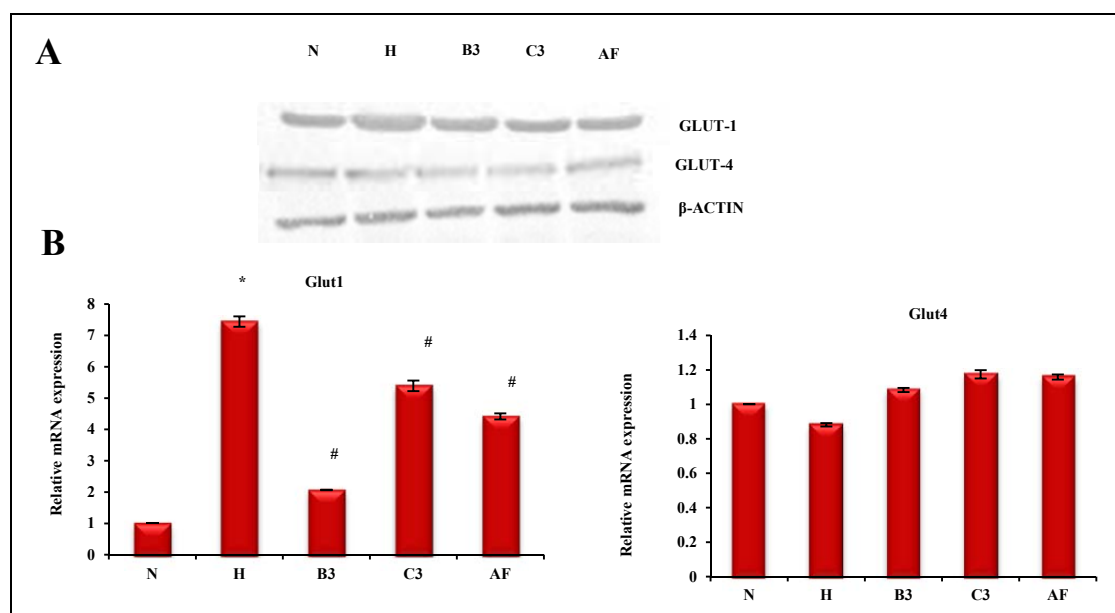
Fig. 4.6 Expression of GLUT-1 and GLUT-4 in normoxic and hypoxic groups: A) Immunoblot analysis of GLUT-1 and GLUT-4 in normoxic and hypoxic groups B) Quantification of mRNA level expression of Glut-1 and Glut-4 normalised to β-Actin in normoxic and hypoxic groups. N-normoxia, H-hypoxia, B3-50 µM of bilobalide, C3-20 µM of curcumin and AF-5 µm of acriflavine, treated hypoxic groups. Values are means, with standard deviations represented by

vertical bars (n=3).* Mean value are significantly different from the control cells (P≤0.05). # Mean values are significantly different from hypoxia treated cells (P≤0.05).

4.3.6 Hypoxia induces increased expression of PPAR-γ in adipocyte
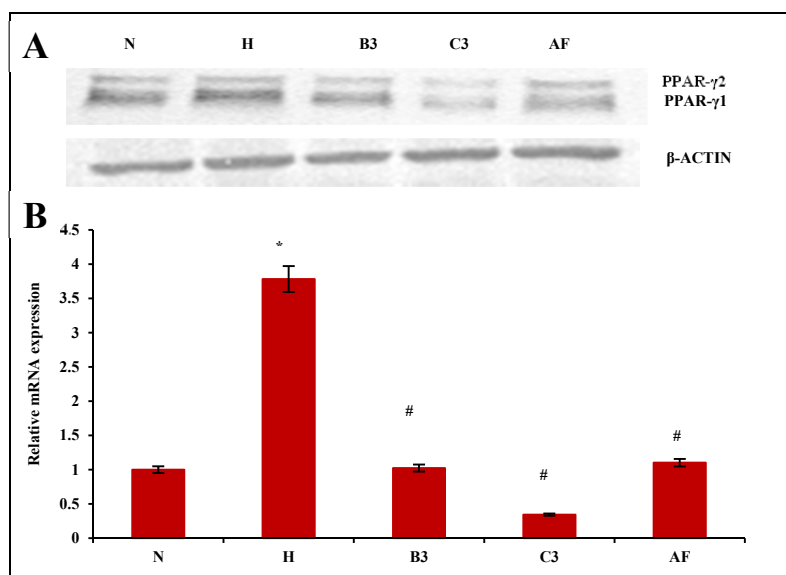
Fig. 4.7 Expression of PPAR-γ in normoxic and hypoxic groups: A) Immunoblot analysis of PPAR-γ. B) mRNA level expression of PPAR-γ normalized to β-Actin in normoxic and hypoxic groups. N-normoxia, H-hypoxia, B3-50 μM of bilobalide, C3-20 μM of curcumin and AF-5 μm of acriflavine, treated hypoxic groups. Values are means, with standard deviations represented by vertical bars (n=3).* Mean value are significantly different from the control cells (P≤0.05). # Mean values are significantly different from hypoxia treated cells (P≤0.05).

Hypoxia significantly (P≤0.05) upregulated PPAR-γ expression at mRNA and protein level in adipocytes. Bilobalide, curcumin and acriflavine significantly lowered its expression in hypoxic adipocytes (Fig 4.7A & B).

4.3.7 Hypoxia induces the release of proangiogenic factors

Hypoxia significantly increased (P≤0.05) the expression of proangiogenic factors (VEGF, MMP-2, MMP-9) in 3T3-L1 adipocytes after 24 hrs of hypoxia. Bilobalide and curcumin significantly reduced (P≤0.05) the expression of proangiogenic factors in hypoxic adipocytes (Fig. 4.8A & B). The secretion of angiopoietin 4 like protein was also monitored in conditioned media by ELISA, in normoxic and hypoxic adipocytes. Results showed a significantly (P≤0.05) high secretion of angiopoietin like protein 4 (angptl 4) in hypoxic adipocytes (2.99 fold) compared to normoxic adipocytes. The treatment with bilobalide (5, 10 and 20 μM), curcumin (5, 10 and 20 μM), and acriflavine (5 μM)

significantly (1.18, 1.73, 1.90; 1.27, 1.83, 1.26; 1.83 fold respectively; P≤0.05) prevented hypoxia induced secretion of angptl4 (Fig. 4.8C).
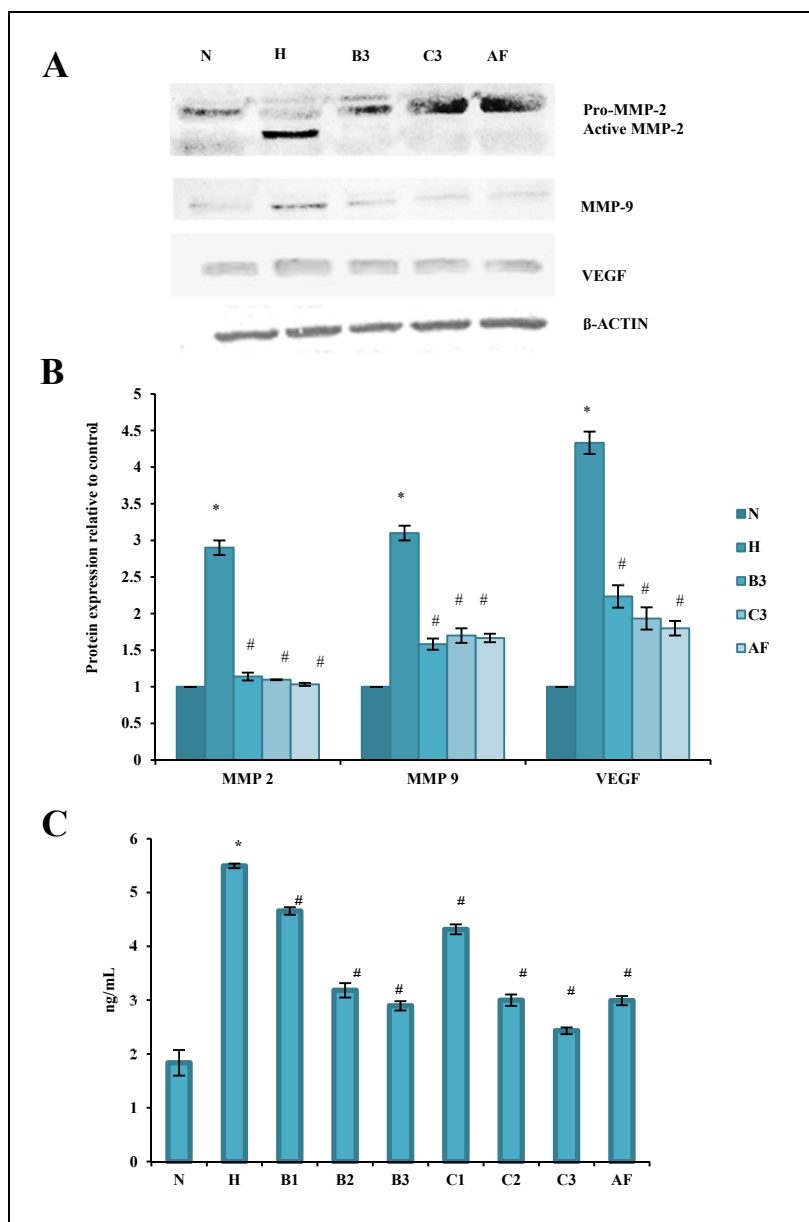
Fig. 4.8 Expression of proangiogenic factors in hypoxic and normoxic groups: A) Immunoblot analysis of proangiogenic factors in normoxic and hypoxic groups B) Quantification of protein level expression of pro-angiogenic factors normalised to β-Actin in normoxic and hypoxic groups C) Angiopoietin like protein 4 release in normoxic and hypoxic groups.
N-normoxia, H-hypoxia, B1-10 μM, B2-20 μM, B3-50 μM of bilobalide, C1-5 μM, C2-10 μM, C3-20 μM of curcumin and AF-5 μM of acriflavine, treated hypoxic groups. Values are means, with standard deviations represented by vertical bars (n=3).* Mean value are significantly different from the control cells (P≤0.05). # Mean values are significantly different from hypoxia treated cells (P≤0.05).

4.4 Discussion

Obesity leads to inflammation in adipose tissue. A large number of studies have shown that an increased body mass index correlates with increased plasma concentrations of inflammatory cytokines. This systemic inflammation is associated with insulin resistance leading to type 2 diabetes mellitus as well as increased risk of cardiovascular disease and certain types of cancer (Greenberg and Obin, 2006; Shoelson et al., 2007). The proposed reasons for development of inflammation in obesity include oxidative stress, ER stress, FFA and local hypoxia. Of these, adipose tissue hypoxia is considered as key factor since it can directly trigger inflammation as well as other factors (ER stress, ROS, FFA) that may induce inflammation in adipose tissue (Trayhurn, 2013). In the present study, we investigated the link between hypoxia induced inflammation and insulin resistance in adipocytes. Our study also demonstrates the protective role of two well-known phytochemicals bilobalide and curcumin against hypoxia induced inflammation and other complications.

Adipokines play major roles in the regulation of food intake, insulin sensitivity, energy metabolism, and the vascular microenvironment (Kawada et al., 2008). Among adipokines, TNF-α, IL-6, MCP-1, IFN-γ, IL-1β, resistin and adiponectin are strongly associated with obesity-induced inflammation, insulin resistance and other obesity-related pathologies. Our study showed increased secretion of TNF-α, IL-6, IL -1β, MCP-1 and IFN-γ in hypoxia compared with normoxia. TNF-α, which is overexpressed in adipose tissue as well as muscle tissues of obese humans, and mice, play significant role in obesity induced insulin resistance (Hotamisligil et al., 1993; Hotamisligil et al, 1995). Targeted gene deletion of TNFα or its receptors significantly improves insulin sensitivity in rodent obesity (Uysal et al., 1997). At cellular level TNF-α has been shown to reduce the expression of genes related to insulin signaling including GLUT4, IRS-1 as well as PPARγ (Hotamisligil et al., 1995). Like TNF-α, elevated level of IL-6 is closely associated with obesity and insulin resistance (Fernández-Real and Ricart, 2003). It impairs insulin signaling in part by down-regulation of IRS and up-regulation of SOCS-3 (Rieusset et al., 2004). IL-1β is also a potent inhibitor of insulin signaling and action, affecting early steps in the insulin signaling cascades (Jager et al., 2007). Hypertrophied adipocytes, observed in obesity, secrete MCP-1 and contribute to macrophage infiltration into adipose tissue, insulin resistance, and hepatic steatosis (Kanda et al., 2006). IFNγ, a major T-cell

inflammatory cytokine, attenuates insulin signaling, lipid storage, and differentiation in human adipocytes (Mc Gillicuddy et al., 2009). Hence, these evidences strongly support inflammation induced insulin resistance in obese subjects. Bilobalide and curcumin treatment significantly reduced the release of these inflammatory markers in a dose-dependent manner.

Adiponectin is an antidiabetic adipokine (Kadowaki et al., 2006), which enhances insulin sensitivity via suppression of gluconeogenesis, and regulation of fatty acid metabolism (Awazawa et al., 2009; Berg et al., 2002). In obese model mice with insulin resistance, hypoadiponectinemia (Yamauchi et al., 2001) often coexists with downregulation of insulin signaling. Hypoxia was shown to reduce adiponectin expression in adipocytes by several independent labs (Jiang et al., 2013; Yu et al., 2011). We also reported reduction in adiponectin level after 24 hrs of hypoxia. This also contributes to hypoxia induced insulin resistance in adipocytes. Bilobalide and CCN treatment significantly improved adiponectin level in hypoxia treated groups.

The stimulation of leptin secretion in differentiated adipocytes, by hypoxia has been demonstrated in several studies and this was also observed here (Lolmède et al., 2003; Hausman and Richardson, 2004; Wang et al., 2007). The leptin level in adipocytes and plasma are positively correlated with total adiposity. Leptin levels are also increased by feeding and decreased by fasting (Couillard et al., 2000). Leptin impairs insulin signaling in adipocytes and contributes to insulin resistance (Denroche et al., 2012). Resistin is an important protein which is secreted from adipocytes. Serum resistin levels are elevated in rodent models of obesity and diabetes (Kusminski et al., 2005). Administration of recombinant resistin to mice worsens glucose tolerance, whereas injection of neutralizing antibody into obese mice improved insulin sensitivity, suggesting that resistin contributes to the pathogenesis of insulin resistance in obesity (Steppan et al., 2001). Increased expression of the adipokine gene resistin in hypoxic/ischaemic mouse brain is also reported (Wiesner et al., 2006). Chronic intermittent hypoxia induced elevated level of resistin is also reported in non-obese rats (Fu et al., 2015). Our results showed an increased expression of resistin mRNA level and bilobalide and curcumin restored its expression to normal level. These evidences suggest that hypoxia mediated secretion of inflammatory cytokines significantly contribute to the progression of insulin resistance in obesity.

The potential mechanisms by which hypoxia promote the development insulin resistance in adipocytes is not well studied. In this chapter we discuss the possible pathways that links hypoxia induced inflammation and insulin resistance in 3T3-L1 adipocytes. Toll-like receptor (TLR) 4 is a major factor that drives the inflammatory NF-κB pathway (Yuan et al., 2001) and JNK pathway (Nguyen et al., 2007). Recently, free fatty acids have been identified as ligands of TLR4 (Shi et al., 2006; Shoelson et al., 2007), linking obesity, TLR4 and inflammation. We observed an increased TLR4 mRNA expression in hypoxic adipocytes. This may be due to increased release of free fatty acids during hypoxia in adipocytes. In a recent study, hypoxia has been reported to upregulate TLR-4 (Toll-like receptor 4) expression via HIF-1 in RAW2647 cells (Kim et al., 2010). The basal lipolysis in adipocytes was determined in hypoxic adipocytes by glycerol release and an increased release of glycerol was found in this study indicating increased release of free fatty acids. Enhanced TLR4 activation in combination with increased free fatty acid concentrations is likely to activate inflammatory signaling. In support of this mechanism, both NF-κB and JNK signaling were up-regulated in hypoxia.This is in line with previous reports that obesity activates inflammatory signaling pathways, mainly NF-κB and JNK pathways (Solinas and Karin, 2010). In the absence of activation, NF-κB is associated with Iκ-Bα inhibitor and retained in the cytoplasm. When cells are stimulated by extracellular signals, activation of IKK2 leads to phosphorylation, ubiquitination and degradation of Iκ-Bα protein. In the absence of Iκ-Bα, NF-κB will be activated and translocated into the nucleus to initiate transcription of target genes. Our study also supports the nuclear translocation of NF-κB p65 to nucleus and subsequent activation of inflammatory cytokines.

Abnormal production of inflammatory adipokines and increased concentrations of FFAs are crucial players in obesity-induced insulin resistance. Both inflammatory cytokines and FFA activates JNK1 by phosphorylation, which in turn phosphorylates IRS-1 at serine 307 (Hirosumi et al., 2002). We found an increased phosphorylation of JNK1 and IRS-1 at Ser 307 in hypoxic adipocytes. Tyrosine (Tyr) phosphorylation of IRS-1 mediates insulin stimulated responses, while Ser 307 phosphorylation inhibits downstream insulin signaling cascade. Hence activation of NF-κB and JNK signaling pathways by hypoxia and subsequent higher expression of cytokines impair insulin signaling cascade. We also observed a reduction in expression of IRS-2, a signaling intermediate downstream

of the insulin, in hypoxic adipocytes. IRS-2 expression is preferentially decreased in the livers of obese model mice (Shimomura et al., 2000), and disruption of hepatic IRS-2 leads to insulin resistance (Kubota et al., 2000), suggesting that IRS-1 as well as IRS-2 is critical for the pathogenesis of systemic insulin resistance. Bilobalide and curcumin ameliorated hypoxia-induced inflammation in 3T3-L1 adipocytes. Bilobalide exerts its anti-inflammatory properties by inhibiting TLR4/NF-κB signaling pathway, thereby lowering production of inflammatory cytokines (Goldie and Dolan, 2013). Several *in vitro* and *in vivo* studies have demonstrated that curcumin inhibits activation of the TLR-4 and NF-κB proinflammatory signaling pathways in diverse cell types including macrophages (Shakibaei et al., 2007; Bharti et al., 2004; Weisberg et al., 2008) and protects cells from inflammation mediated insulin resistance.
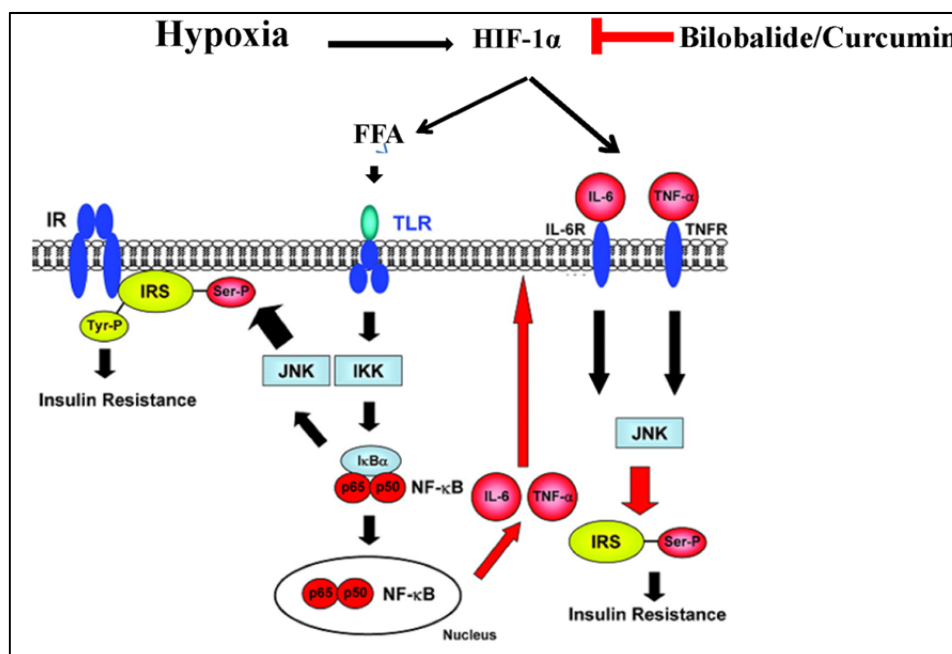
Fig. 4.9 Proposed mechanism of hypoxia induced inflammation and insulin resistance in 3T3-L1 adipocytes and protection with bilobalide and curcumin: The enhanced TLR4 activation in combination with increased FFA release by hypoxia activated inflammatory pathways, NF-κB and JNK signaling in 3T3-L1 adipocytes. Activation of NF-κB and JNK signaling pathways and subsequent higher expression of cytokines impaired insulin signaling cascade by mediating serine phosphorylation of IRS-1. Bilobalide and curcumin ameliorated hypoxia-induced inflammation in 3T3-L1 adipocytes and improved insulin signaling.

We observed an increased basal glucose uptake in 3T3-L1 adipocytes after 24 hrs of hypoxia. This increased glucose uptake is attributed to a metabolic adaptations to reduced O_2 environment, with cells switching to anaerobic glycolysis thereby producing

less cellular ATP per glucose molecule. Consequently, the demand for glucose rises leading to an increase in expression of glucose transporters (Wood et al., 2007). Here, we observed increased GLUT1 expression at mRNA and protein levels in 3T3-L1 adipocytes after 24 hrs of hypoxia. This induction of GLUT-1 is mainly responsible for the increased glucose uptake. Upregulation of GLUT-1 protein represents a response to chronic hypoxia (Zhang et al., 1999), and its expression is directly regulated by HIF-1α (Ebert et al., 1995). There were no significant changes in expression of GLUT4 after 24 hrs of hypoxia. But prolonged exposure to hypoxia can downregulate GLUT4 expression and compromise insulin dependent glucose uptake in adipocytes (Yin et al., 2009). The treatment with bilobalide and curcumin reduced GLUT 1 mediated glucose uptake in hypoxic adipocytes in an HIF-1α dependent manner.

White adipose tissue (WAT) expansion associated with weight gain requires high rates of angiogenesis to support the expanding tissue mass (Kim et al., 2013). The main objective of the present study is to see the influence of hypoxia on the expression and secretion of adipocyte-derived proangiogenic factors. We also assessed the protective role of bilobalide and curcumin against hypoxia mediated release of proangiogenic factors. Since vascular endothelial growth factor (VEGF), and matrix metalloproteinases, MMP-2, MMP-9 are main factors involved in the process of angiogenesis, in this study we analysed the expression of these factors in hypoxic adipocytes. The present results clearly demonstrate the increased expression of VEGF, and MMPs in hypoxic adipocytes, which is in line with the discovery of Lolme`de et al. (2003). VEGF promotes angiogenesis, a process that is required for adipocyte differentiation and adipose tissue growth. Hypoxia is a potent inducer of VEGF and secretion of biologically active VEGF during hypoxia is mediated by HIF-1 (He et al., 2011). Vascular endothelial growth factor (VEGF) induces matrix metalloproteinase expression and enhances the degradation of the basement membrane and extracellular matrix allowing endothelial cell migration as well as proangiogenic factor release (Pufe et al., 2004). The release of angptl 4, a protein which plays important roles in vascular development and angiogenesis (Zhu et al., 2012) also increased in hypoxic adipocytes. Bilobalide and curcumin significantly reduced the expression of all these proangiogenic factors via reducing inflammation and hypoxic upregulation of VEGF.

In conclusion, hypoxia activates NFκB and JNK pathway, leading to the secretion of inflammatory cytokines and inhibitory phosphorylation of IRS-1 which promotes insulin resistance. This provides an important link between hypoxia mediated inflammation and insulin resistance in adipocytes. Bilobalide and curcumin protected adipocytes from hypoxia induced inflammation and insulin resistance mainly by reducing inflammatory adipokine secretion, improving adiponectin secretion, reducing NF-κB/JNK activation, and inhibiting serine phosphorylation of IRS-1 receptors of insulin signaling pathway.

References

Awazawa M, Ueki K, Inabe K, Yamauchi T, Kaneko K, Okazaki Y, Bardeesy N, Ohnishi S, Nagai R, Kadowaki T. (2009). Adiponectin suppresses hepatic SREBP1c expression in an AdipoR1/LKB1/AMPK dependent pathway. *Biochem Biophys Res Comm*, 382: 51-56.

Berg AH, Combs TP, Scherer PE. (2002). ACRP30/adiponectin: an adipokine regulating glucose and lipid metabolism. *Trends Endocrinol Metab*, 13: 84-89.

Bharti AC, Takada Y, Aggarwal BB. (2004). Curcumin (diferuloylmethane) inhibits receptor activator of NF-κB ligand-induced NF-κB activation in osteoclast precursors and suppresses osteoclastogenesis. *J Immunol*, 172: 5940-5947.

Christiaens V, Lijnen HR. (2010). Angiogenesis and development of adipose tissue. *Mol Cell Endocrinol*, 318: 2-9.

Couillard C, Mauriège P, Imbeault P, Prud'homme D, Nadeau A, Tremblay A, Bouchard C, Després JP. (2000). Hyperleptinemia is more closely associated with adipose cell hypertrophy than with adipose tissue hyperplasia. *Int J Obes Relat Metab Disord*, 24: 782-788.

Denroche HC, Huynh FK, Kieffer TJ. (2012). The role of leptin in glucose homeostasis. *J Diabetes Investig*, 3: 115-129.

Ebert BL, Firth JD, Ratcliffe PJ. (1995). Hypoxia and mitochondrial inhibitors regulate expression of glucose transporter-1 via distinct Cis-acting sequences. *J Biol Chem,* 270: 29083-29089.

Fernández-Real JM, Ricart W. (2003). Insulin resistance and chronic cardiovascular inflammatory syndrome. *Endocr Rev*, 24: 278-301.

Fu C, Jiang L, Zhu F, Liu Z, Li W, Jiang H, Ye H, Kushida CA, Li S. (2015). Chronic intermittent hypoxia leads to insulin resistance and impaired glucose tolerance through dysregulation of adipokines in non-obese rats. *Sleep Breath*, 2015 Feb 28.

Goldie M, Dolan S. (2013). Bilobalide, a unique constituent of Ginkgo biloba, inhibits inflammatory pain in rats. *Behav Pharmacol*, 24: 298-306.

Goossens GH, Bizzarri A, Venteclef N, Essers Y, Cleutjens JP, Konings E, Jocken JW, Cajlakovic M, Ribitsch V, Clément K, Blaak EE. (2011). Increased adipose tissue oxygen tension in obese compared with lean men is accompanied by insulin

resistance, impaired adipose tissue capillarization, and inflammation. *Circulation*, 124: 67-76.

Greenberg AS, Obin MS. (2006). Obesity and the role of adipose tissue in inflammation and metabolism. *Am J Clin Nutr*, 83: 461S-465S.

Guilherme A, Virbasius JV, Puri V, Czech MP. (2008). Adipocyte dysfunctions linking obesity to insulin resistance and type 2 diabetes. *Nat Rev Mol Cel Biol*, 9: 67-77.

Hammarstedt A, Graham TE, Kahn BB. (2012). Adipose tissue dysregulation and reduced insulin sensitivity in non-obese individuals with enlarged abdominal adipose cells. *Diabetol Metab Syndr*, 4: 1-9.

Hausman GJ, Richardson RL. (2004). Adipose tissue angiogenesis. *J Anim Sci*, 82: 925-934.

He Q, Gao Z, Yin J, Zhang J, Yun Z, Ye J. (2011). Regulation of HIF-1α activity in adipose tissue by obesity-associated factors: adipogenesis, insulin, and hypoxia. *Am J Physiol Endocrinol Metab*, 300: E877-E885.

Hirosumi J, Tuncman G, Chang L, Görgün CZ, Uysal KT, Maeda K, Karin M, Hotamisligil GS. (2002). A central role for JNK in obesity and insulin resistance. *Nature*, 420: 333-336.

Hotamisligil GS, Arner P, Caro JF, Atkinson RL, Spiegelman BM. (1995). Increased adipose tissue expression of tumor necrosis factor-α in human obesity and insulin resistance. *J Clin Invest*, 95: 2409-2415.

Hotamisligil GS, Shargill NS, Spiegelman BM. (1993). Adipose expression of tumor necrosis factor-α: direct role in obesity-linked insulin resistance. *Science*, 1259: 87-91.

Jager J, Grémeaux T, Cormont M, Le Marchand-Brustel Y, Tanti JF. (2007). Interleukin-1beta-induced insulin resistance in adipocytes through down-regulation of insulin receptor substrate-1 expression. *Endocrinology*, 148: 241-251.

Jiang C, Kim JH, Li F, Qu A, Gavrilova O, Shah YM, Gonzalez FJ. (2013). Hypoxia-inducible factor 1α regulates a socs3-stat3-adiponectin signal transduction pathway in adipocytes. *J Biol Chem*, 288: 3844-3857.

Jiang C, Qu A, Matsubara T, Chanturiya T, Jou W, Gavrilova O, Shah YM, Gonzalez FJ. (2011). Disruption of hypoxia-inducible factor 1 in adipocytes improves insulin

sensitivity and decreases adiposity in high-fat diet–fed mice. *Diabetes*, 60: 2484-2495.

Jung UJ, Choi MS. (2014). Obesity and its metabolic complications: the role of adipokines and the relationship between obesity, inflammation, insulin resistance, dyslipidemia and nonalcoholic fatty liver disease. *Int J Mol Sci*, 15: 61840-6223.

Kadowaki T, Yamauchi T, Kubota N, Hara K, Ueki K, Tobe K. (2006). Adiponectin and adiponectin receptors in insulin resistance, diabetes, and the metabolic syndrome. *J Clin Invest*, 116: 1784-1792.

Kanda H, Tateya S, Tamori Y, Kotani K, Hiasa K, Kitazawa R, Kitazawa S, Miyachi H, Maeda S, Egashira K, Kasuga M. (2006). MCP-1 contributes to macrophage infiltration into adipose tissue, insulin resistance, and hepatic steatosis in obesity. *J Clin Invest*, 116: 1494-1505.

Kawada T, Goto T, Hirai S, Kang MS, Uemura T, Yu R, Takahashi N. (2008). Dietary regulation of nuclear receptors in obesity-related metabolic syndrome. *Asia Pac J Clin Nutr*, 1: 126-130.

Kim D-H, Gutierrez-Aguilar R, Kim H-J, Woods SC, Seeley RJ. (2005). Increased adipose tissue hypoxia and capacity for angiogenesis and inflammation in young diet-sensitive C57 mice compared to diet-resistant FVB mice. *Int J Obes (Lond)*, 37: 853-860.

Kim SY, Choi YJ, Joung SM, Lee BH, Jung Y-S, Lee JY. (2010). Hypoxic stress up-regulates the expression of Toll-like receptor 4 in macrophages via hypoxia-inducible factor. *Immunology,* 129: 516-524.

Kubota N, Tobe K, Terauchi Y, Eto K, Yamauchi T, Suzuki R, Tsubamoto Y, Komeda K, Nakano R, Miki H, Satoh S, Sekihara H, Sciacchitano S, Lesniak M, Aizawa S, Nagai R, Kimura S, Akanuma Y, Taylor SI, Kadowaki T. (2000). Disruption of insulin receptor substrate 2 causes type 2 diabetes because of liver insulin resistance and lack of compensatory beta-cell hyperplasia. *Diabetes*, 49: 1880-1889.

Kusminski CM, McTernan PG, Kumar S. (2005). Role of resistin in obesity, insulin resistance and Type II diabetes. *Clin Sci (Lond)*, 109: 243-256.

Lolmède K, Durand de Saint Front V, Galitzky J, Lafontan M, Bouloumié A. (2003). Effects of hypoxia on the expression of proangiogenic factors in differentiated 3T3-F442A adipocytes. Int *J Obes Relat Metab Disord*, 27: 1187-1195.

Mc Gillicuddy FC, Chiquoine EH, Hinkle CC, Kim RJ, Shah R, Roche HM, Smyth EM, Reilly MP. (2009). Interferon gamma attenuates insulin signaling, lipid storage, and differentiation in human adipocytes via activation of the JAK/STAT pathway. *J Biol Chem*, 284: 31936-31944.

McArdle MA, Finucane OM, Connaughton RM, McMorrow AM, Roche HM. (2013). Mechanisms of obesity-induced inflammation and insulin resistance: insights into the emerging role of nutritional strategies. *Front Endocrinol*, 4: 52. doi:10.3389/fendo.2013.00052.

Nguyen MT, Favelyukis S, Nguyen AK, Reichart D, Scott PA, Jenn A, Liu-Bryan R, Glass CK, Neels JG, Olefsky JM. (2007). A subpopulation of macrophages infiltrates hypertrophic adipose tissue and is activated by free fatty acids via Toll-like receptors 2 and 4 and JNK-dependent pathways. *J Biol Chem*, 282: 35279-35292.

Pufe T, Harde V, Petersen W, Goldring MB, Tillmann B, Mentlein R. (2004). Vascular endothelial growth factor (VEGF) induces matrix metalloproteinase expression in immortalized chondrocytes. *J Pathol*, 202: 367-374.

Regazzetti C, Peraldi P, Grémeaux T, Najem-Lendom R, Ben-Sahra I, Cormont M, Bost F, Le Marchand-Brustel Y, Tanti JF, Giorgetti-Peraldi S. (2009). Hypoxia decreases insulin signaling pathways in adipocytes. *Diabetes*, 58: 95-103.

Rieusset J, Bouzakri K, Chevillotte E, Ricard N, Jacquet D, Bastard JP, Laville M, Vidal H. (2004). Suppressor of cytokine signaling 3 expression and insulin resistance in skeletal muscle of obese and type 2 diabetic patients. *Diabetes*, 53: 2232-2241.

Schaeffler A, Gross P, Buettner R, Bollheimer C, Buechler C, Neumeier M, Kopp A, Schoelmerich J, Falk W. (2009). Fatty acid-induced induction of Toll-like receptor-4/nuclear factor-κB pathway in adipocytes links nutritional signalling with innate immunity. *Immunology*, 126: 233-245.

Shakibaei M, John T, Schulze- Tanzil G, Lehmann I, Mobasheri A. (2007). Suppression of NF-κB activation by curcumin leads to inhibition of expression of cyclo-oxygenase-2 and matrix metalloproteinase-9 in human articular chondrocytes:

implications for the treatment of osteoarthritis. *Biochem Pharmacol,* 73: 1434-1445.

Shi H, Kokoeva MV, Inouye K, Tzameli I, Yin H, Flier JS. (2006). TLR4 links innate immunity and fatty acid-induced insulin resistance. *J Clin Invest*, 116: 3015-3025.

Shimomura I, Matsuda M, Hammer RE, Bashmakov Y, Brown MS, Goldstein JL. (2000). Decreased IRS-2 and increased SREBP-1c lead to mixed insulin resistance and sensitivity in livers of lipodystrophic and ob/ob mice. *Mol Cell*, 6: 77-86.

Shoelson SE, Herrero L, Naaz A. (2007). Obesity, inflammation, and insulin resistance. *Gastroenterology*, 132: 2169-2180.

Solinas G, Karin M. (2010). JNK1 and IKKβ: molecular links between obesity and metabolic dysfunction. *FASEB J*, 8: 2596-2611.

Steppan CM, Bailey ST, Bhat S, Brown EJ, Banerjee RR, Wright CM, Patel HR, Ahima RS, Lazar MA. (2001). The hormone resistin links obesity to diabetes. *Nature*, 409: 307-312.

Tacchini L, Gammella E, De Ponti C, Recalcati S, Cairo G. (2008). Role of HIF-1 and NF-κB transcription factors in the modulation of transferrin receptor by inflammatory and anti-inflammatory signals. *J Biol Chem*, 283: 20674-20686.

Trayhurn P, Wang B, Wood IS. (2008). Hypoxia in adipose tissue: a basis for the dysregulation of tissue function in obesity? *Br J Nutr*, 100: 227-235.

Trayhurn P, Wood IS. (2004). Adipokines: inflammation and the pleiotropic role of white adipose tissue. *Br J Nutr*, 92: 347-355.

Trayhurn P. (2013). Hypoxia and adipose tissue functions and dysfunctions in adipocytes. *Physiol Rev*, 93: 1-21.

Uysal KT, Wiesbrock SM, Marino MW, Hotamisligil GS. (1997). Protection from obesity-induced insulin resistance in mice lacking TNF-α function. *Nature*, 389: 610-614.

Wang B, Wood IS, Trayhurn P. (2007). Dysregulation of the expression and secretion of inflammation-related adipokines by hypoxia in human adipocytes. *Pflug Arch Eur J Phy*, 455: 479-492.

Weisberg SP, Leibel R, Tortoriello DV. (2008). Dietary Curcumin significantly improves obesity-associated inflammation and diabetes in mouse models of Diabesity. *Endocrinology*, 149: 3549-3558.

Wiesner G, Brown RE, Robertson GS, Imran SA, Ur E, Wilkinson M. (2006). Increased expression of the adipokine genes resistin and fasting-induced adipose factor in hypoxic/ischaemic mouse brain. *Neuroreport*, 17: 1195-1198.

Wood IS, Wang B, Lorente-Cebrián S, Trayhurn P. (2007). Hypoxia increases expression of selective facilitative glucose transporters (GLUT) and 2-deoxy-d-glucose uptake in human adipocytes. *Biochem Biophys Res Commun,* 361: 468-473.

Yamauchi T, Kamon J, Waki H, Terauchi Y, Kubota N, Hara K, Mori Y, Ide T, Murakami K, Tsuboyama-Kasaoka N, Ezaki O, Akanuma Y, Gavrilova O, Vinson C, Reitman ML, Kagechika H, Shudo K, Yoda M, Nakano Y, Tobe K, Nagai R, Kimura S, Tomita M, Froguel P, Kadowaki T. (2001). The fat-derived hormone adiponectin reverses insulin resistance associated with both lipoatrophy and obesity. *Nat Med*, 7: 941-946.

Ye J, Gao Z, Yin J, He Q. (2007). Hypoxia is a potential risk factor for chronic inflammation and adiponectin reduction in adipose tissue of ob/ob and dietary obese mice. *Am J Physio Endocrinol Metab*, 293: E1118-E1128.

Ye J. (2009). Emerging role of adipose tissue hypoxia in obesity and insulin resistance. *Int J Obes*, 33: 54-66.

Yin J, Gao Z, He Q, Zhou D, Guo Z, Ye J. (2009). Role of hypoxia in obesity-induced disorders of glucose and lipid metabolism in adipose tissue. *Am J Physiol Endocrinol Metab*, 296: E333-E342.

Yu J, Shi L, Wang H, Bilan PJ, Yao Z, Samaan MC, He Q, Klip A, Niu W. (2011). Conditioned medium from hypoxia-treated adipocytes renders muscle cells insulin resistant. *Eur J Cell Biol*, 90: 1000-1015.

Yuan M, Konstantopoulos N, Lee J, Hansen L, Li ZW, Karin M, Shoelson SE. (2001). Reversal of obesity and diet-induced insulin resistance with salicylates or targeted disruption of Ikkbeta. *Science*, 293: 1673-1677.

Zhang JZ, Behrooz A, Ismail-Beigi F. (1999). Regulation of glucose transport by hypoxia. *Am J Kidney Dis*, 34: 189-202.

Zhu P, Goh YY, Chin HF, Kersten S, Tan NS. (2012). Angiopoietin-like 4: a decade of research. *Biosci Rep*, 32: 211-219.

CHAPTER 5
SUMMARY AND CONCLUSION

Obesity is a major public health and economic problem of global significance. It increases the risk of coronary heart disease, stroke, high blood pressure, type 2 diabetes, and cancer. Obesity is attributed to hypertrophy and hyperplasia of adipocytes. In obesity, adipocytes become hypertrophic and their size increases up to 140–180 μm in diameter. Adipocytes have a limited capacity for hypertrophy; one reason for this is considered the diffusion limit of oxygen, which is at most 100-120 μm. This limits adequate oxygen supply and leads to localized hypoxia. Hypoxia modulates the production of proteins involved in inflammation, angiogenesis, glucose utilization, and so on. Hypoxia may therefore be an important factor underlying adipose tissue dysfunction in obesity. HIF-1, a master signal mediator of hypoxia response, is elevated in obese adipose tissue. Weight loss, on the other hand, down-regulates the expression of HIF-1 in obese adipose tissue. Since the loss of HIF-1 activity improves metabolic functions, compounds that inhibit HIF-1 function in adipose tissue might have significant therapeutic potential in reducing obesity associated metabolic complications.

Numerous trials have been conducted to find and develop new anti-obesity drugs through herbal sources to minimize adverse reactions associated with the present anti-obesity drugs. The weight management programmes often include diet control, physical activity and herbal remedies. A number of new dietary slimming aids are being marketed with an aim to combat obesity. There are numerous investigations on the effectiveness of medicinal plants as natural supplement to reduce body weight. Phytochemicals isolated from medicinal plants offers an opportunity as lead compounds for the development of newer therapeutics. Recent studies have shown the role of adipose tissue hypoxia in obesity related metabolic complications. In present study, natural products were used to target HIF-1, the master signal mediator of hypoxia for the prevention of obesity related complications. Two well-known phytochemicals bilobalide and curcumin were used for this study.

Bilobalide is a sesquiterpene trilactone which is found in extracts of *G. biloba*. It has been shown to protect against cerebral edema, decrease cortical infarct volume, and reduce cerebral ischemic damage. The mitochondria are the the main target for the

terpenoid constituents of *Gingko biloba* extract. Bilobalide allows mitochondria to maintain their respiratory activity in ischaemic conditions by protecting complex I and probably complex III activities. Bilobalide also prevent hypoxia induced decrease in ATP in cultured endothelial cells by protecting mitochondria coupling. Curcumin, a polyphenol from *Curcuma longa* possess antioxidant, anti-inflammatory, anticancer, anti-angiogenesis, chemopreventive and chemotherapeutic properties. Curcumin is a potent inhibitor of the activation of various transcription factors including NF-κB, JNK, HIF-1α, VEGF, PPAR-γ etc. These transcription factors regulate the expression of genes that contribute to inflammation, cell survival, cell proliferation, invasion, and angiogenesis.

In the present study we demonstrated the protective effect of bilobalide and curcumin against hypoxia induced dysfunctions in 3T3-L1 adipocytes emphasising on oxidative stress, ER stress, mitochondrial dysfunctions, inflammation, and insulin resistance. Hypoxia was induced in differentiated 3T3-L1 adipocytes on 9th day by incubating in a hypoxic chamber at an atmosphere of 1% O_2, 94% N_2, 5% CO_2, and at 37^oC for 24 hrs. The control cells were incubated in an atmosphere of 21% O_2 and 5% CO_2 at 37^oC. The cells were treated with different concentrations of bilobalide (10 µM, 20 µM & 50 µM) and curcumin (5 µM, 10 µM & 20 µM) during hypoxic period (24 hrs). Acriflavine (5 µM) was used as positive control.

The induction of hypoxia was confirmed by evaluating the expression of HIF-1α expression in hypoxic adipocytes. Hypoxic adipocytes showed a significant expression of HIF-1α compared to normoxic control. The treatment with bilobalide and curcumin significantly reduced the gene and protein level expression of HIF-1α. By molecular docking experiment using Autodock 4.2 and iGEMDOCK v2.1, appropriate binding and conformation of bilobalide, curcumin, and acriflavine to the LBD of HIF-1α was found. Bilobalide and curcumin exhibited a high binding affinity with LBD of HIF-1α similar to positive control acriflavine which is a known HIF-1α inhibitor. Hypoxia showed increased PDK-1 expression along with elevated lactate release in 3T3-L1 adipocytes, exhibiting a metabolic shift from aerobic to anaerobic respiration. The treatment with bilobalide and curcumin significantly reduced lactate release and PDK-1 expression. Next we analysed hypoxia induced oxidative stress in 3T3-L1 adipocytes. Hypoxia caused significant ROS generation compared with normoxia. Bilobalide and curcumin treatment reduced intracellular ROS generation, lipid and protein oxidation in hypoxic adipocytes and

enhanced the activities of endogenous antioxidant enzymes, showing protection from hypoxia induced oxidative stress. In addition, bilobalide and curcumin augmented Nrf2 mediated HO-1 expression in order to protect hypoxic adipocytes from oxidative stress. Hypoxia induced ROS significantly upregulated ER stress markers (GRP78, ERO1-Lα, PDI, PERK, IRE-1α, ATF-6 & CHOP) in 3T3-L1 adipocytes compared to normoxia. Bilobalide and curcumin attenuated the expression of ER stress markers and protected 3T3-L1 adipocytes from hypoxia induced ER stress.

In hypoxia, mitochondria act as major source of ROS production. Hypoxia elicits the release of superoxide from complex III into the cytosol, where it is converted to H_2O_2 to activate oxidant-dependent signaling pathways resulting in the activation of HIF. So mitochondria are emerging as one of the important targets in the management adipose tissue hypoxia and other associated complications. In this background, we designed further studies to evaluate the protective potential of bilobalide and curcumin against mitochondrial dysfunction in hypoxic 3T3-L1 adipocytes. Hypoxia for 24 hrs substantially increased ROS, and mitochondrial superoxide production. Surplus ROS impaired mitochondrial membrane potential and integrity of permeability transition pore. Hypoxia also reduced mitochondrial biogenesis, oxygen consumption, ATP synthesis, and proteins involved in oxidative phosphorylation. Hypoxia also impaired fusion/fission balance in adipocytes. Bilobalide and curcumin protected the 3T3-L1 adipocytes from adverse effects of hypoxia by enhancing mitochondrial biogenesis, mitochondrial functional performance and by controlling mitochondrial dynamics.

In obesity, chronic inflammation and reduced adiponectin in the white adipose tissue contribute to pathogenesis of insulin resistance. Hypoxia is considered as a potential risk factor for chronic inflammation. In obesity, hypoxic adipocytes produce reactive oxygen species and enhance ER stress, which worsen the inflammatory pathways. Here we studied the molecular mechanism underlying hypoxia induced inflammation, and insulin resistance and, also secretion of proangiogenic factors in 3T3-L1 adipocytes and possible reversal with bilobalide and curcumin. Hypoxia significantly increased the release of TNF-α, IL-6, IL-10, MCP-1 and IFN-γ, leptin, and resistin, the adipokines that induce inflammation and insulin resistance in adipocytes. But the secretion of adiponectin, a beneficial antidiabetic adipokine was significantly reduced in hypoxic adipocytes. Hypoxia also showed an increased mRNA expression of TLR4 receptors. Enhanced TLR4

activation in combination with increased glycerol release activated inflammatory pathways, NF-κB and JNK signaling in hypoxic groups. Activation of NF-κB and JNK signaling pathways by hypoxia and subsequent higher expression of cytokines impaired insulin signaling cascade by mediating serine phosphorylation of IRS-1 and by downregulating the expression of IRS-2. However, we observed an increased basal glucose uptake in hypoxia, in response to increased GLUT1 expression. But there were no significant changes in expression of GLUT4 after 24hrs of hypoxia. Bilobalide and curcumin ameliorated hypoxia-induced inflammation in 3T3-L1 adipocytes and improved insulin signaling. Hypoxia also increased the release proangiogenic factors (MMP-2, MMP-9, VEGF, angiopoietin like protein 4) in 3T3-L1 adipocytes. Bilobalide and curcumin significantly reduced the expression of proangiogenic factors via reducing hypoxia and inflammation.

From overall results of this study, we concluded that hypoxia altered all vital parameters of adipocytes. Hypoxia substantially increased HIF-1α expression, lactate release and PDK-1 expression, ROS production, ER stress and unfolded protein response inducers. Hypoxia also significantly altered mitochondrial functions in 3T3-L1 adipocytes. In addition, hypoxia impaired insulin signaling cascade through increased inflammatory response. The treatment with bilobalide and curcumin protected adipocytes from hypoxia induced dysfunctions by scavenging free radicals and by inhibiting the expression of HIF-1α. This study establishes that HIF-1α, as an appropriate target for ameliorating the detrimental effects of hypoxia on adipose tissue function and the development of obesity-associated disorders.

LIST OF PUBLICATIONS

♦ **Priyanka** A, Nisha VM, Anusree SS, Raghu KG (2014). Bilobalide attenuates hypoxia induced oxidative stress, inflammation, and mitochondrial dysfunctions in 3T3 L1 adipocytes via its antioxidant potential. **Free radical research.** 48(10):1206-1217. doi: 10.3109/10715762.2014.945442.

♦ **Priyanka A,** Anusree SS, Nisha VM, Raghu KG (2014). Curcumin improves hypoxia induced dysfunctions in 3T3 L1 adipocytes by downregulating oxidative stress, inflammation, and mitochondrial alterations. **Biofactors.** 40(5):513-523. doi: 10.1002/biof.1175.

♦ Anusree SS, **Priyanka A**, Nisha VM, Das AA, Raghu KG (2014). An in vitro study reveals the nutraceutical potential of punicic acid relevant to diabetes via enhanced GLUT4 expression and adiponectin secretion. **Food and Function**. 24;5(10):2590-2601. doi: 10.1039/c4fo00302k.

♦ Nisha VM, **Priyanka A**, Anusree SS, Raghu KG (2014). (-)-Hydroxycitric acid attenuates endoplasmic reticulum stress-mediated alterations in 3T3-L1 adipocytes by protecting mitochondria and downregulating inflammatory markers. **Free Radical Research**. 48(11):1386-1396. doi: 10.3109/10715762.2014.959514.

♦ Nisha VM, Anusree SS, **Priyanka A**, Raghu KG (2014). Apigenin and Quercetin Ameliorate Mitochondrial Alterations by Tunicamycin-Induced ER Stress in 3T3-L1 Adipocytes. **Applied Biochemistry Biotechnology**. 174(4):1365-1375. doi: 10.1007/s12010-014-1129-2.

List of presentations in scientific conferences

♦ Poster presentation on "Bilobalide improves hypoxia induced alterations in 3T3-L1 adipocytes by ameliorating oxidative stress and protecting mitochondria." at Indian Academy of Biomedical Sciences, 9th - 11th, January, 2015, Hyderabad.

♦ Poster presentation on "An *in vitro* investigation on protective effect of Curcumin and Bilobalide in hypoxia induced alterations in adipocytes" at International conference on "Phytochemicals in Health and Disease: Challenges and Future Opportunities (ICPHD-2013), JAN 23-25, Annamalai University.